Master's thesis

NTNU
Norwegian University of Science and Technology
Faculty of Medicine and Health Sciences
Department of Clinical and Molecular Medicine

Haelin Kim

Molecular tools and model systems for studying inflammasome activation

Master's thesis in Molecular Medicine
Supervisor: Kai Sandvold Beckwith
June 2019

NTNU
Norwegian University of
Science and Technology

Haelin Kim

Molecular tools and model systems for studying inflammasome activation

Master's thesis in Molecular Medicine
Supervisor: Kai Sandvold Beckwith
June 2019

Norwegian University of Science and Technology
Faculty of Medicine and Health Sciences
Department of Clinical and Molecular Medicine

NTNU
Norwegian University of
Science and Technology

NTNU
Norwegian University of Science and Technology
Master's thesis
Faculty of Medicine and Health Sciences
Department of Clinical and Molecular Medicine
Centre of Molecular Inflammation Research

Acknowledgements

This master's project was carried out at Centre of Molecular Inflammation Research (CEMIR), Department of Clinical and Molecular Medicine, Norwegian University of Science and Technology.

First of all, I would like to express my sincere appreciation to my main supervisor Kai Sandvold Beckwith. Thank you so much for your guidance and support throughout my thesis work. Your unsurpassed knowledge and expertise amazed me every single day. You continuously inspired and motivated me to push myself forward to achieve the best and grow personally and professionally. Also, thank you for always being approachable and caring whenever I needed your help.

To my co-supervisor Trude Helen Flo, thank you for giving me the opportunity to join and complete my master's thesis in your research group. All the experiences that I had, motivated me to be become hard-working and dedicated person in science. Thank you for your helpful critique and support for my project. It was a great pleasure to be involved where I could feel your enthusiasm for immunology.

I wish to acknowledge the help provided by Anne for western blot, cell culture techniques and for always being there whenever I needed help in the lab. Especially to Claire, thank you for allowing me to stay in your office so I could focus with the writing, Hany for your candid advice and help whenever I just dropped by at your office, Alexander for teaching me how to use ImageJ, Marianne for teaching me ELISA, Ragnhild for your help with calculations and being my lab partner, and Sunniva for helping with the grammar check. Thank you to all the people at CEMIR for support and encouragement throughout this long journey.

Last but not least, I would like to thank my family, especially to my mother and sister, and friends for supporting and praying for me. I also thank God who led me all the way for giving me strength and for His love.

Abstract

Upon cellular stress or invasion by pathogens such as *Mycobacterium tuberculosis (Mtb)*, inflammasomes are activated as an innate immune response, an important host-defense mechanism to resist pathogens. Activation of NLRP3 recruits ASC and caspase-1 for oligomerization and eventually to IL-1β secretion and pyroptosis through gasdermin D. In the first part of this study, we knocked out NLRP3 and GSDMD genes with CRISPR/Cas9 technology and confirmed their essential roles in canonical inflammasome pathway by using different genetic and molecular tools. We have compared the efficiency of different guide RNAs and verified the functional roles of inflammasome proteins. Additionally, we attempted to knock out secretory autophagy related proteins FIP200 and SEC22B for they were found to play additional roles in IL-1β secretion, and ESCRT machinery proteins ALIX and ALG-2 for they play major role in balancing cell death and viability and IL-1β release in inflammasome activation. We also wished to explore other recent model systems, BlaER1 cells, for (human) inflammasome research that might show different responses. In the last part of this study, we performed molecular cloning to insert epitope and fluorescent tags within GSDMD in order to visualize intracellular localization and GSDMD cleavage during pyroptotic cell death. Overall, this project established genetic and molecular tools to study inflammasome activation, and have demonstrated the importance of different genes in inflammasome regulation and pyroptotic cell death.

Abbreviations

AIM2: Absent in melanoma
ALG2: Apoptosis linked gene-2
ALIX: ALG2 interacting protein X
APCs: Antigen presenting cells
ASC: Apoptosis-associated speck like protein containing a CARD
ATP: Adenosine triphosphate
BP: Base pair
BSA: Bovine serum albumin
CARD: Caspase recruitment domain
Ca2+: Calcium
CIITA: C2TA or MHC class 2 transcription activator
CLR: C-type lectin receptors
CRISPR: Clustered regulatory interspaced short palindromic repeats
crRNA: CRISPR RNAs
DAMPs: Damage associated molecular patterns
DD: Death domain
DMEM: Dulbecco's modified eagle's medium
DMSO: Dimethyl sulfoxide
DNA: Deoxyribonucleic acid
DSB: Double strand break
EDTA: Ethylenediaminetetraacetic acid
ELISA: Enzyme linked immunosorbent assay
ESCRT: Endosomal sorting complex required for transport
FADD: Fas-associated protein with death domain
FCS: Fetal calf serum
FIP200: ULK-interacting protein
GFP: Green fluorescent protein
GSDMD: Gasdermin D
HCL: Hydrochloric acid
HEPES: Hydroxyethyl piperaazineethanesulfonic acid
HET-E: incompatibility locus protein from *Podospora anserina*
HDR: Homologous direct repair
HIV: Human immunodeficiency virus
HRP: Horseradish peroxidase
HSP90: Heat shock protein 90
ICE: IL-1β converting enzyme
IFN: Interferons
IkBa: Nuclear factor of kappa light polypeptide gene enhancer in B-cells inhibitor
IKK: IkB kinase
IL-1β: Interleukin 1 beta
INT: Iodonitrotetrazolium
KB: Kilobase
KDA: Kilodaltons
KO: Knockout
K+: Potassium
LB: Lysogeny broth
LDH: Lactate dehydrogenase
LLOME: L-leucyl-L-leucine methyl ester
LPS: Lipoplysaccharides

LRR: Leucine rich repeats
mtDNA: Mitochondrial DNA
MCC: MCC950,NLRP3 inhibitor
M-CSF: Macrophage colony-stimulating factor
mIRFP: Monomeric near-infrared fluorescent protein
MLKL: Mixed lineage kinase domain like oligomers
MOPS: 3-(*N*-morpholino) propanesulfonic acid buffer
mSC: Monomeric red fluorescent protein
MSU: Monosodium urate crystals
Mtb: Mycobacterium tuberculosis
MQ: Milli-Q water
MYD88: Myeloid differentiation primary response 88
NACHT: Nucleotide binding domain
NaCl: Sodium chloride
NAIP: NLP family apoptosis inhibitor protein
NADPH: Nicotinamide adenine dinucleotide phosphate oxidase
NETs: Neutrophil extracellular traps
NF-kB: Nuclear factor-kappa B
NHEJ: Non-homologous end joining
NLR: NOD-like receptors
NOD: Nucleotide-binding oligomerization domain
NP40: Nonyl phenoxypolyethoxylethanol buffer
PAM: Photospacer adjacent motif
PAMPs: Pathogen associated molecular patterns
PBMC: Peripheral blood mononuclear cell
PBS: Phosphate-buffered saline
PCR: Polymerase chain reaction
PDCD6: Programmed cell death protein 6 (ALG-2 gene in humans)
PM: Plasma membrane
PMA: Phorbol 12-myristate 13-acetate
PRR: Pathogen recognition receptor
P/S: Penicillin-Streptomycin
PYD: Pyrin domain
PYCARD: PYD and CARD domain containing, ASC
P2X7R: P2X purinoceptor 7
RIPA: Radioimmunopreciptation assay buffer
RLR: Retinoic acid-Inducible gene I (RIG-I)-like receptors
RNA: Ribonucleic asic
RPMI: Roswell Park Memorial Institute medium
ROS: Reactive oxygen species
sgRNA: Single guide RNA
SEC22B: Vesicle-trafficking protein
SEM: Standard error of the mean
SG: Single guide
SGT1: Ubiquitin ligase-associated protein
SOC: Super optimal broth with catabolite repression
TAE: Tris acetate electrophoresis
TALEN: Transcription activator like effector nucleases
TB: Tuberculosis
TBS: Tri-buffered saline
TBS-T: TBS with Tween

TIDE: Tracking of indels by decomposition

TLR: Toll-like receptor

TNF: Tumor necrosis factor

TP-2: Telomerase associated protein

tracrRNA: trans-activating crRNA

WB: Western blot

WT: Wild type

ZFNs: Zinc finger nucleases

Table of Contents

1 Introduction

1.1 Overview of the Immune System

The human body's first line of defense is skin and mucosa that create mechanical and chemical barriers against pathogens such as bacteria, fungi, virus and parasites. But when those barriers are penetrated by pathogens, the immune system protects the host with its innate and adaptive response. Unlike adaptive response that is specific and takes days to arise, innate immune response by phagocytic cells such as macrophages and antigen presenting cells (APCs) reacts quickly to control and eradicate pathogens (Figure 1). The innate immune system relies on conserved molecular structures called pattern recognition receptors (PRRs) to detect structural microbial molecules called "pathogen associated molecular patterns" (PAMPs) and "damage associated molecular patterns (DAMPs) from aged and damaged cells. Currently, there are four classes of PRR families identified. These are membrane bound PRRs called Toll-like receptors (TLRs) and C-type lectin receptors (CLRs), also cytoplasmic PRRs such as RIG-I-like receptors (RLRs) and NOD-like receptors (NLRs). These PRRs on phagocytes recognize the extracellular and intracellular pathogens which eventually leads to induction of pro-inflammatory cytokines, chemokines and type 1 interferons (IFN). Finally, the adaptive immune system takes over when the exposure to pathogens overtakes the ability of innate immunity to handle and generates antigen-specific B and T lymphocytes that provide long term immunological memory. (This section is based upon[1,2] unless otherwise stated).

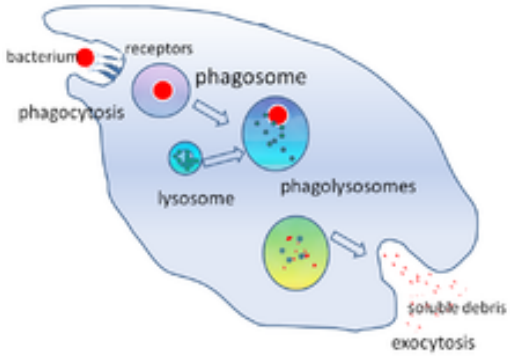

Figure 1. The stages of phagocytosis. *Phagocytes stretch their plasma membrane to ingest the bacteria forming phagolysosome, and kills the bacterium with their hydrolytic enzymes. They also release signaling proteins such as cytokines and chemokines that act as messengers between cells and initiators of inflammatory response. Figure is taken from*[3]

1.2 NLR Family

Nod-like receptors (NLRs) are a family of PRRs that detect variety of PAMPs and DAMPs in the cytosol to activate inflammatory response[1]. They are intracellular sensors that are organized with common NOD (nucleotide-binding oligomerization domains, NACHT: NAIP, CIITA,HET-E, TP-2) domain that is involved in signalling complex activation via ATP-dependent oligomerization effector N-terminal domain (CARD/PYD) for protein interaction and C-terminal leucine rich repeats (LRRs) domain for binding microbial ligands [4,5]. The N-terminal domain divides NLRs to five different subfamilies which are NLRA (acidic transactivation domain), NLRB (baculoviral inhibitory repeat like domain), CARD/NLRC (caspase activation and recruitment domain) and NLRP (the pyrin domain), and NLRX (unknown domain) [4,6]. Currently, there are 23 human NLR genes identified, and these are mainly expressed in immune cells though some are expressed in epithelial cells[7]. NLRs recognize wide range of different ligands such as peptidoglycan, viral RNA, ATP, cholesterol crystals, silica, alum.[4] and once activated, NLRs can either undergo signal transduction, inflammasome formation, transcription activation and autophagy [4,7,8].

1.3 NLRP3 and Inflammation Complex

Some NLRs (NLRP1, NLRP2, NLRP3, NLRP6, NLRP7, NLRP12, NLRC4, NAIP) and absent in melanoma (AIM2) form inflammasome complex on detection of cytosolic PAMPs [8,9]. Inflammasome is a multi protein complex that mediate host immune responses resulting in recruitment of ASC, activation of caspase-1(canonical) or 4/5/11 (non-canonical) and secretion of proinflammatory cytokines IL-1β and IL-18 [10]. Out of these NLRs, NLRP3 (also known as NALP3 or cryopyrin) is the most well-characterized and interesting complex so far. NLRP3 is structured with these three domains: LRRs that recognize stimuli, NACHT that mediates self-oligomerization and N-terminal PYD (pyrin) domain that mediates downstream protein interaction[8,10]. The PYD domain in NLRP3 aggregated with PYD domain in ASC and CARD domain associates with CARD domain in caspase-1 leading to formation of NLRP3 inflammasome complex[11] (Figure 2). Activation of NLRP3 is triggered by numerous ligands and stimuli that are derived from pathogens such as *Listeria monocytogenes*[12,13], *Candida albicans*[14,15], *Mycobacterium abscessus*[16], *Staphylococcus aureus*[17], *influenza A virus*[18,19], sterile activators (ATP, cholesterol crystals, uric acid, LLOME), and environment-derived stimulants (alum, silica,UV radiation) [4,8]. However, its molecular mechanism and consensus

on exact ligand binding are not fully understood yet. Nevertheless, to activate NLRP3 canonically, two steps are required: priming and activation.

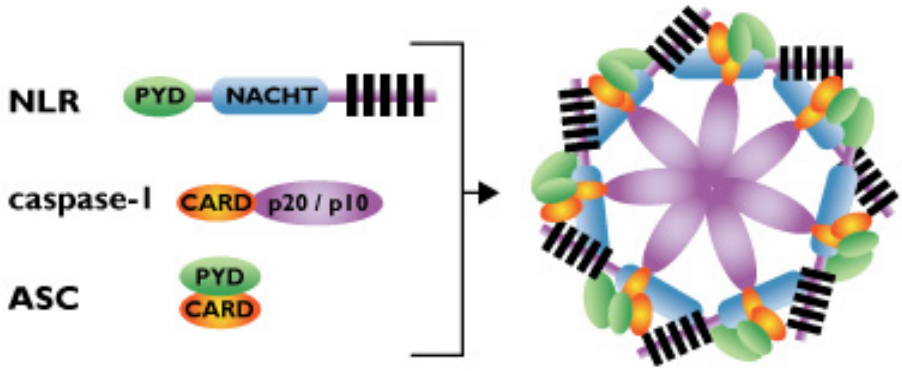

Figure 2. Structure of NLRP3 inflammasome complex. *The sensor NLRP3 protein directly binds to ASC adaptor protein through PYD-PYD interactions. This leads to recruitment of effector protein caspase-1 via CARD-CARD interaction. Figure is taken and modified from* [20]

1.3.1 Priming

The priming step is crucial to obtain strongly enhanced NLRP3 expression because resting macrophages are insufficient for inflammasome activation and IL-1β production [10,21]. This first signal is commonly induced by TLR ligands such as lipopolysaccharide LPS, peptidoglycan, bacterial flagella (PAMPs),[22] but endogenous cytokines such as TNF-alpha and IL-1β can activate the priming signal[23]. Also recently, Grung *et al*. have shown that FADD and caspase 8 are also regulators of NLRP3 expression[24]. The TLR4 agonist, LPS, stimulation triggers MYD88 adaptor protein that activates IkB kinase (IKK) which then phosphorylates IkB-alpha leading to activation of nuclear factor kappa B (NF-kB) transcription factor (Figure 3) [10,21,25] to be translocated into the nucleus[26]. This is a crucial step for both up-regulation of NLRP3 and induction of pro-IL-1β since they are not sufficiently expressed for inflammation formation yet. NLRP3 is in its inactive ubiquitinated state in cytosol until priming signal is initiated. This leads to LRR domain oligomerization by BRCC3 deubiquitinase[27,28] and, studies have shown that knockdown of BRCC3 resulted failure of inflammasome activation[27 28,29]. In addition, chaperones heat shock protein 90 (HSP90), ubiquitin ligase-associated protein (SGT1), and JNK1-mediated phosphorylation are needed for proper inflammasome activity and stability[27,30,31].

1.3.2 Activation

The activation step involves distinct mechanisms in assembly of NLRP3 inflammasome, activation of caspase-1 and IL-1β processing (Figure 3). This step occurs through reduction of intracellular potassium (K+) level, generation of mitochondrial reactive oxygen species (ROS), and lysosomal leakage driven by various agents[10]. For example, ATP (adenosine triphosphate) from microbial pathogens activate P2X7 cell receptor (P2X7R) and results in intracellular K+ efflux thus activating NLRP3 [5,10]. A number of bacterial pore-forming toxins such as nigericin (Streptomyces hygroscopicus) and beta-hemolysin (Group B Streptococcus) can also result low intracellular K+ concentration and activate NLRP3 [32,33]. Blocking the potassium channel and elevating the extracellular potassium level inhibited NLRP3 inflammasome activation[28,34,35] , therefore K+ migration out of the cell is necessary for NLRP3 activation. While it is still controversial, studies show that calcium (Ca 2+) signaling is necessary in NLRP3 activation for blocking Ca2+ signaling inhibits NLRP3 activation[10,36-38]. However, a study by Katsnelson *et al.* suggested that increased level of Ca 2+ is dispensable for NLRP3 activation for Ca 2+ was not necessary for NLRP3 activation[39]. ROS are released upon mitochondrial damage by NAPDH oxidase and can lead NLRP3 inflammasome activation[10,28,40,41] but excessive production of ROS may inhibit caspase-1 activation[23]. Also, a study implied that K+ efflux is not an requirement for ROS inducers like imiquimod and CL097 to activate NLRP3 inflammasome[42]. Oxidized mitochondrial DNA (mtDNA), in response to LPS and ATP, could also be NLRP3 inflammasome triggerer[43]. Furthermore after phagocytosis, phagolysosome may rupture and release lysosomal enzymes such as cathepsin and bacterial mRNA into the cytosol activating NLRP3 inflammasome[10,23]. Upon activation, NLRP3 associates with ASC adaptor protein, which eventually recruits pro-caspase 1 to secrete proinflammatory cytokines leading to pyroptosis. Contradictorily, recent studies have shown that human PBMCs (peripheral blood mononuclear cell) could secrete mature IL-Iβ with only LPS itself, without having K+ efflux dependency and pyroptosis[44]. It is certain that NLRP3 is activated with multiple molecular events and that many signals either require or do not require K+ efflux, but it is still debated how all these activation stimuli can interplay together.

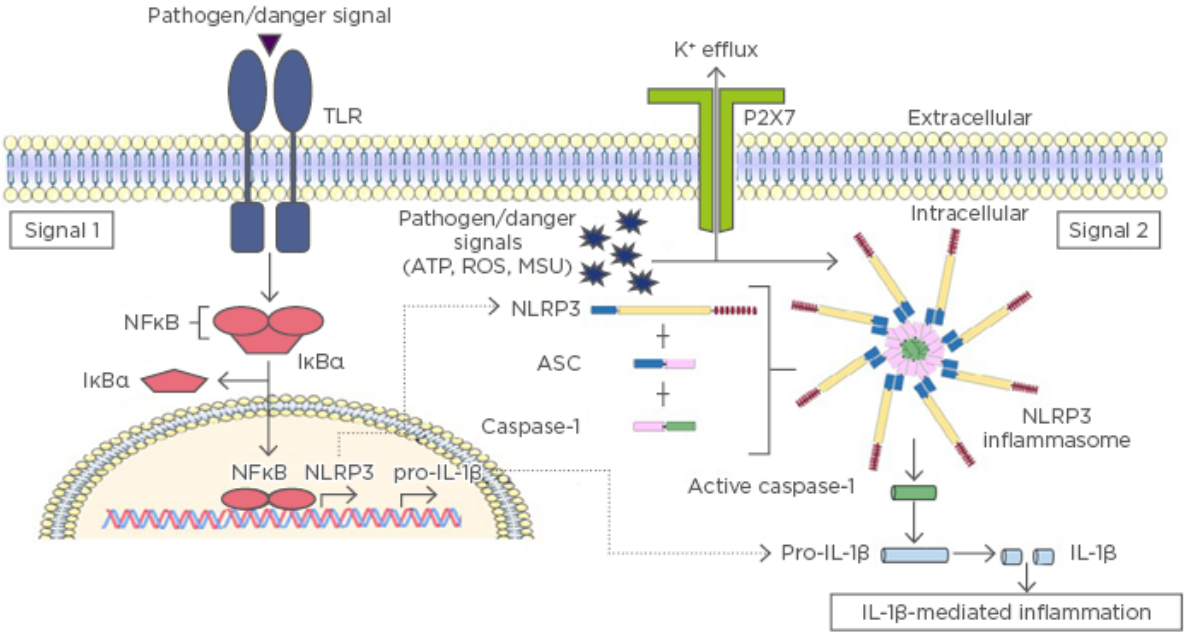

Figure 3. NLRP3 inflammasome activation requires two signals. *Signal 1 or priming is provided by PAMPS/DAMPS that leads to dimerization of TLR leading to initiation of transcription and translation of NLRP3 and pro-inflammatory cytokines by NF-kB signalling pathway. Signal 2 or activation is provided by numerous stimuli that induces K+ efflux and therefore activates NLRP3 inflammasome. NLRP3 inflammasome complex is formed by associating ASC and caspase-1 domains. Eventually, this leads to IL-1β mediated inflammasome. Figure is taken from* [45]

1.3.3 ASC Adaptor Protein

ASC (Apoptosis-associated speck like protein containing a CARD) or PYCARD (PYCARD human gene, located in 16p11.2)[46] plays a crucial role in both inflammation and cell death[47]. ASC is a central adaptor protein that contains two death domains (DD), C-terminal caspase recruitment domain CARD and N-terminal pyrin PYD domain connected by a linker. The PYD domain in ASC binds to other PYD domain in NLRP protein (PYD/PYD interaction) and ASC recruits caspase-1 via CARD/CARD interaction[47,48]. Normally ASC is localized in the nucleus of macrophages, but upon infection, ASC is re-localized to cytoplasm, ER, and mitochondria[49]. In macrophages, a supramolecular ASC complex called pyroptosome, mediator of pyroptosis, is formed[50]. ASC recruitment is absolutely necessary for NLRP3; failure to do so, results in no NLRP3 inflammasome complex. Mariathasan *et al.* showed that ASC-deficient mouse models had impaired IL-1β production and therefore a key mediator for caspase-1 activation[51].

1.3.4 Caspase-1

Caspases are part of the cysteine protease family that are involved in mediating programmed cell death through activation and implementation of cellular demise[7,52]. Caspase-1, also known as interleukin-1β (IL-1β) converting enzyme (ICE) regulated by NF-kB and, is responsible as innate immune response mediator[53,54]. After forming active dimers on inflammasome, caspase-1 processes inflammatory response by cleaving pro-IL-1β to mature IL-1β[7,52]. Caspase-1 is called the main mediator of inflammatory processes because caspase-1 activation results not only in rapid secretion of IL-1β but also pyroptosis[54]. Fink *et al.*, has shown that pyroptosis is dependent on caspase-1 stimulated nuclease activity for pore formation on plasma membrane during bacterial infection[55,56]. Recent studies have shown that human caspases 4,5, and 11 participate in non-canonical inflammasome signaling upon LPS recognition; these caspases interact with caspase 1, activate NLRP3 inflammasome, and lead to pyroptosis[5,57-59].

1.3.5 IL-1β

Known as a potent pro-inflammatory cytokines, Interleukin-1β (IL-1β), are produced mainly by monocytes and macrophages which are upregulated during infection and inflammation[5,60]. In its inactive form, pro-IL-1β is synthesized as 31 kDa in response to PAMPs or DAMPs and processed to its active 17 kDa form. As mentioned previously, pro-1L-1β expression is induced during the priming step and secreted as IL-1β after further activation. Cogswell *et al*., shows that IL-1β expression is regulated by NF-kB transcription factor and that only low levels are detectable before pro-inflammatory stimuli such as LPS[5,26,61]. The mechanism of how mature IL-1β is secreted after caspase-1 dependent processing are suggested with multiple mechanisms including lysosomal exocytosis, microvesicle shedding, plasma translocation and lytic release [62,63]. The secreted IL-1β increase accessibility of effector cells, activates vascular endothelium, initiate inflammatory responses such as fever to help eliminate infections, and help to synthesize acute-phase proteins in the liver[1,64].

1.4 Pyroptosis and Gasdermin D

Studies regarding pathogen induced cell death have demonstrated the importance of similar yet different cell death mechanisms. Unlike apoptosis where caspase 1 is not involved, pyroptosis is a lytic, caspase (1 or caspase 4/5/11) dependent programmed cell death that leads to cell swelling and cell membrane damage in response to infection or danger[5,65]. The burst of cell membrane results release of cytokines thereby attracting other immune cells to help and fight the infection[1]. Previously explained NLRP3, caspase-1 and ASC specks all contribute in the activation of pyroptosis. Although necroptosis is quite similar to pyroptosis with common feature of cell membrane rupture, the morphology and mechanism are different. Pyroptotic cells results in flattening of plasma membrane while necroptotic cells go through cell explosion[62,66]. While necroptosis is mediated by channel-forming MLKL (mixed lineage kinase domain-like oligomers) inducing influx of ions, pyroptosis is executed by pore-forming gasdermin-D (GSDMD) after caspase-1 or 11 cleavage that does not depend on osmolarity for disruption[62,66].

GSDMD, a substrate of caspase-1, are non-ion selective channel pores with dimension of 10-20nm[60,62,67,68]. GSDMD is cleaved into 31kDa N-terminus (GSDMD-Nterm) and 22kDa C-terminus (GSDMD-Cterm) by caspase-1 during inflammasome activation and is a necessary step for pyroptosis to occur (Figure 4)[62]. After cleavage, GSDMD-Nterm is translocated into the plasma membrane[66,67] while C-terminal is released to the aqueous environment[69]. Sborgi *et al.,* showed that N-terminal of GSDMD induces pore formation in liposomes by targeting the cellular membranes. They found that GSDMD-Nterm expression gave high level of LDH and that GSDMD-Nterm induced cell death gave phenotype associated with pyroptosis[67]. The evidence that IL-1β cytokines are exited into the extracellular space through GSDMD pores has been shown by Evavold *et al.* and that IL-1β cytokines are released in intact cells through GSDMD pores before lytic membrane rupture[69,70]. Recently, work by Taabazuing *et al*. revealed bidirectional crosstalk between apoptosis and pyroptosis in macrophages and monocytes[62,71]. Here they confirmed that GSDMD is the only substrate of caspase-1, for caspase-1 activated caspase-3/7 in the absence of GSDMD. Also, caspase-3 and-7 blocked pyroptosis by cleaving GSDMD to inactivate the protein. Interestingly, Orning *et al.* suggested that caspase-8, a controller of apoptotic cell death, could process IL-1β, cleave GSDMD and lead to pryoptosis [72,73].

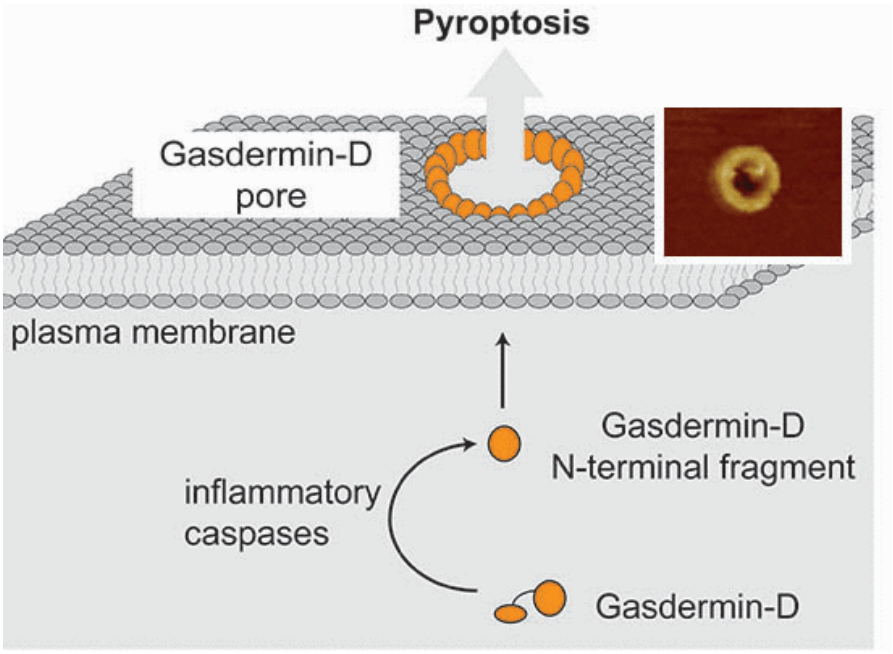

Figure 4. Formation of GSDMD pore during pyroptosis and visualization by atomic force microscopy. *Upon caspase-1 cleavage of GSDMD, the GSDMD-Nterm fragment is translocated into the plasmas membrane to form a giant pore leading to pyroptosis and release of IL-1β. Figure is taken from*[67].

1.5 Autophagy and ESCRT

Autophagy is part of homeostatic mechanism in eukaryotic cells where it degrades cytosolic components for cell survival[74-77]. Its main role is to remove damaged organelles such as mitochondira[74,76], kill intracellular pathogens[78], and supply energy and nutrients to the cell [75,76]. Autophagy is mediated by autophagsosome, which results from cystoplasmic cargo fusion with lysosome[74]. Recently studies proposed that proinflammatory cytokines IL-1β is secreted through secretory autophagy pathway where R-SNARE SEC22B and autophagy initiator ATG17 (FIP200 in mammalian gene)[79] are involved transporting autophagy cargo to the plasma membrane[80]. In addition, induction of autophagy seem to contribute to the enhancement of IL-1β production[76]. On the other hand, Ca2+ dependent endosomal sorting complex required for transport (ESCRT) complex has been linked with pyroptosis[81]. Upon plasma membrane excision, ESCRT with its accessory proteins result in membrane budding, shedding or patching for restoration[81-83]. Ruhl *et al*. found that some cells do not go into pyroptosis regardless inflammasome formation and that ESCRT machinery gets recruited upon GSDMD activation[81]. Apoptosis linked gene-2 (ALG2) and ALG2 interacting protein X (ALIX) are part of ESCRT[84-86]. Studies have found that these proteins are early indicators of ESCRT mediated membrane

repair and requirement for plasma membrane healing [82,83]. To understand more of these multiple mechanisms involved in the interplay between plasma membrane damage and inflammasome will give a deeper insight on studying host innate defense.

1.6 Clinical Relevance of Inflammasome

While NLRP3 plays an important role in fighting invader in innate immunity, its dysregulation causes various disorders such as inflammation, cancer and infection[75]. Gout is an inflammatory arthritis due to accumulation of monosodium urate (MSU) crystals, a crystallized form of uric acid that is released from dying cells[75,87]. Martinon *et al*., found that MSU crystals activate NLRP3 inflammasome resulting pro-inflammatory cytokine production[88]. This promotes neutrophil influx and aggregation into the joint fluid and develops neutrophil extracellular traps (NETs) that leads to abrupt pain attacks and eventually joint destruction[75,87-89]. To control and relieve the pain, therapies blocking the IL-1β maturation and pathway with caspase-1 inhibitor (VX-765)[90] and IL-1β inhibitor (canakinumab) are currently on development[89].

Remaining controversial in the field of cancer, increased concentration of IL-1β and involvement of NLRP3 have been found to promote tumor growth and metastasis in breast cancer models[91,92]. Guo *et al*. showed decrease level of tumor growth and metastasis in NLRP3 and caspase-1 KO mice after mammary tumor injection and proved low level of mature IL-1β in those knockout cell lines[91]. On the other hand, NLRP3 inflammasome seem to suppress metastasis of liver colon cancer[93] and in colitis-associated cancer[94]. The underlying theory whether inflammation contributes positively or negatively to tumor progression is still elusive, therefore further studies are necessary[92].

Mycobacterium tuberculosis (*Mtb*) bacteria is the cause of tuberculosis (TB) which causes chronic and deadly infectious disease worldwide[95,96]. When macrophages engulf *Mtb* for degradation, mycobacteria do not fuse with the lysosome for degradation, leading to phagosomal maturation arrest and this leads to persistent infection[97,98]. But when *Mtb* translocate to the cytosol to kill the host cell to replicate, NLRP3 is activated[99], and IL-1β secretion in response to *Mtb* by macrophages is important host cell defense[100,101]. Studies by Mayer Barber *et al*. show that knockout mice of IL-1β are prone to *Mtb* for they displayed acute mortality and high levels of bacterial load in the lungs[101]. However, caspase-1 and ASC

was not requirement for IL-1β production in *Mtb* for both KO mice since they did not show impairment in IL-1β production. Inhibition of host cell inflammasome response by *Mtb* has also been discovered[100,102]. Studies show that ZMP1 (Zn-metalloprotease) from *Mtb* blocks NLRP3 activation, ESX-1 system inhibits AIM-2 inflammasome, and that *Mtb* may limit NLRP3 activation[100,102,103]. This complex relationship between *Mtb* and inflammasome is still being investigated and, a tremendous amount of research is being conducted to elucidate this complex mechansim. To get a deeper understanding of host innate immune response in regards to *Mtb* infection and inflammasome disorders will accelerate drug and vaccine development.

2 Aim and objectives of the study

The overall aim of this project was to establish model systems using CRISPR/Cas9 technology in order to study *Mtb*-induced inflammasome activation. Studies have shown that NLRP3 is expressed in many inflammatory cells which are important in host defense response to PAMPs and DAMPs[1,4,10]. Since NLRP3 inflammasome complex is formed by oligomerization of caspase-1 and ASC[4,11], and secretion of IL-1β is mediated by GSDMD leading to pyroptosis[104], the usage of knockout cell lines are important tools on studying protein function and inflammasome activation mechanism. Our group's overall interest is towards the relationship between *Mtb*, ESCRT plasma membrane repair and inflammasome activation, and between secretory autophagy and inflammasome activation and IL-1β secretion during *Mtb* infection. Therefore, investigating how all these different routes interact and finding out their essentiality during inflammasome activation and/or Mtb infection is of our interest. Due to safety issues, work with virulent *Mtb* was restricted therefore sterile triggers and *Mtb* $mc^2$6206 auxotroph strain were used to study the model systems.

To achieve our goal, the specific objectives were:

- Establish a protocol to verify knockout cell lines using current genetic and molecular tools

- Establish stable knockout cell lines of GSDMD, NLRP3, ALIX, ALG2,FIP200 and SEC22B especially in ASC_mNG background

- Evaluate BLaER1 monocytes as an alternative model for inflammasome research

- Establish overexpressed GSDMD constructs with fluorescent mNG tag and FLAG epitope tag to study localization and cleavage of GSDMD

3 Theory

3.1 CRISPR/Cas9

Recently, the development of CRISPR/Cas gene editing technology has captured the world's attention. Unlike transcription activator-like effector nucleases (TALENs) and zinc-finger nucleaes (ZFNs) which are protein-guided cleavage methods, CRISPR/Cas is based on small RNAs which guides nucleases to the target DNA. The high efficiency, specificity and uniqueness of CRISPR/Cas have facilitated efficient genome editing in many cells and organisms. Currently, three types (1, 2, and 3) of CRISPR/Cas have been identified, among which type 2, Cas protein 9 (Cas9) is the one best characterized and most used in genetic engineering.

Originally CRISPR (Clustered Regulatory Interspaced Short Palindromic Repeats)/Cas9 system is an adaptive immunity of bacteria, *Streptococcus pyogenes*, to fight themselves from virus[105]. It is based on the insertion of short sequences of viral or plasmid DNA into the CRISPR region of bacterial genome. These inserted sequences are then transcribed to CRISPR RNAs (crRNAs) which hybridizes with trans-activating crRNA (tracrRNA). This crRNA and tracrRNA modules can be simply fused into a chimeric, single guide RNA (sgRNA) which forms a hairpin structure to dock onto Cas9 and recognizes ~20bp DNA "spacer" or "target" sequence. The sgRNA guides the endonuclease Cas9 to cleave the foreign double stranded DNA. It is important that in order for Cas9 to perform a double stranded break (DSB), the DNA target sequence must come right before protospacer adjacent motif at the 5' end (5′-NGG PAM).

Once double strand breaks by Cas9 in the specific target sequence, the post cleavage sites are repaired by cellular repair mechanism to complete the editing process. DNA repair can be achieved by these two repair mechanisms: non-homologous end joining (NHEJ) or homologous direct repair (HDR). In NHEJ, the DNA ends are rapidly re-ligated creating small insertions or deletions, called indels. This may either result premature stop codon, alteration in the promoter region, or interruption on exons leading to frameshift mutations. On the other hand, HDR allows exogenous donor template to repair the damage or generate precise modification on the target genome. Thus, with CRISPR/Cas9 genomic editing tool, production of knock-out and knock-in models can be achieved. (This section is based upon [106-108] unless otherwise stated).

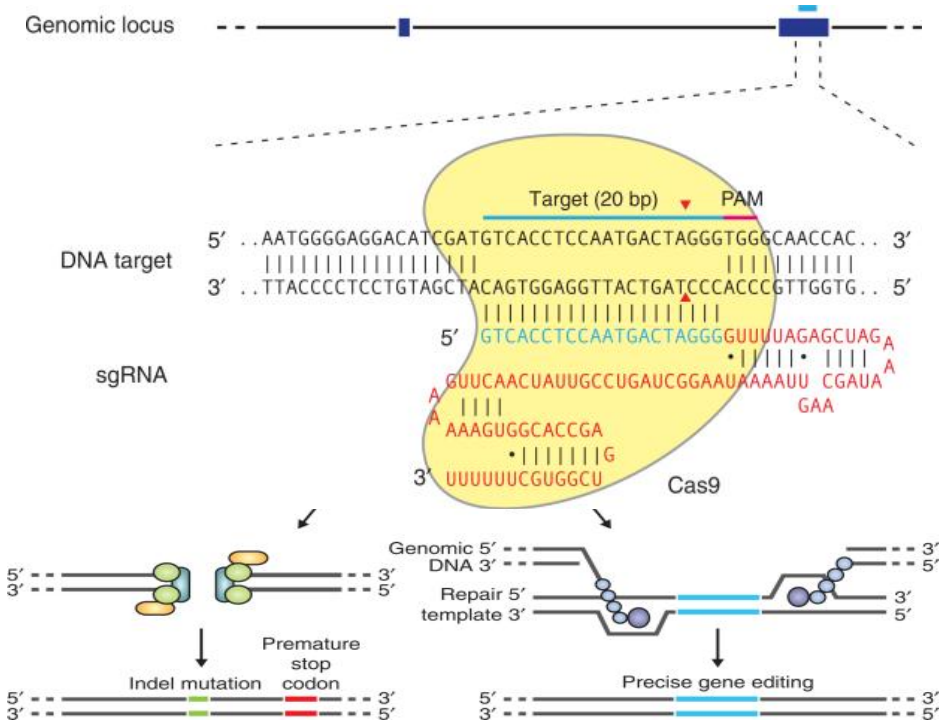

Figure 5. sgRNA guided Cas9 nuclease and DSB repair mechanisms. *Cas9 protein identifies the corresponding DNA sequence ~20bp upstream of PAM motif and initiates DSB. The cells can repair either by error-prone NHEJ where random indel mutation silences the targeted gene or by precise HDR editing where specifically designed template is introduced to the target "correcting" the damage. Figures modified and taken from*[106]

3.2 Genomic Cleavage Detection Kit Assay

The Geneart Genomic Cleavage Detection Kit (Thermofisher) is a method to detect specific genomic DNA cleavage in the locus. After CRISPR/Cas9 gene editing, insertions and deletions (indels) are created during the repair with NHEJ. The gene-specific double-strand break are PCR amplified, denatured and re-annealed so that the strand is regenerated with a re-annealed indel with a different indel or no indel. Next, these mismatches are cleaved and detected by detection enzyme, and the resultant bands can be seen on gel electrophoresis. The percent of cut bands calculated by cleaved efficiency equation estimates the percent of editing or indels. (This section is based upon [109]).

3.3 Western blot

Western blot or immunoblotting is a method widely used to identify specific proteins in cell extracts[110]. The protein mixtures are separated by size or molecular weight by gel electrophoresis. The gel is transferred to a membrane to produce a band and incubated with antibody probes to detect the target proteins. The membrane is washed off to remove the unbound antibody following membrane development to detect the antibody-bound protein of interest. The thickness or intensity of the band corresponds to the amount of protein present, and the bands are relatively quantified with housekeeping gene/ loading control[110].

3.4 GATEWAY cloning technology

Gateway cloning (Invitrogen)[111] (Figure 6) is a method that is based on the site specific recombination used by lambda bacteriophage to infect *Escherichia coli (E. coli)* bacteria. This mediates DNA fragments to shift between plasmids with the help from recombination enzymes and without changing the reading frame. Lambda bacteriophage and *E. coli* have specific recombination sites called *att*P and *att*B respectively. This recombination results in new recombination sites *att*L and *att*R that flank integrated lambda phage DNA. The *att* sites on gateway vectors can be modified so that desired DNA sequence can be easily cloned. After choosing the gene of interest, forward/reverse primers with *att*B1 and *att*B2 flanking sites are designed to amplify the gene. A donor vector is chosen with *att*P1 and *att*P2 sites with selectable markers and *ccdB* gene, a DNA gyrase poison which kills the cell. After transformation, all growing colonies on antibiotic selection are assumed to be successful gene integration since *ccdB* gene is removed. In this study, Gateway cloning method was used to create lentivectors containing GSDMD gene, and expression vectors with tagged mNG and FLAG for the use in THP1 cells. (This section is based upon [111]).

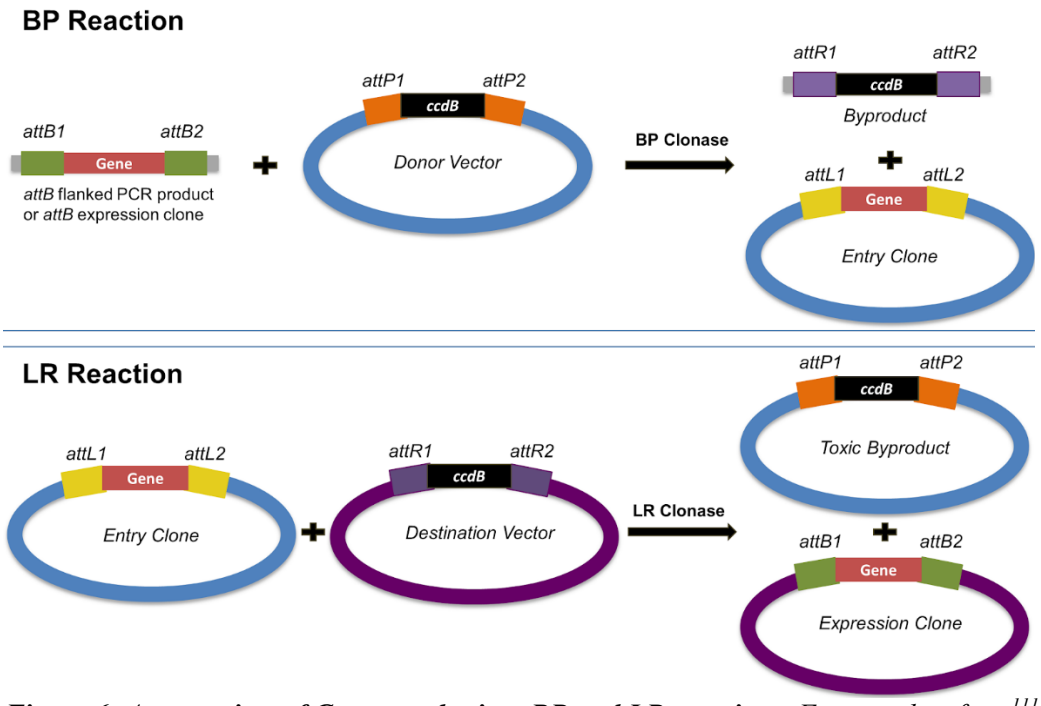

Figure 6. An overview of Gateway cloning, BP and LR reactions. *Figure taken from*[111]

3.5 PCR

Polymerase chain reaction (PCR) (Figure 7) is used to amplify the targeted sequence region with DNA polymerase. This is a very useful tool since very tiny amount of DNA could be replicated over and over again for a high yield[112].

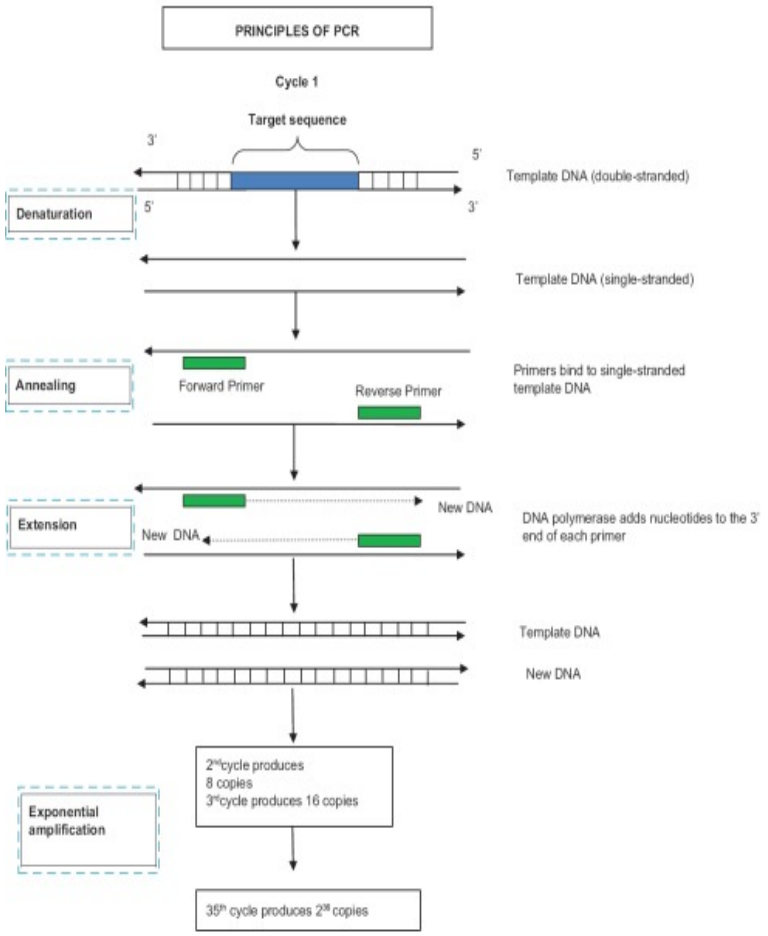

Figure 7. Principles of PCR[112]. *In PCR, the cycle begins by heating the reaction to 94~98°C to denature the double strand DNA by breaking the hydrogen bonds. Next in the annealing process, the temperature is lowered to 50~65°C for the primers to bind to the complementary single-stranded DNA template. The temperature is raised again for the thermostable Taq polymerase to add nucleotides to the 3' ends of each primers. This extension step gives two strands of target DNA is formed. Denaturation, annealing, and extension steps are repeated up to 20~40 cycles to produce trillion copies of DNA molecule. Lastly, the temperature is lowered to 4~12°C to keep the products for short term storage. Figure taken from[112]*

3.6 LDH Cytotoxicity Colorimetric Assay

Lactate dehydrogenase (LDH), a cytoplasmic enzyme, is released from the cell upon cell death due to plasma membrane damage. The level of LDH activity is measured with an enzymatic colorimetric reaction that gives red color. First, there is catalytic conversion of lactic acid to pyruvic acid due to reduction of NAD+ to NADH/H+. Then, an enzymatic reaction converts INT (iodonitrotetrazolium or tetrazolium salt) to formazan by diaphorase. The amount of color that is produced is proportional to the amount of damaged or dead cells.[113,114]

3.7 ELISA (Sandwich)

Enzyme linked immunosorbent assay (ELISA) is an immunological assay that is used to detect and quantify proteins, antibodies and hormones. In this study, sandwich ELISA assay was used to measure natural human interleukin Il-1β. Sandwich ELISA uses two layers of antibodies (capture and detection antibody) to measure the analyte. First, the wells of the plate is coated with primary capture antibody which allows the protein of interest (IL-1β) to bind. When the protein becomes bound to the wells, enzyme-linked secondary detection antibody is added and washed away to remove unbound proteins. Lastly, horse radish peroxidase (HRP) substrate is added and converted by enzyme to produce chromogenic (yellow) signals if the target protein is present. The signal is detected with spectrophotometer and the results are compared to a standard curve to measure the concentrations. [115]

4 Method

4.1 Cell culture

4.1.1 THP-1

THP-1(human leukemic monocytic cell line) purchased from ATCC was cultured in Roswell Park Memorial Institute (RPMI-1640) medium (Sigma) supplemented with 10% Fetal Calf Serum (FCS, Gibco, Life Technologies), L-glutamine (Sigma). 10mM Hepes (Gibco), and 1% PenStrep (100 U/mL Penicilium and 100 µg/mL Streptomycin from Sigma) Cell lines were incubated in T25 and T75 flasks (NUNC) at *37°C 5% CO_2*. Cells were split into 200,000 cells/ml twice a week. Some of the cells lines were differentiated into macrophage like cells using 100 ng/ml PMA (Sigma) for 48-72 hours (NUNC 6-well plate 750,000 cells/ml in 2 ml total volume/well, NUNC 96-well plate 300,000 cells/ml in 100 µl total volume /well). The medium was changed to fresh complete RPMI medium (without PMA) after 72 hours and left one day to rest before proceeding with experiments.

4.1.2 HEK293T

HEK293T (human embryonic kidney 293 with SV40 T antigen) from (ATCC) was grown in a complete Dulbecco's Modified Eagle's Medium (DMEM from BioWhittaker) with 10% FCS and 100nM PenStrep in T75 flask. To split HEK cells, the culture medium was removed, and the cells were washed with 10 ml Dulbecco's Phosphate Buffered Saline (PBS, Sigma). 3 ml of Trypsin/EDTA (Sigma) was added and incubated for 3 minutes. Next, 17 ml of fresh DMEM medium was added and dispersed by pipetting up and down. The cells were transferred to 50 ml falcon tube and spun down for 6 minutes 1.1x1000 rpm, and after resuspended in fresh DMEM medium, 1 ml of resuspended cell culture and 7 ml of fresh DMEM media were transferred to new T75 flasks and placed in *37°C 5% CO_2* incubator. Generally the cells were split twice a week, when the cells reached ~80% confluency.

4.1.3 BLaER1

BLaER1 cell lines (based on RCH-ACV line) are suspension cells originating from B cell precursor leukemia[116]. These cell lines (single-cloned) were produced and provided by Dr. Holger Heine's lab in Research Center Borstel, Leibniz Lung Center, Borstel, Germany. The

cell lines were cultured in fresh complete RPMI medium and split every 2-3 days to maintain the cell density at 1-2x10^6 cells/ml.

BLaER1 transdifferentiation took 7 days and the protocol was followed from Hornung *et al*. "Modeling Primary Human Monocytes with the Trans-differentiation Cell Line BLaER1"[117]. On Day 0, the cell lines were treated with fresh complete RPMI medium that contained 10 ng/ml rh IL-3, rh M-CSF 10ng/ml (Peprotech), and 100 nM beta-Estradiol E2 (Sigma-Aldrich)) for trans-differentiation. 70,000 cells/ml undifferentiated BLaER1 cells were spun down at 400 x *g* 5 minutes and resuspended in 100 µl differentiation medium and seeded into flat 96-well plate. On Day 2 and 5, half of the medium was changed to fresh medium with IL-3, M-CSF and beta-Estradiol. On Day 7, BLaER1 monocytes became adherent and ready to be used for functional assays.

4.1.4 Freezing the cells

All the knockout cell lines were cryopreserved in 2 ml cryovials. In 500 µl of 2x10^6 cells/ml diluted in fresh RPMI medium, 500 µl Freezing media (complete RPMI + 20% FCS + 10% Dimethyl sulfoxide DMSO (Sigma)) was added drop by drop. The vials were frozen in an isopropanol chamber at -80°C and transferred to liquid nitrogen the next day.

4.2. CRISPR sgRNA cloning

The target sequence cloning protocol from CEMIR, Systems Inflammation Group SOP_003 v1.1 was followed to perform cloning of sgRNA oligos into plasmid.

4.2.1 CRISPR sgRNAs design

The main purpose of using CRISPR/Cas9 technology was to knockout GSDMD, FIP200, SEC22B, PDCD6, ALIX and NLRP3 genes in THP-1 cells. The targets of sgRNA were designed based on the genome sequences of these genes using Genetic Perturbation Platform Web Portal from Broad Institute (https://portals.broadinstitute.org/gpp/public/analysis-tools/sgrna-design)[118]. The desired CRISPR enzyme *S. pyogenes* (NGG PAM) and target genome *Human GRCh38* were selected. The most suitable two sgRNAs were chosen for each genomic target region by the highest on-target scoring ("Rule Set 2" method, Doench, fusi *et al*[119]), off target scoring, and target cut length %. The sgRNA oligos with suitable overhangs

and the corresponding primers were designed with the help of my supervisor K. S. Beckwith. The oligonucleotides were ordered from Sigma Aldrich and diluted to appropriate stock and working solutions. See Appendix I for the list of sgRNAs and primers used in this study.

4.2.2 Preparation of plasmid

The lentiviral plasmid LentiCRISPR_v2 (AddGene-52961/sig_P_016) glycerol stock was provided by CEMIR. A small amount was scraped off with 10µl pipette tip and inoculated in 5ml LB media (10g NaCl (EMSURE),10g Tryptone (OXOID), 5g yeast extract (OXOID), distilled water up to 1000ml) and 100µg/ml ampicillin overnight in shaker incubator (300rpm) at 30°C. Next day. The inoculated bacterial plasmid was isolated using PureYield Plasmid Miniprep Start-up (Promega) Kit. The DNA concentration was measured by NanoDrop.

4.2.3 Gel-based purification of LentiCRISPR_V2 to prepare backbone

The LentiCRISPR_v2 plasmids were digested by BsmbI restriction enzyme (5µg lenticrispr_v2, 2µl BsmbI (NEB), 5µl NEB 2.1 buffer, MQ water up to total volume of 50µl) which were incubated at 55°C for 1 hour and additional heat inactivation for 20 minutes at 80°C. Next, incubation with 5.5µl of Antarctic phosphatase buffer and 1µl Antarctic phosphatase proceeded for 30 minutes at 37°C. To confirm if the digestion was successful, the entire sample (50µl sample, 8ul of 6x loading dye per sample) was ran in agarose gel electrophoresis (40µl 0.7% agarose gel in 1X TAE buffer, 4µl GelGreen dye) for 30 minutes at 100V. This gave two bands, and the upper band was purified using the Monarch DNA gel extraction kit. Total volume of 10ul of vector backbone was eluted.

4.2.4 Annealing of sgRNA pair

Each pair of sgRNAs were phosphorylated, ligated, and annealed (1 µl of forward_sgRNA 100µM, 1µl of reverse_sgRNA, 1 µl 10x T4 ligation buffer, 0.5µl T4 PNK (polynucleotide kinase), MQ water 6.5 µl) using a thermocycler with the settings below:

Thermocycler conditions for annealing sgRNA pair	
37°C	30 minutes
95°C	5 minutes
Ramp down	5°C/minutes
25°C	∞

4.2.5 Ligation of annealed sgRNA with LentiCRISPR_V2 backbone

After sgRNA pair annealing, sgRNA oligos were ligated into the plasmid (Vector backbone 50ng, 1 ul of 1:100 diluted annealed sgRNA, 1µl 10x T4 ligation buffer, 1µl T4 ligase, MQ water up to total volume of 10µl). One vial with MQ water (instead of sgRNA) was included as a negative control. The reaction was incubated overnight at 16°C in cold room.

4.2.6 Transformation

Transformation is the process where a genetic material is introduced and taken up by bacteria. In this study, heat shock transformation was mainly used. A sudden increase in temperature creates pores in the bacterial plasma membrane allowing exogenous DNA to enter the bacterial cell. After transformation, bacteria were plated on agar plates with antibiotic for selection. Plasmids contain antibiotic resistance gene, therefore bacteria without plasmid will not survive.

Heat shock competent *E.coli* DH5alpha cells were thawed on ice for 20~30 minutes on ice. 1ul of plasmid from the ligation reaction was gently mixed into 50µl of competent cells and left on ice for 30 minutes. Next, the samples were heat shocked for 45 seconds at 42°C and back on ice for two minutes. 200µl of SOC media (without antibody) was added and grown in 30°C shaker incubator (300rpm) for 1 hour. 100 ul of the product was plated on carbenicillin agar plates at 30°C overnight. Next day, the plates were checked for the colony growth, and two single colonies from each plate were picked and inoculated on falcon tube containing 5ml LB media and 5µl of 100µg/ml ampicillin. The reaction was incubated on 30°C shaker incubator (300rpm) overnight.

4.2.7 Isolation of plasmids

Prior to plasmid isolation, glycerol stocks (100µl of 85% glycerol and 450µl of overnight inoculated culture) were made in cryovial to preserve the CRISPR oligos and kept in -80°C. Next, the remaining plasmids were purified following the manual instruction on QIAprep Spin Miniprep Kit (Qiagen), and DNA concentration was measured with NanoDrop. The plasmid samples were stored at -20°C.

4.2.8 Sequencing

The isolated CRISPR oligo plasmids were verified by Sanger sequencing at GATC Biotech in Germany. Each sample was diluted to a concentration of 100ng/µl with MQ water (5µl total) and mixed with 5µl of 5µM U6_CRISPR_Seq3 primer (GACTATCATATGCTTACCGT).

4.3 Lentivirus production

Lentiviruses, such as human immunodeficiency virus (HIV), are able to deliver and replicate their genes into either dividing or non-dividing mammalian cells. Therefore, they are an efficient gene delivery tool for cell transfection and transduction. After transfection of HEK 293T cells the supernatants, containing lentiviral recombinant vectors, are used to transduce the target cells. Once the vectors are in the target cells, reverse transcription of viral RNA occurs and the viral DNA gets integrated in to the host genome.[120,121]

4.3.1 HEK293T cell preparation

The day before transfection, 250,000 HEK 293T cells/ml were plated in 6-well plate, total volume of 2ml in DMEM growth medium (with L-Glutamine, FCS,P/S) per well. Next day, the cells were checked under the light microscope to make sure the cell confluency was 50~80% for transfection.

4.3.2 Transfection

Day 1

For transfection, a total of 1µg DNA was used. In a sterile 1.5ml eppendorf tube, 2µl of jetprime packaging mix (home-made: mix of a 3rd generation lentivirus packaging system, consisting of pRSV-Rev, pMDLg/pRRE and pMD2.G at 500ng/µL), 1µg of DNA, and 200µl of jetprime

buffer (Polyplus) were added together, vortexed for ten seconds and shortly spun down. 4µl of jet prime buffer was added, then vortexed and shortly spun down again. The samples were incubated at room temperature for ten minutes. The entire ~250µl volume of transfection reagent/DNA mixture was evenly distributed dropwise into 293T cells. *It is important to gently rock the dish and not swirl!* The cells were incubated overnight at *37℃ 5% CO_2.*

Day2

The transfection mixture was removed and replaced with new DMEM medium (with only L.glutamine, FCS). Incubated overnight at *37℃ 5% CO_2.*

Day3

The supernatants were harvested in 15ml tube with a syringe (size) and 0.45µM sterile filter (approximately total volume of 1.5ml). 1.5µl of 1000xPB and 1.5µl of F108 were added to the supernatants and mixed carefully by rolling the tube.

1ml (800,000 ~ 1,000,000 cells/ml) of target THP-1 cells were transferred to a screwed 1.5ml eppendorf tubes and spun down for 5minutes at 4°C 0.3x1000 rcf . After centrifugation, the supernatants were removed. 1ml of filtered supernatants were directly added to the target cell pellets and carefully resuspended. Next, the cells were spinoculated for 90 minutes at 32°C 1.2x1000 rcf. After spinoculation, the cells were carefully resuspended and transferred to 24-well plate for overnight incubation at *37℃ 5% CO_2.*

Day4

The cells were collected in 1.5ml screwed eppendorf tubes and spun down for 5min at 4°C 0.3x1000rcf. The supernatants were discarded and resuspended in 2ml RPMI medium in 6 well-plate (with FCS, L.glutamine, HEPES, P/S). Appropriate antibiotic (1µg/ml puromycin for CRISPR) was added for antibody selection. The cells were incubated overnight at *37℃ 5% CO_2.*

Day6~8

After 48 hours post- transduction, the cells were expanded in T25 flasks for further growth (still in antibiotic selection) and monitored for dead cells. Once the cells were normally growing, the KO cells were analyzed with appropriate analytical assays.

4.4 Gateway cloning

4.4.1 Gateway cloning primer design and PCR amplification

The forward and reverse primers with *att*B1 and *att*B2 sites were designed with the help from my supervisor, K.S. Beckwith using the Snapgene software and following the Multisite Gateway Pro manual. The F/R primers and gene sequences are provided in Appendix I.The length of the primers were designed with optimal annealing temperature, GC content, and stability to amplify the gene of interest. The stock primer was diluted into 100 µM in RNase-free water and to a working primer concentration, 10µM (10µl of primer stock solution and 90µl RNase-free water).

For Gateway cloning, Q5 Highfidelity 2X MasterMix kit (New England BioLabs NEB) was used to amplify the gene of interest from the original plasmids with *att*B1 and *att*B2 flanking sites.

4.4.2 Generation of entry clone (BP reaction)

BP reaction is catalyzed by BP Clonase 2 Enzyme Mix 2 (Invitrogen) that swaps *att*B site containing the DNA with *att*P site containing donor vector. This generates an entry vector with *att*L1 and *att*L2 sites, and by-product *ccdB* gene with attR1 and attR2 flanking sites.

Suitable *att*B primers were designed and *att*B-PCR products (Appendix I) were synthesized for recombination with the donor vector (pDONOR™ 221, Thermo Fisher) to generate the entry clone. The reagents of BP reaction are listed on Table 1 and the protocol was followed from Multisite Gateway Pro BP recombination reaction.

Table1. Gateway BP reaction reagents

Component	Amount (5µl reaction)	Final concentration
*att*B PCR product	1µl	8ng/500bp, 12.5ng/750bp, 16ng/1000bp
pDONR221 (donor vector)	1µl	100ng/µl
BP clonase 2 enzyme mix	1µl	
TE buffer	2µl	

After terminating the reaction by adding 0.5 µl Proteinase K. solution (Invitrogen), 1µl of entry vector reaction was heat-shock transformed in competent DH5 alpha *E. coli* strain (provided by CEMIR) and plated on 50 µg/ml kanamycin agar plate for selection. The plates were incubated at *37°C 5% CO_2* for 16~24 hours. The entry clone DNA was purified using Pureyield ™ Plasmid Miniprep System kit, and the DNA concentration was measured with NanoDrop.

4.4.3 Generation of expression clone (LR reaction)

In LR reaction, recombination of *att*L sites from the entry clone and *att*R sites from the destination vector produce the expression vectors, flanked by *att*B sites. The protocol was followed from Multisite Gateway Pro LR recombination reaction using the substrates (Table 2.) in Gateway LR Clonase Enzyme Mix 2 (Invitrogen) to perform the recombination. Destination vector pLex_307 Addgene (see Appendix II) was used to make expression clone. After terminating the LR reaction with 0.5µl Protein K. solution, the ligation reaction was proceeded for transformation in DH5 alpha *E. coli* cells and grown on ampicillin 100 µg/ml agar plates for selection. The plates were incubated at *37°C 5% CO_2* for 16~24 hours. Next, DNA purification was done with Qiagen Plasmid Midi Kit and DNA concentration was measured with NanoDrop.

Table2. Gateway LR reaction reagents

Component	Amount (5µl reaction)	Final concentration
Entry vectors	0.5µl each	100ng/µl
Destination vector	1µl	100ng/µl
LR clonase 2 enzyme mix	1µl	
TE buffer	2.5 µl	

4.4.4 Restriction enzyme digestion

To confirm the presence of the genes, the entry vector was digested using FastDigest™ (ThermoFisher) buffer and MIuI enzyme, and expression vector was digested using TimeSaver™ (New England Biolabs) buffer and restriction enzyme BsrGI. Reagents on Table 3 were prepared in 1.5 ml eppendorf tube:

Table3. Reagents for restriction digest

Component	Sample (10µl reaction)
10X FastDigest™ buffer/ NEB™ buffer 3.1	1µl
Restriction enzyme (FastDigest MIuI/NEB BsrGI)	0.5 µl
DNA plasmid	~20 ng
RNase free water	Up to 10 µl

*The enzyme was kept on ice.

After thawing the buffer at room temperature, all the components were mixed together, vortexed and shortly spun. The mixture was incubated for 5-10 minutes at 37°C, and heat inactivated for ~10minutes at 80°C. The 10 µl sample was loaded on to 1% gel electrophoresis, as previously described.

The correct entry vector gave 2 bands (one at 932bp and 1600bp+insert size). And if the expression vector gave correct bands (one band for insert and one band for remaining vector), the expression vector plasmid was proceeded for transfection.

4.4.5 Sequencing pEntry plasmids

To ensure that the constructs were properly inserted, the entry plasmids were sent for sequencing to GATC, Germany. The plasmid sample was sent using 5µl M13Forward sequencing primer (ThermoFisher) (5pmol diluted in RNase free water) and 5µl of plasmid (concentration of 100ng/µl diluted in RNase free water). An additional tube with 5µl M13Reverse sequencing primer (Thermofisher) with the same plasmid was sent if the insert was over 1000bp. The obtained data was analyzed with Snapgene with the help from my supervisor.

4.4.6 GoTaq Green Colony PCR

In addition to sequencing, bacteria colony GoTaq Green MasterMix PCR (Promega) was performed for pEntry vectors from BP reaction and expression plasmids from LR reaction to see either presence or absence of insert in DNA plasmid. This protocol is a quick screening method where colonies are picked and used directly in the PCR reaction to determine the insert size. The reaction set up is shown above (PCR section).

4.5 Gel electrophoresis

Agarose gel electrophoresis is a method to separate, identify, and purify the DNA according to molecular size. The gel was prepared by dissolving appropriate concentration of agarose powder in 1X TAE (Tris-Acetate Electrophoresis) buffer (Sigma). In this study, 0.7%, 1%,2% agarose (SeaKem) was prepared to run gel electrophoresis. The mixture was heated up and boiled until the solution was clear. 1:10 dilution of GelRed or GelGreen (Biotium) solution was mixed with the agarose solution and left to dry for the wells to form. Next the DNA samples (mixed with 6X loading dye ThermoFisher) and 1 kb DNA ladder (ThermoScientific Appendix XIII) were loaded into the wells and ran in 100V for 30 minutes. The bands were visualized by High Performance UV-transmitter (UVP) and captured by Gel Logic 212 Pro (Carestream).

For purifying PCR products, entire PCR product (25 or 50µl) was loaded with 6X loading dye on 40 ml 0.7% agarose gel with GelGreen. The gel was visualized on blue light transilluminator and the bands were cut and purified with Monarch DNA Gel Extraction Kit (NewEngland Biolabs).

4.6 PCR

For this study, PCR was used to amplify genes for gateway cloning, cleavage kit assay and CRISPR cloning. Also, colony PCR was performed to verify the inserts in the transformed bacterial colonies.

Table 4. Thermocycling conditions for Q5 High-Fidelity 2X Mastermix PCR:

Stage	**Temp.**	**Time**	
Enzyme activation	98°C	30 seconds	
Denature Anneal Extend	98°C 50-72°C 72°C	5-10 seconds 10-30 seconds 20-30 seconds/kb	25 cycles
Final extension	72°C	2 minutes	
Hold	4-10°C	∞	

*The annealing temperature was adjusted with NEB ™ Calculator based on the primers used.
*The extension time was adjusted based on the size of templates.

Table 5. Reaction setup for Q5 High-Fidelity 2X Mastermix (NEB) PCR:

Component	Sample (25ul reaction)	Final concentration
Q5 High-Fidelity 2X Master Mix	12.5µl	1X
10µM Forward Primer	1.25µl	0.5µM
10µM Reverse Primer	1.25µl	0.5µM
DNA Template	1-4µl	< 1000 ng
RNase free water	up to 25µl	

*The DNA concentration was measured with Nanodrop.

Table 6. Thermocycling conditions for GoTaq-green analysis/colony PCR:

Stage	Temp.	Time	
Enzyme activation	95°C	2 minutes	
Denature Anneal Extend	98°C ~55°C 72°C	45 seconds 45 seconds 1 minute/kb	15 cycles
Final extension	72°C	3 minutes	
Hold	4-10°C	∞	

*The annealing temperature was adjusted to 50C for pEntry vector and 55C for pExpr vector.

Table 7. Reaction setup for GoTaq-green analysis/colony PCR:

Component	Sample (10ul reaction)
GoTaqGreen 2X MasterMix (Promega)	5µl
10µM Forward Primer	0.5 µl
10µM Reverse Primer	0.5 µl
DNA Template (1ng/µl)	1 µl
RNase free water	3µl

*The DNA concentration was measured with Nanodrop.

*For colony PCR, 1µl of DNA template was replaced by picking a small part of colony.

* M13F/R primers were used for pEntry vectors and attB1/2 universal primers for pExp vectors.

Table 8. Thermocycling conditions for Cleavage kit assay PCR:

Stage	Temp.	Time	
Enzyme activation	95°C	10 minutes	
Denature Anneal Extend	95°C 55°C 72°C	30 seconds 30 seconds 30 seconds/kb	40 cycles
Final extension	72°C	7 minutes	
Hold	4°C	∞	

*The annealing temperature was adjusted based on the primers used.

Table 9. Reaction setup for Cleavage kit assay PCR:

Component	Sample (50µl reaction)	Control
Cell lysate	2 µl	
10µM Forward Primer	0.5 µl	
10µM Reverse Primer	0.5 µl	
Control template & primers		1 µl
Q5 High-Fidelity 2X Master Mix	25µl	25µl
RNase free water	22 µl	24µl

*AmpliTaqGcold 360 Master Mix (Thermofisher) was used for GSDMD knockout reaction.

4.7 Cleavage assay kit

The PCR primers were designed following the recommended PCR design guidelines from the kit's protocol. All the reagents were provided in the kit.

4.7.1 Cell lysis and DNA extraction

50,000 and no more than 2 million cells/ml (kit recommendation) were spun down at 1.5 x 1000 rpm for 5 minutes at 4°C and the supernantants were removed. 50 µl Cell Lysis Buffer and 2µl Protein Degrader was mixed in a eppendorf tube, and 50 µl of Cell Lysis Buffer/Protein Degrader was mixed to each cell pellets. Next, the mixture was transferred to a PCR tube and the following program was run on thermal cycler:

Temp.	Time
68°C	15 minutes
95°C	10 minutes
4°C	∞

*The cells were stored at -20°C if not immediately proceeded to the next step, PCR amplification.

4.7.2 PCR amplification

The cell lysates were briefly vortex and PCR components were added. See Table 8 and 9. for the ingredients and parameters. After PCR amplification, 3 µl PCR product was mixed with 10 µl Water (RNase free) and 2 µl 6x loading dye to be run by 1% gel electrophoresis for 30 minutes at 100V. The gel was viewed using UV transilluminator. The cells were stored at -20°C if not immediately proceeded to the next step, Denaturation and Reannealing.

4.7.3 Denaturation and reannealing

In this step, PCR fragments are randomly annealed with or/and without indels. 1 µl of PCR products, 1 µl 10X Detection Reaction Buffer, 7 µl Water was mixed into a new PCR tube (duplicate was made for each samples as negative controls). The mixture was briefly spun to eradicate the bubbles, and was run on thermal cycler with the following program:

Temp.	Temp/Time
95°C	5 minutes
95°C-85°C	-2°C/sec
85°C-25°C	-0.1°C/sec
4°C	∞

*The cells were stored at -20°C if not immediately proceeded to the next step, Enzyme Digestion.

4.7.4 Enzyme digestion

In this step, the heteroduplex DNA with indels is cleaved by the detection enzyme. 1 µl Detection Enzyme was added to all samples and 1µl Water was added to all negative control samples. The mixture was briefly vorted and incubated at 37°C for one hour. After the incubation, the cells were vortexed quick and spun down. The entire 10 µl sample was mixed

with 10 µl Water and 2 µl 6X loading dye and was run on 1% gel electrophoresis for 30 minutes 100V. The gel was viewed using UV transilluminator.

4.7.5 Cleavage efficiency formula

The histogram of band intensity of PCR products was measured using ImageJ software.

1) Cleavage Modification Efficiency = 1- (1-fraction cleaved)
2) Fraction Cleaved= Sum of intensity of cleaved bands/ (cleaved bands + parental band intensities)

4.8 EVOS FL auto 2 Cell Imaging System

EVOS (Life Technologies) epifluorescence microscopy is a high-performance automated imaging that can be used for time-lapse live-cell imaging, image tiling and Z stacking. EVOS was used to check for the presence of live cells, dead cells, and ASC specks. Prior to fluorescence imaging, the cells were stained with DRAQ7 (Far-Red fluorescent live-cell impermeant DNA dye BIoLegend) diluted 1:1000 in complete RPMI medium. The GFP excitation was 470/22 and emission at 510/42. CY5/DRAQ7 at 628/40 and emission at 692/40. The objective used was Plan Fluor 10x LWD PH.

4.9 LDH

300,000 cell/ml were resuspended in fresh RPMI medium and 100µl of cell suspension (~ 30,000 cell/per well) was seeded in round bottom (or flat bottom for PMA differentiated cells) 96-well plate. 2-3 replicates were prepared for each sample including positive control with 0.1% Triton X-100 and negative control cultures only in medium.

4.9.1 LPS + Nigericin treatment

1 µg/ml or (10ng/ml for PMA differentiated cells) EB UB LPS (Invivogen) was added into the wells and incubated for 2-4 hours at *37℃ 5% CO_2*. 5µg/ml nigericin (Invivogen) was added to each LPS-primed wells and was left for 1 hour at *37℃ 5% CO_2*. Next, the plate was put on ice to stop the reaction.

4.9.2 M. tuberculosis treatment

M. tuberculosis mc^{2}6206 (BL2-certified *Mtb* auxotroph strains) was provided by CEMIR and prepared by Ragnhild Sætra. The bacteria were diluted to optical density (OD) 0.01-0.02 in RPMI medium containing HEPES, L-glutamine, and 10% human serum A+. 100µl of diluted bacteria was added into the wells and incubated for 30-45 minutes at *37℃ 5% CO_2*. The cells were washed once with 100 µl Hank's Balanced Salt Solution buffer (Sigma). Next, fresh 100µl RPMI media with DRAQ7 was added to the wells and incubated overnight at *37℃ 5% CO_2*.

After treating the cells with stimuli, 0.1% Triton X-100 (Sigma) was added to the positive control wells and carefully pipetted up and down. The cells were spun down in plate centrifuge for 3 minutes at 1000*g*. The supernatants were harvested, and 30 µl of supernatants were transferred to new flat bottom 96-well plate (the remaining supernatants were frozen in -20°C for IL-1β ELISA analysis).

LDH reagents, Solution A and B, (Takara) were thawed and mixed according to the Takara LDH Cytotoxicity Detection Kit protocol (for one 96-well plate, 3.5ml of solution B was mixed with 77.8µl solution A). 30 µl of mixed LDH reagents was carefully mixed with 30 µl of supernatants in the flat bottom 96-well plate. The plate was mixed carefully by rotating and tilting. The plate was incubated for 30 minutes at room temperature covered in aluminum foil. The reaction was measured on plate reader at 490 nm and the cell death % was calculated by ((positive control-negative control/treated control-negative control) *100)

4.10 ELISA

Detection of human IL-1β secretion was done by using reagents in the DuoSet ELISA Development System Human IL-1β /IL-1F2 (R&D Systems) kit and following the manufacture's protocol.

The 96-well ELISA plate was incubated with 50 µl of 4 µg/ml Human IL-1β Capture Antibody (diluted in Reagent Diluent: 1%BSA in PBS) overnight at room temperature, sealed with a plastic cover. Next day, the plate was automatically aspirated and washed (total of three washes x2) by BioRad iMark microplate washer. The plate was blocked by adding 150µl of Reagent

Diluent and incubated for one hour at room temperature. The plate was automatically aspirated and washed (total of three washes x2). Next, 50µl of samples (supernatants from experiments described above LDH assay), diluted 1:10 in Reagent Diluent, was added at incubated for two hours at room temperature. The plate was washed again, and 50µl of 150ng/ml Human IL-1β Detection Antibody was added and incubated for two hours room temperature. After another aspiration/wash, 50µl of Streptavidin-HRP R&D system (diluted 1:40 in Reagent Diluent) was added, incubated for 20 minutes in the dark. The plate was aspirated and washed (total of three washes x2). 50µl of TMB-Substrate Solution (Biolegend) was added, incubated in the dark for 20 minutes at room temperature. Lastly, 25µl of Stop Solution (2NH2SO4) was added to stop the reaction. In order to quantify the amount of IL-1β cytokines, the absorbance was measured at 450nm with the plate reader.

4.11 Western blot

4.11.1 Cell lysis (suspension cell protein extraction)

200,000 cells/ml were spun down for 6 minutes 1500rpm. Washed with 1ml ice-cold PBS and spun down again. The supernatants were removed and 150µl of ice-cold lysis buffer was added. The cells were incubated on ice for 15 minutes, vortexed every 5 minutes. Next, the cells were centrifuged for 15 minutes, 4°C, 10 000rpm. The supernatants were transferred to a new eppendorf tube and lysates were stored at -20°C.

4.11.2 Cell lysis (adherent cell protein extraction-6 well plate)

The adherent cells were washed with 1ml ice-cold PBS and incubated with 150µl ice-cold cell lysis buffer for 15 minutes on ice. Next, a cell scraper was used to dislodge the cells and the mixture was pipetted around five times before transferring to an eppendorf tube. The cell mixture was vortexed and incubated on ice for 5 minutes. Centrifuged for 15 minutes ,4°C,10 000 rpm. The supernatants were transferred to a new eppendorf tube and lysates were stored at -20°C.

The recipe for lysis buffers:

1 X NP40 buffer: 100nM Tris/HCL pH 8.0 (Sigma), 300nM NaCl (Gibco), 0.5M EDTA pH 8.0 (Sigma), Nonidet P-40 (IGEPAL CA-630 1%) (Sigma), MilliQ Water

RIPA buffer: 1% Triton-x 100, 150nM NaCl, 5mM EDTA, 50mM Tris/HCL pH 8.0, PhosSTOP phosphatase inhibitor complete mini protease inhibitor, MiliQ water

4.11.3 Loading and running the SDS-page gel

The gel apparatus was assembled with precasted polyacrylamide *NuPAGE™ Novex™* 4%-12% Bis-Tris Gel (Thermofisher) and followed the instruction in the reference leaflet. The chambers were filled with NuPAGE 1x MOPS SDS Runing buffer (Thermofisher); the middle chamber was filled first to check for leakage.

17µl of protein lysate and 8.5µl of loading dye was mixed to an eppendorf tube. The mixture was heated for 5 minutes 80°C to denature the protein. Next, 25µl of the mixture was loaded on to the well and, standards 5µl SeeBlue marker and 1µl MagicMarker (Thermo Fisher Scientific) were loaded in the appropriate lanes. The NuPage gel was sequentially run at two settings: 30 minutes at 100V and 90 minutes at 150V on PowerEase 500 power supply (Invitrogen).

4.11.4 Blotting

Blotting was performed with the iBlot Transfer Stacks iBlot Gel Transfer Device system, 20V for 7 minutes. After transfer, the nitrocellulose membrane was washed with 1X TBS-T (10X 20mM TBS pH 7.5 (Sigma), 10% Tween-20 (Sigma), 5M NaCl (Merck Millipore), distilled water) for 5 minutes.

4.11.5 Blocking and Incubating

Membrane was blocked with 5% BSA in 1X TBS-T for one hour at room temperature with agitation and washed three times with 1X TBS-T for 5 minutes. Next, the membrane was incubated with appropriate dilutions of primary antibody (see Table 10.) in 5% BSA (blocking buffer) overnight at 4°C and HRP-conjugated secondary antibody (see Table 10.) for 1 hour at room temperature.

For signal development, 4ml of SuperSignal West Femto solutions (followed the Pierce/ThermoFisher Scientific kit recommendations) was mixed and added to the membrane and left for 3 minutes. The excess reagent was removed and membrane was transferred to a transparent film. Image was acquired with LI-COR ODYSSEY Fc Imaging system.

Table 10. Primary and secondary antibodies used for Western blotting

Gene of Interest	Primary antibody & Manufacturer	Dilution (in 5% BSA in TBS-T)	Secondary Antibody & Manufacturer (Polyclonal immunoglobulins/HRP)	Dilution (1% BSA in TBS-T)
GSDMD	Mouse , Abcam	1:1000	Goat anti mouse, Dako	1:4000
FLAG	DYKDDDK Tag Rabbit Ab, Cell signalling	1:3000	Goat anti rabbit, Dako	1:5000
NLRP3	Rabbit, Cell signalling	1:1000	Svin anti rabbit, Dako	1:4000
ALIX	Polyclonal Rabbit ,Novusbio	1:1000		
PDCD6 (ALG-2)	Polyclonal Rabbit, Thermofisher	1:500		
IL-1β	Mouse, Abcam	1:1000		
Alpha actin	Mouse,Abcam	1:2000		
Beta actin	Mouse, Abcam	1:2000		
Beta tubulin	Rabbit, Abcam	1:10000		

4.11.6 Stripping the membrane

The membrane was washed 2x for 10 minutes with stripping buffer (62.5mM Tris-HCl pH 6.8 (Sigma TrizmaBase), fuming hydrochloric acid (Merk), 1% SDS (Sigma)). Next, the membrane was washed 2x 10 minutes with PBS, 1x 10 minutes with 1X TBS-T and re-probed with primary and secondary antibodies of interest.

4.12 TIDE

Tracking of Indels by Decomposition (TIDE) accurately determines the spectrum and the frequency of targeted CRISPR/Cas9 mutations. TIDE aligns sgRNA sequence to the control or wildtype sequence to figure out frequency of indel, Cas9 cut site and Cas9 efficiency[122]. TIDE also gives R^2 value for good-fit measurement and p value for indel statistical significance [122]. The PCR products of the knockouts (same products made for cleavage kit assay) were purified using ZymoResearch DNA Clean & Concentrator kit and sent for Sanger sequencing to GATC; the samples were sent with appropriate sequencing primers listed in Appendix I. TIDE Software web tool (https://tide.deskgen.com/)[123] created by Bas van Steensel Lab was used to assess our knockout genome editing after receiving Sanger sequencing result from GATC.

5 Results

5.1. Establishing of knockout cell lines using CRISPR/Cas9 technology

By shutting down or overexpressing a gene of interest, one can study its functions in a biological process. In order to study *Mtb*-induced inflammasome activation, we established our own stable knockout cell lines of GSDMD and NLRP3 using CRISPR/Cas9 technology. NLRP3 plays a crucial role in secretion of pro-inflammatory cytokines and GSDMD is a caspase substrate and known as executor of pyroptosis[62]. Thus, we set out to determine how deletion of GSDMD and NLRP3 protein expressions in monocytes or macrophages affect inflammasome activation and pyroptosis. Recently, Dupont *et al*. and Harris *et al.* has suggested that IL-1β cytokines are unconventionally secreted by autophagosmes[76,124]. To explore the link between IL-1β and autophagy, we set out to generate additional knockout cell lines of FIP200, SEC22B, ALG-2 (PDCD6) and ALIX, which are important proteins in secretory autophagy and membrane repair. Furthermore, ALG-2 and ALIX are ESCRT-associated proteins that repair damaged plasma membrane so by making KO cell lines we could study their role in membrane damage during inflammasome activation and pyroptosis[81].

5.1.1 Verification of KO cell lines

Various guide sequences were selected for GSDMD gene: cc1, cc2, m1, m2 and p1, FIP200, SEC22B, (ALG-2) PDCD6, ALIX genes: sg1 and sg2, NLRP3: sg1 (Appendix I). The data for the genes were gathered from National Center for Biotechnology Information website (https://blast.ncbi.nlm.nih.gov/Blast.cgi). To target the specific protein coding sequence, we used CRISPR design web tool from Broad Institute as described previously. To take GSDMD gene (sg cc1 and cc2) as an example, the analysis showed that guide sequences for exon 5 and 6 scored highest in terms of low off-target effects and high efficiency in target site when compared to other exon parts of the gene. The analysis of exons 5 and 6 had 10.9% and 26.4% target cut site respectively. The off target ranking for exon 5 was 5 while on target ranking was 2. For exon 6, the off-target ranking was 4 and on-target ranking was 35. The overall on-target score for exons 5 and 6 was 0.7401 and 0.6298 respectively (score ranging 0 to1, 1 is the highest).

These oligos were ordered and phosphorylated/annealed (following the protocol as described above) and ligated into pLentiCRISPR_v2 backbone. These ligated plasmids were purified and then sent for DNA sequencing to GATC with U6_CRISPR_seq3 primer to verify if the target sequence has been inserted into the backbone. GSDMD KOs were transduced in wild type THP1, and additionally, sg cc1 and p1 KOs were transduced in pLex_ASC_mNG (mNeonGreen) and ASC_mIRF (near-infrared fluorescent protein) (cell lines provided by K.S.Beckwith) as reporters. Since ASC speck is the readout of inflammasome activation, we decided to use the cell lines overexpressing fluorescently tagged ASC so that we can visualize ASC dependent inflammasome formation. NLRP3, FIP200, SEC22B, ALG-2 (PDCD6) and ALIX were transduced with pLex_ASC_mNG in THP1 (cell line provided by K.S. Beckwith) reporters.

5.1.2 Identifying the best CRISPR sgRNA with cleavage kit assay

The first protocol that was used to verify the knockout clones was using the cleavage kit assay which allows the detection of genomic indels. We wanted to compare the efficiency of different sgRNAs to see which sgRNA is superior. The amplified PCR products of targeted genomic locus of GSDMD, FIP200, SEC22B, ALG2 (PDCD6), NLRP3 and ALIX were ran on 2% agarose gel electrophoresis to verify if sgRNA sequence on pLentiCRISPR_v2 template was amplified (Figure 8A). The expected size of PCR product (around 500bp) had to be present in order to move on to the cleavage detection assay. If there was no single band present on the expected size, PCR conditions were optimized by changing the annealing temperature and amount of lysate volume. The number of cells used in this assay was 400,000 cells/ml. The control sample (provided in the kit - size at 500bp) was added to check if PCR conditions were optimum.

For GSDMD KOs, the amount of lysates were diluted 1:4 in RNase free water after previous gel analysis (data not shown) showed smear bands, which indicated concentrated lysates. All of GSDMD PCR products except sg m1 gave a single band at 500bp which proved successful assembly of targeted genomic region. For GSDMD sgRNA m2, the PCR product did not have clear single band (Figure 8A) but we decided to proceed with it because previous PCR result showed (data not shown) smeared bands before lysates were 1:4 diluted, therefore we thought that this could be just be a smear for lysates being not diluted enough. The gel result after denaturation and reannealing reaction with the digestive enzyme showed that guide RNAs cc1,

cc2, m2 had clear parental and cleaved bands indicating successful gene editing (Figure 8B). Although sgRNA p1 had a clear band after PCR amplification, the cleavage bands were weak and only the parental band was detectable. GSDMD m1 gave two bands under 500bp and one faint band over 500bp which indicated amplification of non-specific products (Figure 8A). PCR result for cc1 and p1 GSDMD KOs overexpressed in pLex_ASC_mIRFP and mNG cell lines can be seen in Appendix III. The gel result of GSDMD KO cc1 and p1 in ASC_mNG and mIRFP cleaved bands were hardly detectable except for the parental bands; this could have happened due to uneven mix of GelRed with the agarose when making the gel cast resulting weak band intensity or not optimal PCR condition.

KOs of FIP200 sg1, SEC22B sg1, PDCD6 (ALG-2) sg2 and ALIX sg2 PCR products gave a single band around 500bp and NLRP3 around 200bp. This again proved successful assembly of targeted genomic regions. The samples were prepared in two different conditions to avoid PCR troubleshooting: lysates diluted 1:4 and lysates undiluted. The gel result showed that diluted lysates on FIP200 sg1, SEC22B sg1, PDCD6 sg2, and ALIX sg1 gave clearer single band than undiluted lysates (Figure 8C) No PCR product on diluted NLRP3 sg1 lysate was visible. All of diluted PCR samples were chosen while for NLRP3 undiluted PCR product was chosen to proceed to the next step. PCR result for FIP200 sg2, SEC22B sg2, PDCD6 sg1 and ALIX sg1 is shown on Appendix IV. PDCD6 sg1 did not gave a single band but multiple bands which indicated amplification of non-specific products.

Amplified PCR products were directly proceeded to the denaturing and re-annealing reaction. A negative control for each samples was included to distinguish the cleavage products from the background. The expected result was to see two smaller bands below the parental band (500 bp). The agarose gels indicated successful cleaved bands (Figure 8.B, D) on all samples except on GSDMD KO sg m1, PDCD6 KO sg1 and all GSDMD KOs overexpressed in reporter cell lines. (Appendix III). In addition, the cleavage efficiency was determined using the previously described formula.

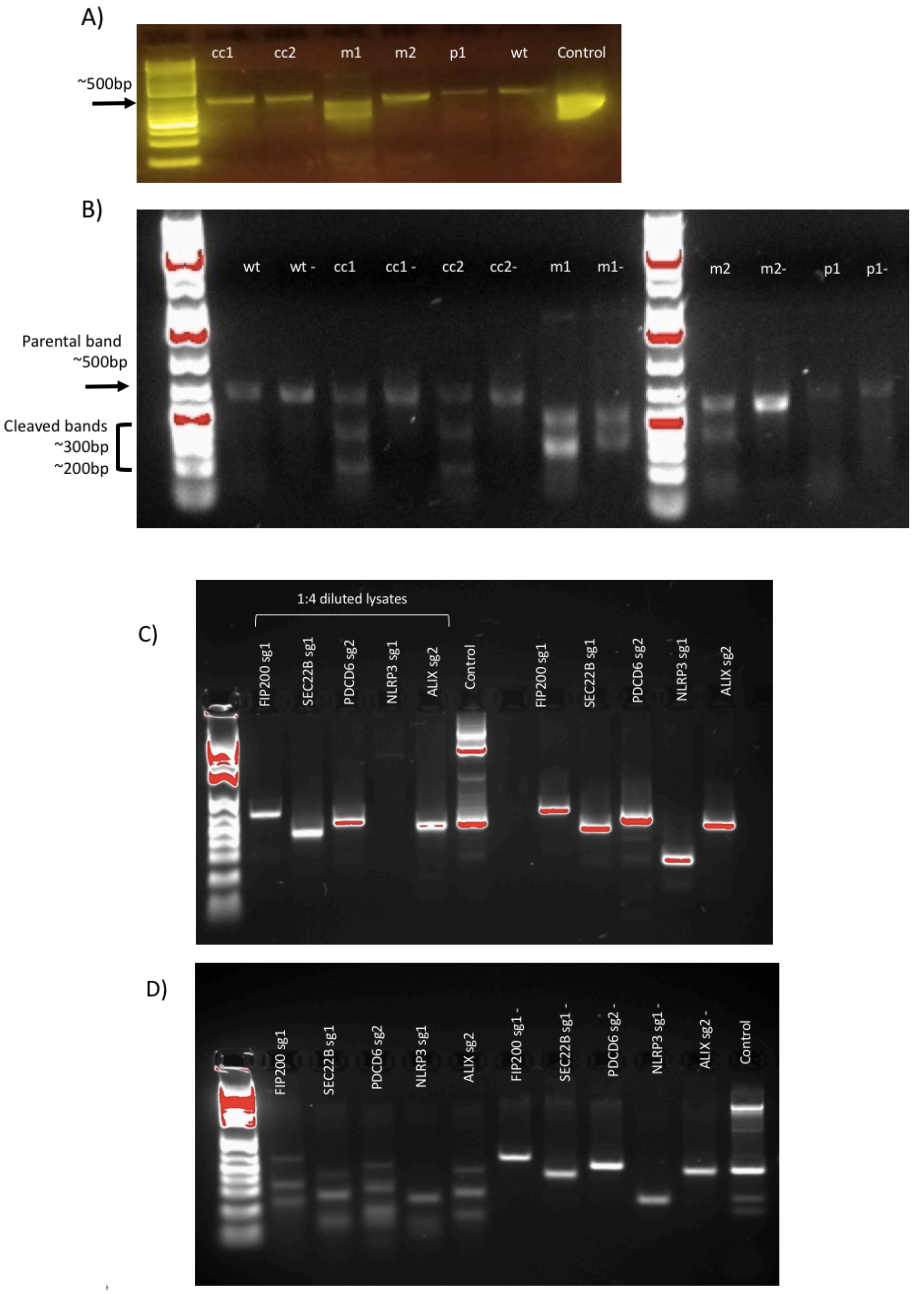

Figure 8. PCR verification of the products and cleaved bands detection on agarose gel for cleavage kit assay. *GeneRuler 1 kb plus ladder (Appendix VIII) was loaded to visualize DNA size. Molecular weight of PCR products and cleavage bands indicated with an arrow. A) Lanes represent amplified PCR products of GSDMD KO with different guide RNAs cc1,cc2,m1,m2,p1 plus control with size ~500bp B) GSDMD KO cleaved products after enzyme digestion including negative controls next to each corresponding samples C) 1:4 sample diluted (lane 1-5), c ontrol, and undiluted (lane 8-12) amplified PCR products of FIP200 sg1, SEC22B sg1, NLRP3 sg1,PDCD6 sg2, ALIX sg2 KO cells D) FIP200 sg1, SEC22B sg1, NLRP3 sg1,PDCD6 sg2, ALIX sg2 KO cleaved products after enzyme digestion (lane 1-5), negative controls of corresponding samples (lane 6-10, positive control (lane 11) with cleavage bands size of 291 and 225).*

5.1.3 Verification of protein KOs with Western blot

In addition to cleavage kit assay, western blotting (WB) was performed to confirm the absence of target proteins in GSDMD, NLRP3, PDCD6 and ALIX KO cell lines. All the targeted samples were normalized to housekeeping proteins such as beta actin, alpha actin and beta tubulin. This was done to equalize the differences in sample loading on the gel because the protein expression levels between different samples might vary. Wild-type THP-1 or a parental cell line ASC_mNG cell line were used as positive controls.

Figure 3.A. shows WB and normalized data for all of GSDMD knockout cell lines. The result showed that cc1, cc2 and m1 GSDMD KOs expressed lowest GSDMD protein amount while m2 had high GSDMD protein expression similar to the wild type THP1. Interestingly, GSDMD sg m2 had the highest protein expression compare to other KOs on WB (Figure 9A) even though we could see clear cleavage bands on the cleavage kit assay (Figure 8B) Also, western blot result of GSDMD sg m1 had low protein expression like sg cc1 and cc2 when PCR amplification and cleavage assay did not seem to have worked properly.

NLRP3 KO cells were differentiated into monocyte-derived macrophages. We decided to stimulate one of the PMA treated well with 10ng/ml LPS overnight to induce more NLRP3 expression. The cells were lysed on 6-well plate with RIPA buffer as described above. When compared to the NLRP3 expression level in parent cell line ASC_mNG, NLRP3 expression on both NLRP3 KO and NLRP3 KO (LPS) had a notable decrease (Figure 9B). LPS induced NLRP3 KO expressed low but slightly higher protein expression than untreated NLRP3 KO; this was expected since LPS must have activated the remaining function NLRP3 proteins.

KO cell lines of ALG-2 and ALIX were also differentiated with PMA but lysed with NP40 buffer. The lysis buffer was changed from RIPA to NP40 after experiencing a problem with viscosity and clumping solution. The ALG-2 and ALIX protein expressions (Figure 9C, D) were notably lowered on KOs than in the parental cell line. Although we concluded that ALG-2 sg2 and ALIX sg1 KOs seemed most-promising due to almost absent expression of the corresponding proteins.

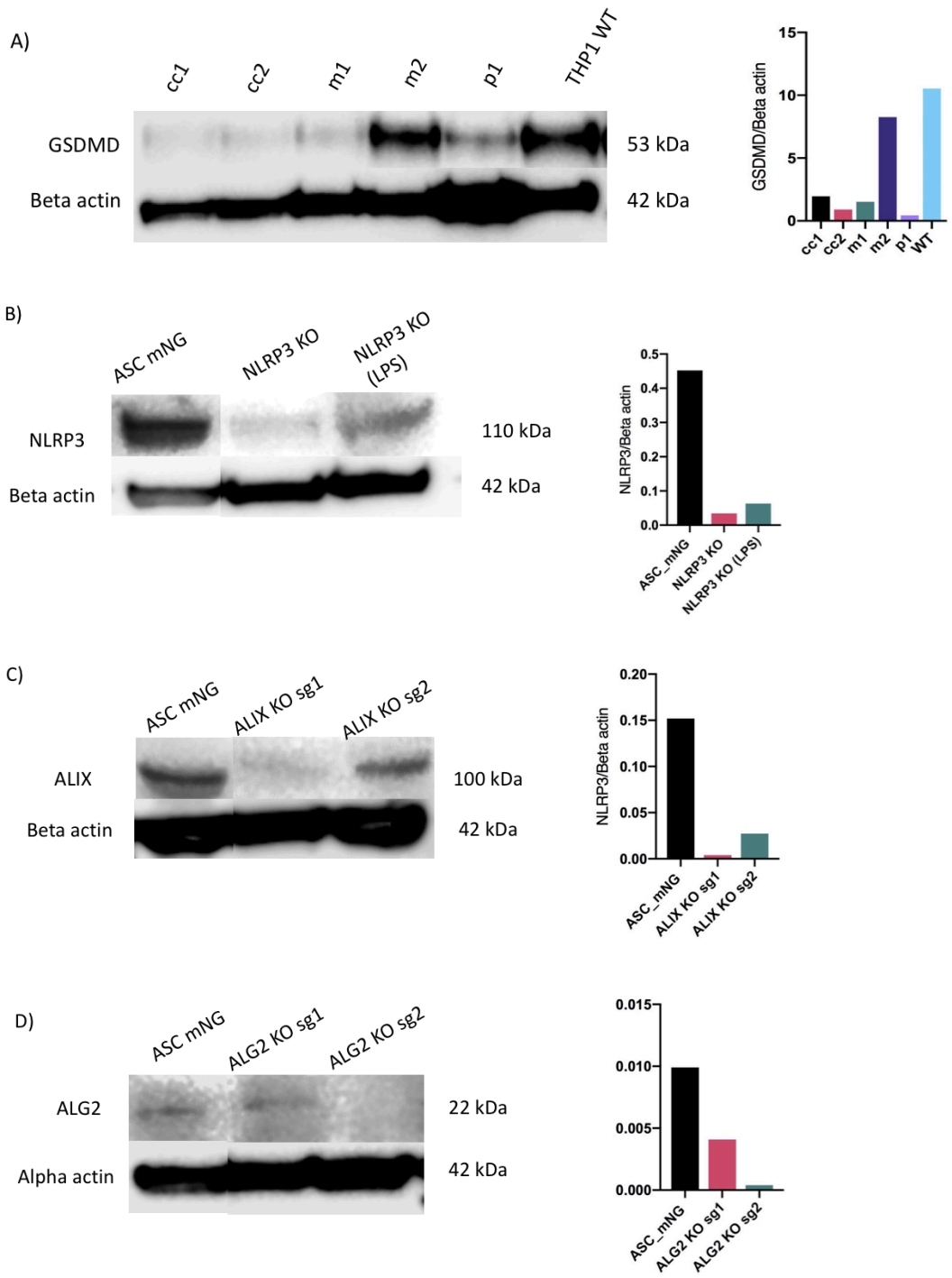

Figure 9. Verification of gene KO on a protein level with WB. *The ladder used to compare the size was MagicMarker. The proteins were stained with appropriate antibodies (see method section) to detect the signal. A) GSDMD KOs stained with anti-GSDMD antibody size 53kDa B) NLRP3 KOs stained with anti-NLRP3 antibody size 110 kDa C) ALIX KOs stained with anti-ALIX antibody size 100kDa D) ALG-2 KOs stained with anti-PDCD6 antibody size 22 kDa. The bands were quantified and normalized to Beta/alpha actin ~42 kDa.*

5.1.4 Assessment of genome editing efficacy by TIDE

In order to confirm successful CRISPR gene editing, we ran TIDE (Tracking of Indels by DEcomposition) analysis using the Sanger sequencing data. The TIDE web tool analyzed sequencing data from one pair of wild type control sample and one pair of edited sample. The TIDE detected indels and their frequencies mediated by NHEJ. We tested this approach on FIP200, SEC22B, PDCD6 (ALG2), NLRP3 and ALIX knockout cells.

The genome editing efficiency of the KO cells was assessed by TIDE and shown in Table 11 (see Appendix VII for indel spectrum). The TIDE result quantified that most of the genome editing efficiency by nuclease was over 50%, which proved promising knockout of the gene. However, for KOs SEC22B sg2 and NLRP3, the genome editing efficiency was only around 20% and also high percentage of sequence without insertions/deletions. In addition to editing efficiency, the TIDE result was elaborated with 1) % aberrant sequence signal in control vs treated sample 2) expected break site 3) decomposition of indel spectrum 4) base composition of +1 insertions. To take one sample in detail, analysis by TIDE resulted that 67.7% of ALG2 sequences in the sgRNA-treated cell pool carried an indel, 43.6% being -1 deletion, 3.3% being -2 deletion, and 3.6% being -5 deletion (Figure 10A). The inserted nucleotide probability (+1) was 0%. The correct targeting by sgRNA was confirmed by the expected cut site which was at 178bp (Figure 10 B, C).

Table. 11 TIDE analysis result (total editing efficiency % of Cas9) for CRISPR KO cell lines

KO cell lines	Total efficiency (%)
FIP200 sg1	47
FIP200 sg2	92
SEC22b sg1	52
SEC22b sg2	19
NLRP3 sg1	20
ALG-2 (PDCD6)	68
ALIX sg1	90
ALIX sg 2	58

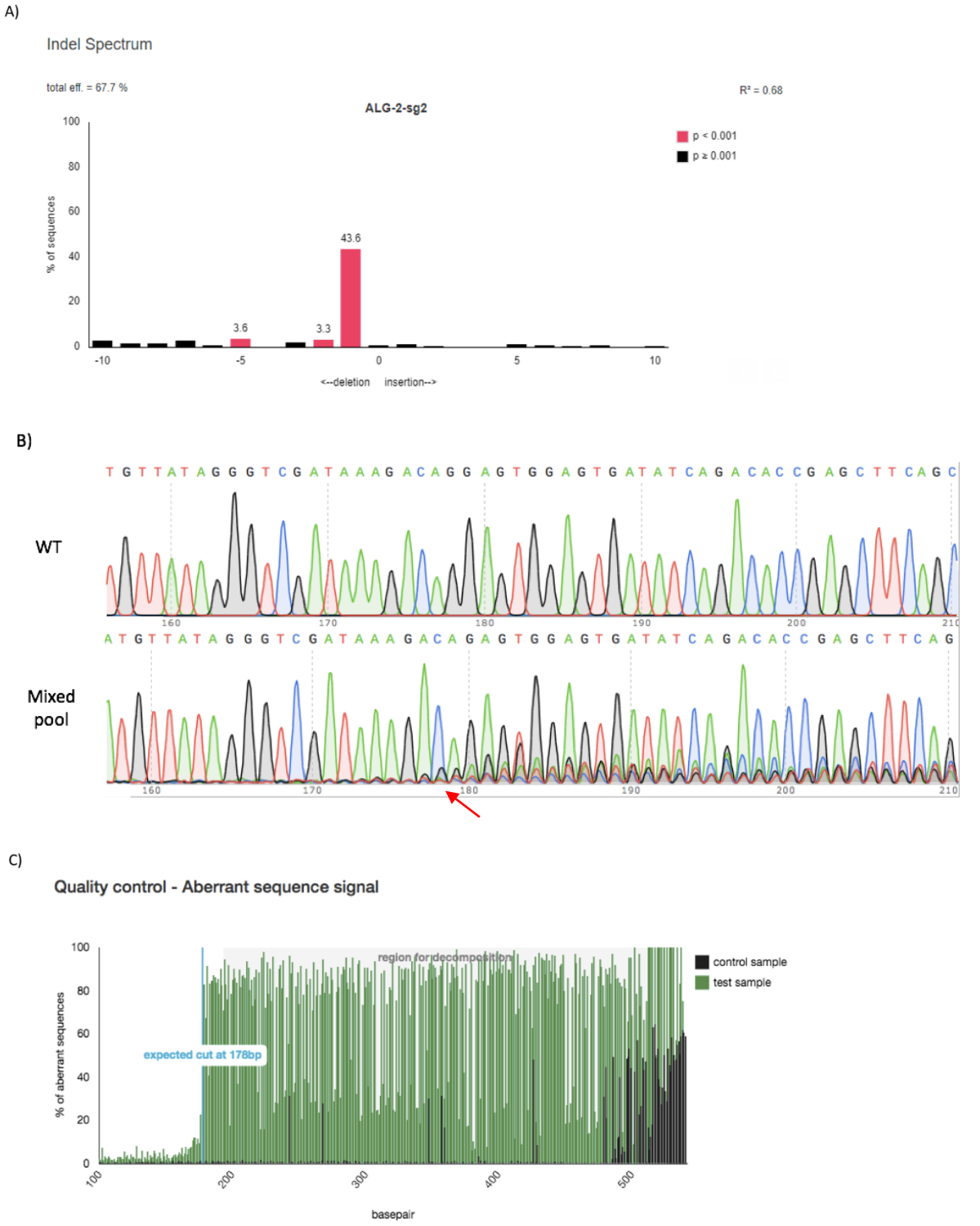

Figure 10. Detailed TIDE analysis result for ALG-2 sg2 knockout cell line. *A) Profile of all insertions and deletions in the edited sample and editing efficiency. The indel spectrum shows 67.7% editing efficiency of CRISPR Cas9 enzyme. B) Chromatogram of Sanger sequencing data. WT and mixed pool (edited sample) Red arrow indicates where the expected cut site is. C) Proportion of aberrant signal between control (black) and ALG-2 test sample (green). Location of break site in blue dotted line.*

5.1.5 Functional assay with LDH release assay and ELISA

Since the release of LDH to the supernatant is one of the marker for dead or dying cells, an enzymatic assay to detect LDH was performed on KO cell lines. GSDMD KO cells were PMA differentiated and treated with LPS for 3 hours and 1 hour with nigericin. Maximum release of cell death was achieved by adding 1% Triton X and spontaneous LDH release was assessed by uninfected cells. Low levels of cell death were observed for gRNA cc1, cc2, m1, p1 knockout cell lines plus gRNA cc1 KO in ASC_mNG reporter cell line (Figure 11A). However, gRNA m2 GSDMD KO cell line had high level of cell death as the control cell line, which we concluded majority of GSDMD protein was still functional and that it was not a strong knockout cell line. ELISA analysis on supernatants revealed that knocking out GSDMD significantly reduced the release of IL-1β in GSDMD KOs. ELISA was performed on supernatants which were collected after LPS+nigericin treatment (Figure 11B). For GSDMD KO with m2 gRNA, there was no reduction in IL-1β production after LPS+nigericin treatment, which is in agreement with the LDH assay result. But GSDMD KO with cc1 sgRNA in ASC_mNG reporter had low LDH and high IL-1β release even for the untreated; this high level of spontaneous IL-1β production might have resulted from overexpression of ASC. ELISA result proved that GSDMD is necessary for IL-1β secretion in addition to pyroptosis.

To study the involvement of FIP200, SEC22B, PDCD6, NLRP3, and ALIX proteins in pyroptotic cell death, macrophages from those KO cell lines (FIP200 sg1, SEC22B sg1, PDCD6 sg2,NLRP3 sg1 and ALIX sg2) were treated with LPS+nigericin and *M.*tub (Figure 12). There was a dramatic decrease in cell death on NLRP3 KO cell line after LPS+nigericin less than 10% cell death, and less than 20% cell death after *M.tub* infection compared to the parental and wild type controls (WT and ASC_mNG) (Figure 12). However, the stimuli did not seem to affect cell death in other KOs. Although LPS+ nigericin triggered lower cell death in ALG2 and ALIX KO cell lines and *M.tub* induced around 30~40% cell death but there were no notable differences in all KOs when compared with the control cell lines.

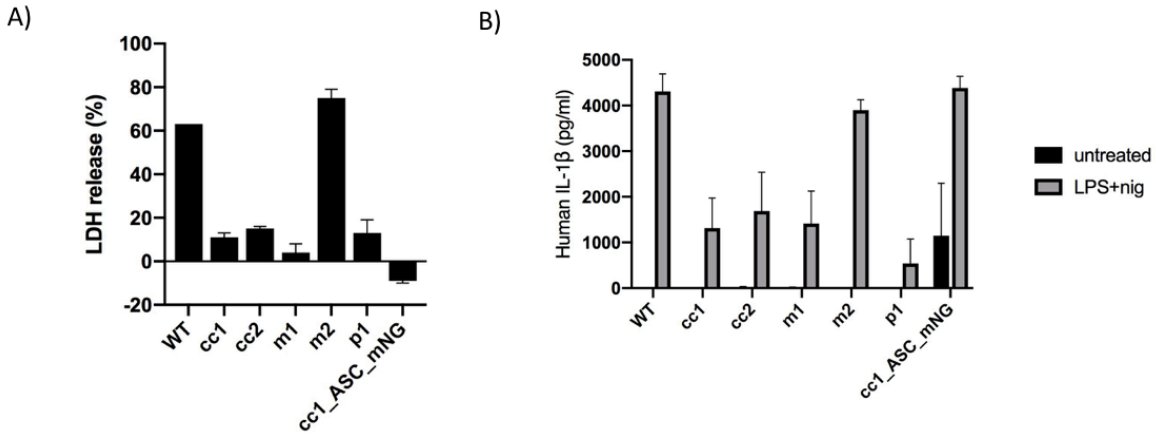

Figure 11. GSDMD KO inhibited pyroptosis and IL-1β release. *A) Cell cytotoxicity assay result for GSDMD KOs. LDH release in the supernatant of GSDMD KOs cells were measured after 1µg/ml LPS priming and 5µg/ml nigericin stimulation. B) IL-1β secretion were measured from the supernatants of GSDMD KO collected after LPS + nigericin treatment. The bars represent mean values and all results show standard error of the means (SEM) within each group from an independent experiment.*

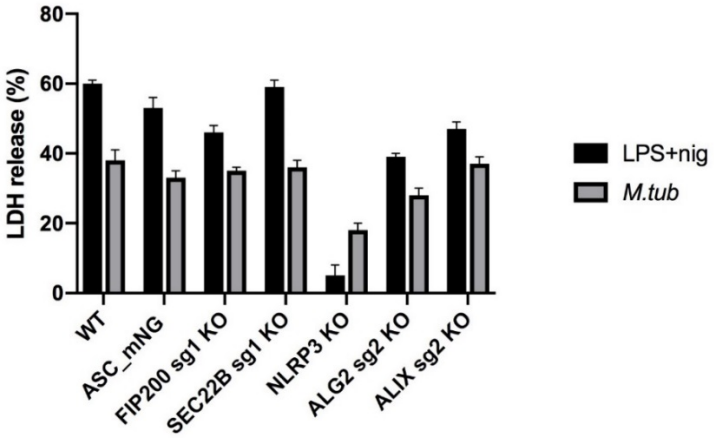

Figure 12. Cell death evaluation by LDH release on FIP200, SEC22B, ALG2, NLRP3 and ALIX KOs. *Cells were PMA treated for 72 hours and 1 day rest before priming the cells with 10ng/ml LPS and 5µg/ml nigericin stimulation and with M.tub. The supernatants were collected and LDH release was measured. The bars represent mean values and all results show standard error of the means (SEM) within each group from an independent experiment.*

5.1.6 Discrimination between live/dead cells after LPS+nigericin and *M.tuberculosis* stimulation with EVOS

Prior to LDH assay, we imaged the cells to count live/dead cells and ASC specks on EVOS epifluorescence microscopy (Appendix VI). Upon inflammasome activation, ASC assembles into a large protein complex called ASC speck. Since we transduced the KO cells into overexpressed ASC_mNG reporter cell lines, we could observe upstream readout of inflammasome activation. EVOS image of NLRP3 and GSDMD KOs were chosen to be analyzed since the phenotype from the LDH assay was the strongest. Technical triplicate replicates were made for the untreated and treated samples for each ASC_mNG and NLRP3 KO cell line. The live and dead cells were automatically counted using algorithm in Fiji ImageJ Software and ASC specks were manually counted. The ratio of live/dead cells and ASC specks were determined by calculating mean from triple replicates (see Appendix VI). NLRP3 KO in ASC_mNG cell line and parent cell line ASC_mNG (as control) were differentiated and stimulated with LPS+ nigericin and infected with *M.tub* optical density (OD) 0.02 for 45 minutes.

There was low < 20 % dead cells in untreated and treated (both LPS+nigericin and *M.tub*) NLRP3 KO cell line (Figure 13 A, B). Overall, there was very few ASC specks (Figure 13C, D) formation that indicated no inflammasome formation due to NLRP3 knockout. In the parental ASC_mNG cell line, more than half of the cells died after LPS+nigericin treatment (Figure 13A, Appendix VIa) and around 50% of ASC specks which meant more than half of the cells went into pyroptotic cell death (Figure 13C). There is a clear cell death after *M.tub* treatment for the control cell line (Figure 13B), and the percentage of ASC specks proves clear speck formation which meant pryoptotic cell death (Figure 13D).

In addition, live/dead cell imaging with EVOS for GSDMD KO cc1 in ASC_mNG cell line after 3 hours 10ng/ml LPS+ 1 hour 10µM nigericin treatment (Figure 14). Comparison with the parental cell line ASC_GFP, the knockout cell line showed almost no cell death and no defects in specks formation (Figure 14B).

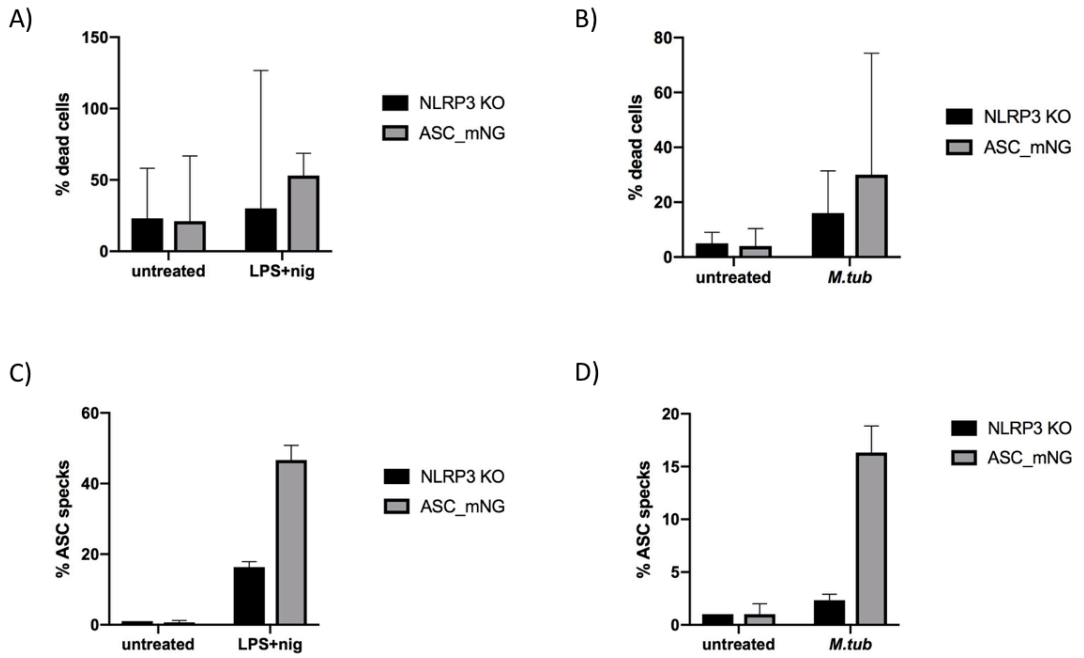

Figure 13. Cell viability assay LPS+nigericin and M.tuberculosis treatment. *A) % dead cells after 10ng/ml LPS+ 5µg/ml nigericing treatment B) % dead cells after o.d 0.002 M.tuberculosis treatment for 45 min. C) % mean of ASC specks after LPS+nigericin D) % mean of ASC specks after M.tub. The bars represent mean values and all results show standard error of the means (SEM) within each group from an independent experiment.*

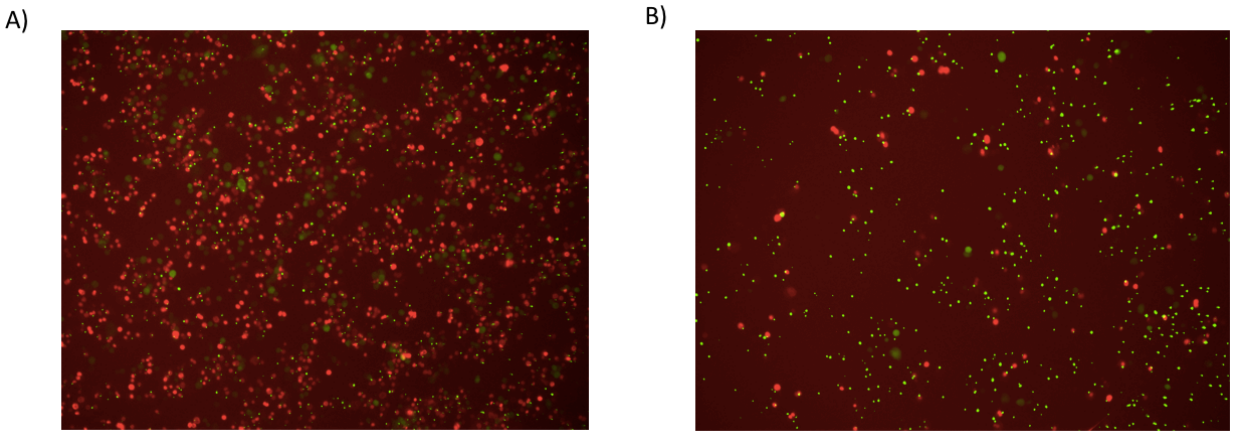

Figure 14. EVOS imaging of GSDMD KO cc1 in ASC_mNG *Live cells in GFP (green), dead cells in Draq7 (red), ASC specks mNG (brighter smaller green). These images were taken after 3 hours 10 ng/ml LPS + 1 hour 10µM nigericin treatment A) parental cell line ASC_GFP cell line B) GSDMD KO cc1 in ASC_mNG reporter*

5.2. BLaER1

5.2.1 Functional assays on BLaER1 cell lines

Recently, alternative inflammasome pathway has been discovered in human monocytes where IL-1β is secreted with only priming signal 1 and without classical inflammasome characteristics such as pyroptosis and K+ efflux dependency[44]. Gaidt *et al.*, and Rapino *et al.* found that BlaER1 cells show this unique pathway that THP-1 cells do not[44,116]. Therefore, we wished to use this alternative human cell line to investigate if inflammasome activation characteristics were similar to THP-1 cells. The BLaER1 cells were trans-differentiated with IL-3, M-CSF, and beta-estradiol, and successful trans-differentiation was confirmed by morphological change from round B-cells to adherent and spread-out monocytes. Functional assays were done to confirm the KO cell lines. After trans-differentiation, the cells were primed with 10ng/ml LPS for 3 hours and treated with 5µg/ml nigericin for 1 hour before supernatants were harvested for LDH assay and ELISA. KOs in all of inflammasome related proteins NLRP3, GSDMD, Caspase-1, ASC resulted low cell death and notable decrease in IL-1β production when compared to wildtype, GFP KO, ASC_mNG cell lines (Figure15).

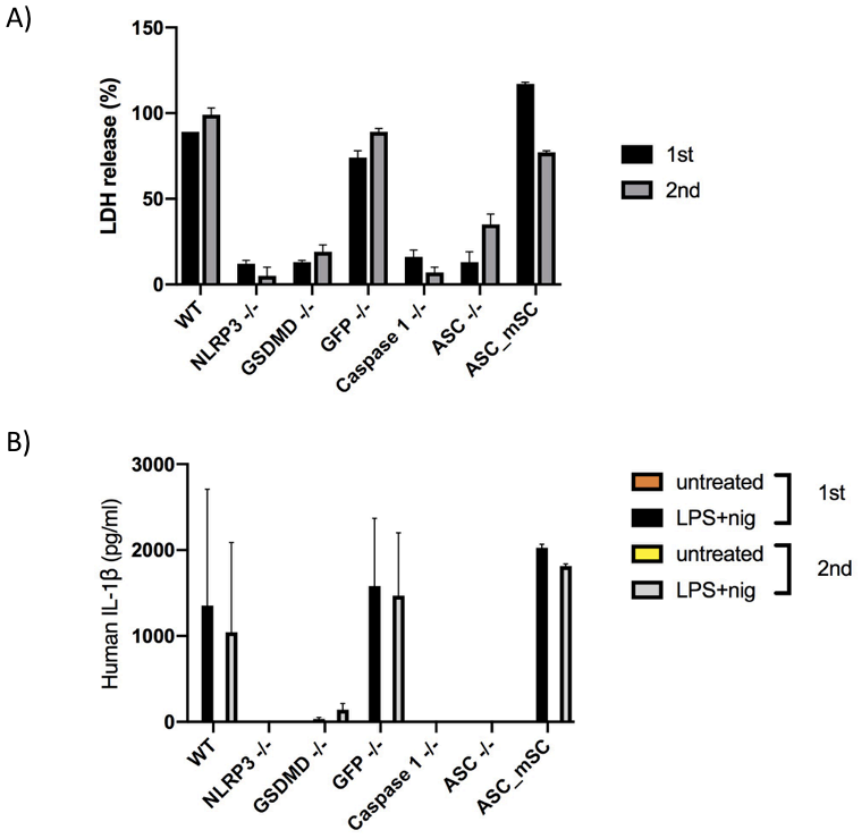

Figure 15. Cell death % and IL-1β release on BLaER1 KO cell lines. *BlaER1 cells were transdifferentiated with the mentioned cytokines for 7 days before primed with 10ng/ml LPS and 5 µg/ml nigericin. The supernatants were collected and two independent experiments were done for A) LDH release in % in the supernatants B) ELISA done on the supernatants collected with same condition and treatments. The bars represent mean values and all results show standard error of the means (SEM) within each group from two independent experiments.*

5.3. GSDMD expression vectors successfully made with Gateway cloning

To make a stable cell line of THP1 expressing GSDMD, pEntry vectors were designed using the Gateway cloning. In addition, GSDMD_mNG and GSDMD_FLAG tagged expression vectors were created. These expression vectors were made so that we could study the relation between GSDMD and ESCRT proteins and detect cleaved GSDMD during different types of inflammasome activation in the future studies.

5.3.1 Successful production of pEntry_GSDMD_L1L2 vector

Normally, the gene of interest could be amplified from plasmid vector. However, we used SuperScript IV Reverse Transcriptase (Invitrogen) to clone GSDMD genes from mRNA using specific 3`UTR primer to make complementary DNA (cDNA) (Appendix I) (done by K.S Beckwith) because plasmid vector with GSDMD-cDNA was not readily available. After getting the GSDMD coding sequence from BLAST, specific primers (forward and reverse) were designed for GSDMD gene with *att*B1 and *att*B2 flanking sites to purify the gene of interest. The PCR program for GSDMD primers was set to 69°C annealing temperature after calculating the correct annealing time for NEB calculator. The successful PCR product was ran on 0.7% agarose gel electrophoresis with GelGreen and purified using the gel extraction kit as mentioned above; the size of GSDMD product on the gel was based on the gene size from the donor vectors. This GSDMD product was now ready to be used for BP cloning reaction.

The BP reaction of GSDMD that contained pDONOR221 plasmid gave positive bacteria colonies on Kanamycin resistant plates, and we assumed that there was correct gene recombination. However, we needed further verification with Mlul restriction enzyme digestion. The predicted pEntry GSDMD vector size when digested by Mlul restriction enzyme was calculated using Snapgene software: one at 932 bp and one at 3067 bp (Figure 16A). We observed correct bands for both colonies on the gel and sent for sequencing with M13F/R

sequencing primers. The sequencing result confirmed correct GSDMD inserts in the plasmid (data not shown).

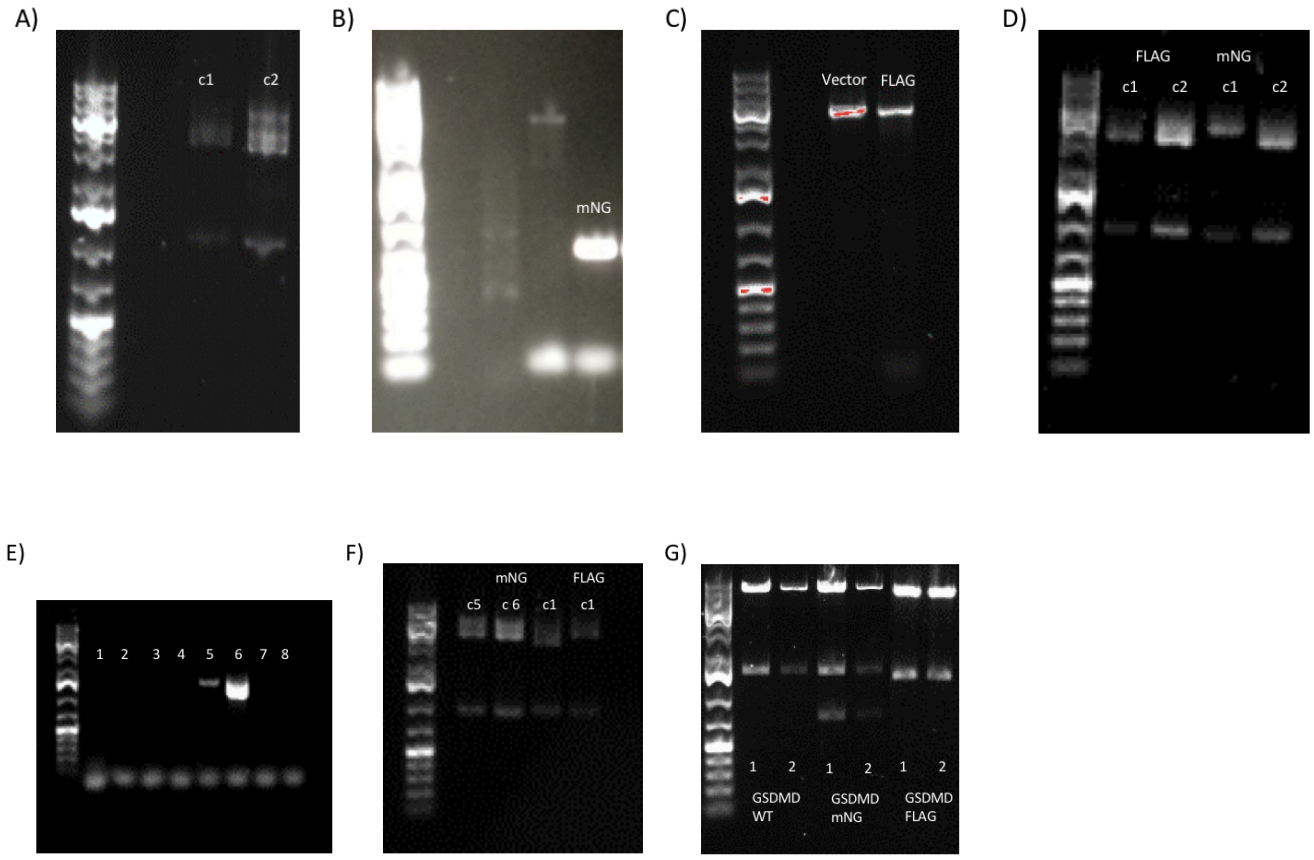

Figure 16. Gel results of GSDMD vectors using Gateway cloning. *All the gels were ran for 30 minutes 100V. A) Purified and digested pEntry_GSDMD products after MluI digestion. Two colonies (c1 and c2) were picked and ran on agarose gel. B) amplified PCR products for mNG with the band size around 754bp C) amplified PCR product of GSDMD vector and FLAG (4023bp) D) Purified and MluI digested pEntry_GSDMD_FLAg and pEntry_GSDMD_mNG E) 8 different colonies of GSDMD_mNG were ran for Go-taq green colony PCR. Only colonies 5 and 6 had amplified mNG gene. F) Purified and MluI digested pEntry_GSDMD_mNG colonies 5 and 6 products after Go-taq green colony PCR. Previously MluI digested pEntry_mNG and FLAG vectors were ran alongside together as a "control". G) Purified and BsrGI digested LR reaction of pLexB_GSDMD_WT, pLexB_GSDMD_mNG, and pLexB_GSDMD_FLAG.*

5.3.2 Modification of pEntry_GSDMD vector with internal mNG and FLAG tag

During pyroptosis, caspase-1 cleaves full-length GSDMD into C- and N- terminal ends; the C-terminal is lost while the GSDMD N-terminal fragment binds to the membrane [125]. To explore and track GSDMD activity, we wanted to add an internal mNG and FLAG tag into entry vector to overexpress GSDMD protein. The reason for internal tag was that N-terminal tagging inhibits GSDMD pyroptotic activity [126-129], and also we were not able to get N-terminal GSDMD antibodies to work. Here, Gateway BP reaction was substituted with HiFi DNA assembly cloning (NEB) for mNG and In-Vivo Assembly (IVA) cloning for FLAG to insert the tag proteins into the vector.

Specific forward/reverse primers were designed to amplify the pEntry_GSDMD_L1L2 vector, FLAG and mNG proteins (Appendix I). The PCR reaction was set as previously described with adjustment of annealing temperature to 69°C and extension time to 90 seconds for FLAG and 10 seconds for mNG reaction. The successful PCR reaction was ran on 1% agarose gel electrophoresis to confirm the gene amplification (Figure 16B, C) and digested with DpnI enzyme to destroy the plasmid template.

After Hifi and IVA reaction was performed to ligate the mNG and FLAG tags into the vector, the plasmids were plated on kanamycin agar plate for positive selection. We chose two colonies for each expression plasmids to be purified: pEntry_GSDMD_mNG L1L2 and pEntry GSDMD_FLAG L1L2. From the gel result after MluI digestion (Figure 16D), the bands gave predicted digested product size (calculated on Snapgene for the MluI enzyme digestion) at 932bp (lower band). We sent both FLAG and mNG for GATC sequencing for further verification.

5.3.3. Go-Taq green PCR screening for positive expression clones

Go-taq green PCR was performed to screen for bacteria colonies that contained mNG tag in pEntry_GSDMD_L1L2. 8 different colonies were picked and used directly in the PCR tubes giving out the result in Figure 16E. After observing the product on the gel, only clone numbers 5 and 6 possessed the correct product at ~1500 bp but no products for all the other clones. These 5 and 6 clones were then inoculated in kanamycin LB culture and digested with MluI restriction enzyme. Figure 16F shows the gel result after MluI digestion. However, the Go-Taq green PCR product bands after enzymatic digestion still gave same band result as pervious MluI digestion for mNG. We concluded to proceed with the transfection anyways with mNG since the top band

was a bit lower than the first digestion, and just assumed that MluI did not cut properly even though mNG was inserted.

5.3.4 Verifying the presence of mNG and FLAG tags in the cloned construct after LR reaction

Gateway LR reaction for pEntry_GSDMD_L1L2, mNG and FLAG vectors was performed into destination vector pLexB (Appendix II), with blasticidin antibody selection marker. This destination vector is Gateway plasmid that contains attR1/2 sites for recombination where entry clones are transferred to generate expression clone[111]. After antibody selection, two colonies were chosen for each expression plasmids purified: pLexB_GSDMD_WT, pLexB_GSDMD_mNG, and pLexB_GSDMD_FLAG, and they were digested with BsrGI restriction enzyme which cuts *att*B1/B2 sites giving the bands of insert and remaining vectors (Figure 16G). Based on the gel result, all of the samples looked promising since they gave predicted product sizes (calculated on Snapgene). To continue with transfection, we chose colony 1s from each of three gene constructs since they had stronger bands.

After transfecting the constructs into HEK293T, we decided to transduce pLexB_GSDMD_mNG and pLexB_GSDMD_FLAG into THP1 WT and pLex_ASC_mIRFP cell lines. The cells were observed under fluorescent microscope to determine the presence of mNG; quantification was not performed to determine the presence of mNG but the presence of mNG was qualified visually by observing the cells. The transfected GSDMD_mNG expressed green fluorescent phenotype during the first two days. However, after blasticidin antibiotic selection, ~90% cells did not express mNG expression and began to die after few days. For GSDMD_FLAG_WT and FLAG_ASC_mIRFP, we could not observe the phenotype under the fluorescent microscope. However, since the majority of the cells survived the antibiotic selection, we expanded the cells and verified with western blot (Figure 17). After running the WB with anti-FLAG antibody, the result was clear in that both cell lines expressed FLAG tags, while negative control did not express any FLAG tag.

In addition, after confirming the FLAG tagged GSDMD, pLexB_GSDMD_FLAG in WT THP1 cells were stimulated with various stimuli (done by K.S.Beckwith): LPS+nigericin, LPS+nigericin+MCC. MCC-950 is a NLRP3 activation inhibitor that therefore inhibits GSDMD cleavage. Western blot was ran on the lysates with GSDMD antibody so that we could detect GSDMD cleavage after inflammasome activation. As expected, there was no cleavage

of GSDMD-N term in the untreated control. After LPS priming and nigericin treatment, GSDMD was cleaved and the N-terminal cleavage product was observed at around 38 kDa (with tag), (Figure 18). There was some N-terminal cleavage after MCC treatment on LPS+nig, but amount of full-length GSDMD expression was stronger. Furthermore, we could detect lower beta actin signals in LPS+nigericin and LPS+nigericin+MCC treated cells as the cells were lost to pyroptosis.

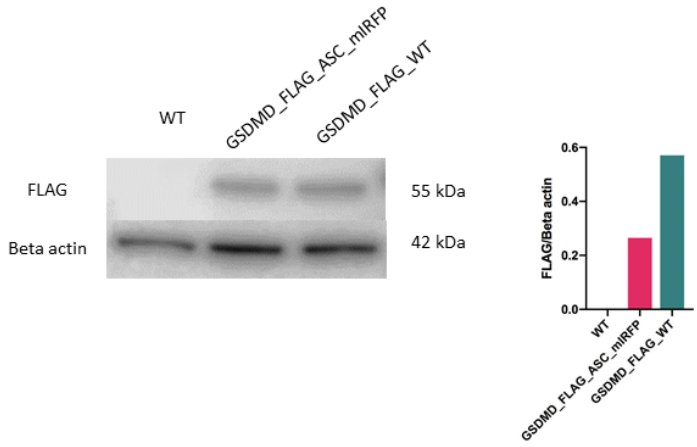

Figure 17. WB of FLAG tagged GSDMD_WT and GSDMD_ASC_mIRFP including normalization. *Wild type cell line lysate was loaded together as a negative control. Both cell lines confirmed to express FLAG tag gene after immunoblotting with anti-FLAG antibody.*

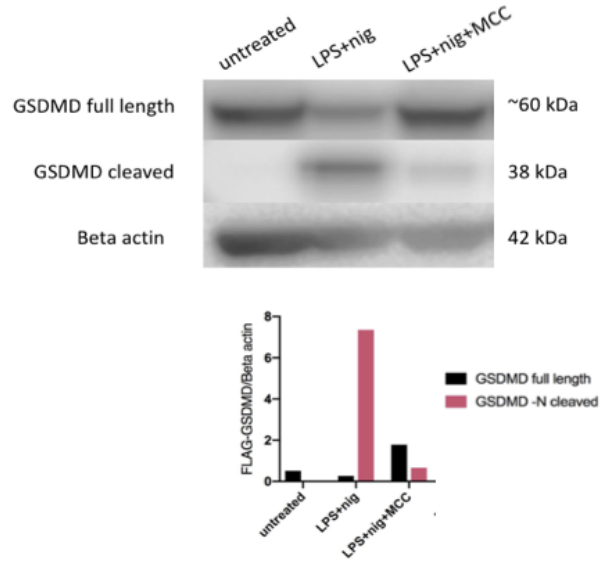

Figure 18. Cleavage of GSDMD on lysates seen on WB with normalization. *WB result of FLAG_GSDMD stimulated with LPS+nigericin, LPS+nigericin+MCC, control FLAG_GSDMD without any stimulation. Cell lysates were analyzed after anti-GSDMD antibody immunoblotting.*

6 Discussion

Inflammasomes are activated upon infection or cellular stress which induces pro-inflammatory cytokines such as IL-1β, which is important in triggering innate immune defense[5]. NLRP3 inflammasome is not a single protein complex, but a multi-protein complex combined with ASC and caspase-1[11]. Recent studies have shown GSDMD is the executor of pyroptosis and the main exit for IL-1β cytokines[62]. The secretion of IL-1β may occur through unconventional pathway of secretory autophagy that involves FIP200 for autophagosome formation and SEC22B for autophagic cargo secretion [79,80,130]. Furthermore, the ESCRT machinery proteins, ALG-2 and ALIX, are essential for cellular homeostasis and survival as they repair the damaged plasma membrane thereby balancing cell viability and pyroptosis[84-86]. We hypothesized that both ESCRT membrane repair and secretory autophagy might be involved in inflammasome activation and IL-1β secretion during *Mtb* infection. Thus, we needed model systems to study all inflammasome components and new possibilities to understand the molecular basis of host defence during infection or cellular stress. The recent discovery of CRISPR/Cas9 has revolutionized genome editing technology by making gene modification efficient and relatively simple to perform. In this study, we attempted to generate knockout cell lines of GSDMD, NLRP3, FIP200, SEC22B, PDCD6 (ALG-2) and ALIX, and verify all the established KOs using different genetic and molecular methods. In addition, we succeeded on making GSDMD expression plasmid vector in order to study cellular localization and protein cleavage. Also, since our group is focused on inflammasome research, testing BLaER1 cell lines was an alternative approach in studying inflammasome pathway.

First, CRISPR/Cas9 technology was used to knockout the proteins of interest. CRISPR genome editing technology uses designed sgRNA-guided Cas9 nuclease enzyme to cleave targeted locus by creating DSB and repairing with NHEJ or HDR [106]. Compared to TALENs and ZFNs that are time-consuming process, CRISPR/Cas9 is more precise and simple to modify DNA[106,131,132]. Some advantages of using CRISPR/Cas are 1) simply designed gRNA, not engineered protein, targets DNA cleavage therefore it is less cumbersome[106] 2) more efficient and time saving first generation knockout production[133] 3)simultaneous introduction of multiplexed mutations[134]. However, there are limitations in using CRISPR/Cas9: production of off-target activity that could interfere normal gene[135] and possibly limited target sequence due to PAM sequence. By using the web based tool, we were able to efficiently design and analyse sgRNAs and obtained indel frequency by using TIDE method.

Since genome editing techniques are frequently used, finding out the efficacy of endonuclease is important for optimization and verification of KO cell lines. Although cleavage assay calculates the % of indels or gene modification (Appendix V), this does not mean that high cleavage efficiency is necessarily the lowest expression. Apart from its low cost, the advantage of using TIDE was that we could accurately detect indels and endonuclease efficiency in the KO cell lines. The cleavage assay was not a best method to check for editing efficiency for it only detects small sequence changes and underestimates accurate endonuclease efficiency[136]. We could not use TIDE analysis for GSDMD KOs because Sanger sequencing results (not shown in this thesis) were impossible to interpret due to failed DNA sequencing or messy and not "clean" chromatogram data peaks. One important requirement for a good sequencing/ TIDE analysis is to have a clear good PCR products. However, in some cases this is difficult due to genome regions with very high AT or CG contents or other unexpected difficulties in PCR primers e.g. off-target binding. Thus, optimal PCR condition or newly designed primers are necessary to get a good PCR products. Although we had clear GSDMD PCR products, our sequencing still did not work; what went wrong with the PCR products sequencing can be difficult to find out.

Moreover, quantifying the amount of protein of interest with western blot provided increased sensitivity and specificity in the KO cell lines. The advantage of using WB was that the results showed disappear or decrease in protein expression which additionally confirmed successful induced mutation by Cas9. However, there still could be functional proteins after NHEJ depending on whether that exon was coding area or not. For example, some exons may not even be involved on generating transcripts or even due to alternative splicing, there may be multiple transcripts. Also, a chance of non-specific band size appearing on the same size of the target protein may give false impression. Therefore, sending in for sequencing and verifying with TIDE are reliable method to see the exact rates of NHEJ in KO cells.

How accurate TIDE sequencing is can be proved by SEC22B sg1 and sg2 TIDE indel spectrum results (Appendix VII). Even though, the cleavage kit assay showed clear cleaved bands after enzyme digestion, this did not accurately determined KO efficiency. During the course of the study, these cell lines only survived one week after transduction; this may have happened due unstable repair process that did not retained the protein activity, low activity of gRNA or that gene must have been essential for the cells. The indel spectrum result for NLRP3 KO showed only 20.1% of Cas9 efficiency and 73 % of no indel in the sequence. However, we observed that NLRP3 was a strong KO after verifying with WB, EVOS, LDH and ELISA. NLRP3

cleaved bands were difficult to detect since the parental band was around 270bp (Figure 8D) so we presumed that there were cleaved bands within the smear. NLRP3 primers were not designed to yield amplicon lengths of ~500bp, as the general guideline of cleavage kit assay recommended. However, if there was no cleavage bands in the first place, this could have meant that CRISPR system could silence transcription and/or translation by other means. Qi *et al.* showed that catalytically inactive Cas9 or modified system CRISPR interference (CRISPRi) may block transcription without changing the target sequence[137]. If this is true, then NLRP3 KO we produced could be a knockdown cell line. Therefore, it is important to keep in mind the location of target sequence effects the gene editing efficiency.

Our central working hypothesis was that pyroptosis and IL-1β secretion are dependent upon inflammasome activation. We provided functional assays to support this claim as well and fluorescent live/dead cell and ASC speck images to confirm the KO cell lines. A direct correlation between LDH and ELISA result of GSDMD KO cell lines was observed for the reduction of cell death due to GSDMD KO decreased IL-1β secretion. This proved that GSDMD is crucial inflammasome components and the main executor of pyroptosis and IL-1β secretion. Also, our EVOS images of GSDMD KO showed that GSDMD is necessary for pyroptosis even with ASC specks. The LDH results on ALIX and ALG-2 showed that KO of these genes resulted an increase in pyroptosis due to perhaps lack of plasma membrane repair. However, this must be investigated more thoroughly for the LDH result was based on one experiment and also check the results for IL-1β secretion including FIP200 and SEC22B KOs.

It is well known that in canonical inflammasome pathway, NLRP3 must be primed with signal 1 such as LPS to activate transcription factor NF-kB to upregulate pro-IL-1β [28] and signal 2 to activate inflammasome. Recent finding suggested that human monocytes can utilise an alternative inflammasome pathway that consists of NLRP3-ASC-caspase-1 signalling with secretion of mature IL-1β without second stimuli[44]. Since Gaidt *et al*. showed that THP-1 did not show this pathway while BLaER1 cell showed this response by inducible nuclear translocation of C/EBPalpha transgene, our lab wanted to establish BLaER1 wild type and KO cell line models to compare inflammasome activation and mechanism with THP-1. LPS is sufficient to induce and secrete mature IL-1β independently of pyroptosis in human monocytes, but since our purpose was to confirm the KOs additional nigericin treatment was added to secrete 10x more fold of IL-1β and promote pyroptosis[44]. The low concentration of LDH and IL-1β release in KOs of NLRP3, caspase-1, GSDMD and ASC proved that these KO cell lines were successfully made, for pyroptosis and IL-1β secretion were inhibited due to deletion of

inflammasome related genes. Evavold *et al*., suggested that intact or hyperactive macrophages release IL-1 through GSDMD pores [104] and that GSDMD is the executor of pyroptosis and IL-1β secretion. As our results have shown, without GSDMD the cells were not able to go into pyroptosis nor release IL-1β. To note, these BLaER1 cells are single-cell clones which could be the reason for clearer LDH and ELISA results than the KO THP1 cells lines we produced.

Unfortunately, we were notified that the BLaER1 cells were infected with active retrovirus particles. Experiments were put on hold until further investigation in this matter is done. However, even if virus is produced our BLaER1 results are still valid for we were just comparing WT with KOs and the effect we see attributes to that particular knockout. Since these cell lines are new for us, we still need more time to observe the cell's behaviour, characterization and stability. Following these BLaER1 KO verification test, producing overexpressed GSDMD with either mNG or FLAG will be a possibility to study GSDMD localization, pore formation, and cleavage in BLaER1 cells during alternative inflammasome pathway. Also, to test other inflammasome inducing stimuli could be an interesting approach to characterize BLaER1 cells. These immortalised cell lines of BLaER1 and THP1 are useful tool in cell biology due to their indefinite cell division. THP-1 has been widely used to study signalling pathways and functional activities in monocytes and macrophages, and also their homogenous genetic background and long-term storage have been advantages over PBMCs[138]. Likewise, discovery of BLaER1 cells has opened a path of studying signalling pathways of canonical, non-canonical and alternative inflammasome pathway. However, very little is known about these BLaER1 cell lines to fully characterize their strength and limitation.

Gateway cloning was used to create pEntry vector and expression vectors of GSDMD. By making these vectors, we were able to use these for lentiviral transfection and transduction in THP-1. As previously mentioned, the expression vector of plexB_GSDMD_mNG became not functional when transfected into HEK293T and transduced in WT THP1. One of the reason could be that mNG tag might have interfered with GSDMD protein folding or downstream signalling in the cell that result transient GSDMD_mNG cell lines. The reason for choosing mNG, a bright monomeric yellow-green fluorescent protein tag over commonly used green fluorescent protein (GFP) was because mNG tag was known to be more stable and brighter in visualization of protein[139]. On the other hand, FLAG is a smaller tag compare to mNG so the protein function would not be so affected resulting successful transfection or transduction in WT THP1. We could easily detect whether majority of cells have survived transfection/transduction with western blot and immunofluorescence technique. However, one

would have hard time doing live cell imaging to observe intracellular localization and translocation. Overexpressed GSDMD cell lines with other fluorescent protein such as mSC or mIRFP could be substituted for mNG, but the chance of producing successful overexpressed cell line is uncertain.

7 Conclusion

In summary, this study focused on using genetic and molecular tools to verify different cell lines on studying inflammasome.

- By using CRISPR/Cas9 technology, we attempted to establish KO cell lines of GSDMD, NLRP3, ALG-2 and ALIX.
- Verification of KO cell lines were accomplished using different molecular methods such as genomic cleavage kit assay, western blot, TIDE, LDH, ELISA, and EVOS
- Introduction of new cell line, BLaER1 to further study inflammasome pathway, both canonical and alternative inflammasome pathway.
- Production of pEntry GSDMD vector and expression vector GSDMD with FLAG tag were established.

Overall, gene editing with CRISPR technology gave some promising results, and generation of NLRP3 and GSDMD models confirmed essential roles for inflammasome and pyroptosis. It was already well known that nigericin induces NLRP3 and leads to GSDMD pryoptosis and IL-1β release, therefore the results were expected from known literatures. However, this thesis work gave some in-house methods and model cell lines to better investigate inflammasome activation during *Mtb* and other less well understood mechanisms. Also, by studying these genes, we could obtain better understanding and establish potential therapeutic application in inflammasome related diseases. Some future experiments that could be done on these knockout cell lines could be stimulation with different inflammasome triggers to investigate how these stimulations affect the KO cells in regards to inflammasome formation and pyroptosis. Also, we could perhaps single-clone the KO cells lines to achieve pure KO population to avoid unwanted mutations. We also attempted to knockout FIP200 and SEC22B but was unsuccessful. One explanation for this could be that those genes were essential for cell function and thus losing the gene was toxic to the cells. For future experiments, investigating more of ESCRT proteins and other autophagy proteins could be worth investigating.

8 References

1 Owen, J. A., Punt, J., Stranford, S. A., Jones, P. P. & Kuby, J. *Kuby immunology*. (W.H. Freeman, 2013).

2 Parham, P. *The Immune System*. (CRC Press, 2014).

3 Colm, G. Vol. 101kb (ed Phagocytosis2) (English Wikipdia, 2009).

4 Kim, Y. K., Shin, J. S. & Nahm, M. H. NOD-Like Receptors in Infection, Immunity, and Diseases. *Yonsei medical journal* **57**, 5-14, doi:10.3349/ymj.2016.57.1.5 (2016).

5 Schroder, K. & Tschopp, J. The Inflammasomes. *Cell* **140**, 821-832, doi:https://doi.org/10.1016/j.cell.2010.01.040 (2010).

6 Kumar, H. *et al. Involvement of the NLRP3 Inflammasome in Innate and Humoral Adaptive Immune Responses to Fungal -Glucan*. Vol. 183 (2009).

7 Franchi, L., Eigenbrod, T., Muñoz-Planillo, R. & Nuñez, G. The inflammasome: a caspase-1-activation platform that regulates immune responses and disease pathogenesis. *Nature immunology* **10**, 241-247, doi:10.1038/ni.1703 (2009).

8 Sun Jin, H., Park, J.-K. & Jo, E.-K. *Toll-like Receptors and NOD-like Receptors in Innate Immune Defense during Pathogenic Infection*. Vol. 44 (2014).

9 Rathinam, V. A. K., Vanaja, S. K. & Fitzgerald, K. A. Regulation of inflammasome signaling. *Nature immunology* **13**, 333, doi:10.1038/ni.2237 (2012).

10 He, Y., Hara, H. & Núñez, G. Mechanism and Regulation of NLRP3 Inflammasome Activation. *Trends in biochemical sciences* **41**, 1012-1021, doi:https://doi.org/10.1016/j.tibs.2016.09.002 (2016).

11 Jo, E. K., Kim, J. K., Shin, D. M. & Sasakawa, C. Molecular mechanisms regulating NLRP3 inflammasome activation. *Cell Mol Immunol* **13**, 148-159, doi:10.1038/cmi.2015.95 (2016).

12 Meixenberger, K. *et al.* Listeria monocytogenes-infected human peripheral blood mononuclear cells produce IL-1beta, depending on listeriolysin O and NLRP3. *J Immunol* **184**, 922-930, doi:10.4049/jimmunol.0901346 (2010).

13 Kim, S. *et al.* Listeria monocytogenes is sensed by the NLRP3 and AIM2 inflammasome. *Eur J Immunol* **40**, 1545-1551, doi:10.1002/eji.201040425 (2010).

14 Gross, O. *et al.* Syk kinase signalling couples to the Nlrp3 inflammasome for anti-fungal host defence. *Nature* **459**, 433-436, doi:10.1038/nature07965 (2009).

15 Hise, A. G. *et al.* An essential role for the NLRP3 inflammasome in host defense against the human fungal pathogen Candida albicans. *Cell host & microbe* **5**, 487-497, doi:10.1016/j.chom.2009.05.002 (2009).

16 Lee, H. M. *et al.* Mycobacterium abscessus activates the NLRP3 inflammasome via Dectin-1-Syk and p62/SQSTM1. *Immunol Cell Biol* **90**, 601-610, doi:10.1038/icb.2011.72 (2012).

17 Munoz-Planillo, R., Franchi, L., Miller, L. S. & Nunez, G. A critical role for hemolysins and bacterial lipoproteins in Staphylococcus aureus-induced activation of the Nlrp3 inflammasome. *J Immunol* **183**, 3942-3948, doi:10.4049/jimmunol.0900729 (2009).

18 Allen, I. C. *et al.* The NLRP3 inflammasome mediates in vivo innate immunity to influenza A virus through recognition of viral RNA. *Immunity* **30**, 556-565, doi:10.1016/j.immuni.2009.02.005 (2009).

19 Thomas, P. G. *et al.* The intracellular sensor NLRP3 mediates key innate and healing responses to influenza A virus via the regulation of caspase-1. *Immunity* **30**, 566-575, doi:10.1016/j.immuni.2009.02.006 (2009).

20 Invivogen. Inflammasome multiprotein complex (Invivogen, 2012).

21 Bauernfeind, F. G. *et al.* Cutting Edge: NF-κB Activating Pattern Recognition and Cytokine Receptors License NLRP3 Inflammasome Activation by Regulating NLRP3 Expression. *The Journal of Immunology* **183**, 787-791, doi:10.4049/jimmunol.0901363 (2009).
22 Jacobs, S. R. & Damania, B. NLRs, inflammasomes, and viral infection. *Journal of leukocyte biology* **92**, 469-477, doi:10.1189/jlb.0312132 (2012).
23 Hornung, V. & Latz, E. Critical functions of priming and lysosomal damage for NLRP3 activation. *Eur J Immunol* **40**, 620-623, doi:10.1002/eji.200940185 (2010).
24 Gurung, P. *et al. FADD and Caspase-8 Mediate Priming and Activation of the Canonical and Noncanonical Nlrp3 Inflammasomes*. Vol. 192 (2014).
25 Qiao, Y., Wang, P., Qi, J., Zhang, L. & Gao, C. TLR-induced NF-κB activation regulates NLRP3 expression in murine macrophages. *FEBS Letters* **586**, 1022-1026, doi:10.1016/j.febslet.2012.02.045 (2012).
26 Liu, T., Zhang, L., Joo, D. & Sun, S.-C. NF-κB signaling in inflammation. *Signal Transduction And Targeted Therapy* **2**, 17023, doi:10.1038/sigtrans.2017.23 (2017).
27 Py, Bénédicte F., Kim, M.-S., Vakifahmetoglu-Norberg, H. & Yuan, J. Deubiquitination of NLRP3 by BRCC3 Critically Regulates Inflammasome Activity. *Molecular Cell* **49**, 331-338, doi:https://doi.org/10.1016/j.molcel.2012.11.009 (2013).
28 Sutterwala, F. S., Haasken, S. & Cassel, S. L. Mechanism of NLRP3 inflammasome activation. *Annals of the New York Academy of Sciences* **1319**, 82-95, doi:10.1111/nyas.12458 (2014).
29 Juliana, C. *et al.* Non-transcriptional priming and deubiquitination regulate NLRP3 inflammasome activation. *J Biol Chem* **287**, 36617-36622, doi:10.1074/jbc.M112.407130 (2012).
30 Mayor, A., Martinon, F., De Smedt, T., Pétrilli, V. & Tschopp, J. A crucial function of SGT1 and HSP90 in inflammasome activity links mammalian and plant innate immune responses. *Nature immunology* **8**, 497, doi:10.1038/ni1459

https://www.nature.com/articles/ni1459 - supplementary-information (2007).
31 Song, N. *et al.* NLRP3 Phosphorylation Is an Essential Priming Event for Inflammasome Activation. *Molecular Cell* **68**, 185-197.e186, doi:https://doi.org/10.1016/j.molcel.2017.08.017 (2017).
32 Costa, A. *et al.* Activation of the NLRP3 inflammasome by group B streptococci. *J Immunol* **188**, 1953-1960, doi:10.4049/jimmunol.1102543 (2012).
33 Greaney, A. J., Leppla, S. H. & Moayeri, M. Bacterial Exotoxins and the Inflammasome. *Front Immunol* **6**, 570, doi:10.3389/fimmu.2015.00570 (2015).
34 Pétrilli, V. *et al.* Activation of the NALP3 inflammasome is triggered by low intracellular potassium concentration. *Cell Death And Differentiation* **14**, 1583, doi:10.1038/sj.cdd.4402195

https://www.nature.com/articles/4402195 - supplementary-information (2007).
35 Lamkanfi, M. *et al.* Glyburide inhibits the Cryopyrin/Nalp3 inflammasome. *J Cell Biol* **187**, 61-70, doi:10.1083/jcb.200903124 (2009).
36 Lee, G. S. *et al.* The calcium-sensing receptor regulates the NLRP3 inflammasome through Ca2+ and cAMP. *Nature* **492**, 123-127, doi:10.1038/nature11588 (2012).
37 Rossol, M. *et al.* Extracellular Ca2+ is a danger signal activating the NLRP3 inflammasome through G protein-coupled calcium sensing receptors. *Nat Commun* **3**, 1329, doi:10.1038/ncomms2339 (2012).
38 Murakami, T. *et al.* Critical role for calcium mobilization in activation of the NLRP3 inflammasome. *Proceedings of the National Academy of Sciences of the United States of America* **109**, 11282-11287, doi:10.1073/pnas.1117765109 (2012).

39 Katsnelson, M. A., Rucker, L. G., Russo, H. M. & Dubyak, G. R. K+ efflux agonists induce NLRP3 inflammasome activation independently of Ca2+ signaling. *J Immunol* **194**, 3937-3952, doi:10.4049/jimmunol.1402658 (2015).
40 Dostert, C. *et al.* Innate immune activation through Nalp3 inflammasome sensing of asbestos and silica. *Science (New York, N.Y.)* **320**, 674-677, doi:10.1126/science.1156995 (2008).
41 Martinon, F., Burns, K. & Tschopp, J. The inflammasome: a molecular platform triggering activation of inflammatory caspases and processing of proIL-beta. *Mol Cell* **10**, 417-426 (2002).
42 Groß, Christina J. *et al.* K+ Efflux-Independent NLRP3 Inflammasome Activation by Small Molecules Targeting Mitochondria. *Immunity* **45**, 761-773, doi:https://doi.org/10.1016/j.immuni.2016.08.010 (2016).
43 Zhong, Z. *et al.* New mitochondrial DNA synthesis enables NLRP3 inflammasome activation. *Nature* **560**, 198-203, doi:10.1038/s41586-018-0372-z (2018).
44 Gaidt, M. M. *et al.* Human Monocytes Engage an Alternative Inflammasome Pathway. *Immunity* **44**, 833-846, doi:10.1016/j.immuni.2016.01.012 (2016).
45 Sinead Kenealy, E. M. C. (EMJ Allergy Immunol. 2018;3[1]:106-113, 2018).
46 Masumoto, J. *et al.* ASC, a novel 22-kDa protein, aggregates during apoptosis of human promyelocytic leukemia HL-60 cells. *J Biol Chem* **274**, 33835-33838, doi:10.1074/jbc.274.48.33835 (1999).
47 de Alba, E. Structure and interdomain dynamics of apoptosis-associated speck-like protein containing a CARD (ASC). *J Biol Chem* **284**, 32932-32941, doi:10.1074/jbc.M109.024273 (2009).
48 Nambayan, R. J. T., Sandin, S. I., Quint, D. A., Satyadi, D. M. & de Alba, E. The inflammasome adapter ASC assembles into filaments with integral participation of its two Death Domains, PYD and CARD. *J Biol Chem* **294**, 439-452, doi:10.1074/jbc.RA118.004407 (2019).
49 Bryan, N. B., Dorfleutner, A., Rojanasakul, Y. & Stehlik, C. Activation of inflammasomes requires intracellular redistribution of the apoptotic speck-like protein containing a caspase recruitment domain. *J Immunol* **182**, 3173-3182, doi:10.4049/jimmunol.0802367 (2009).
50 Fernandes-Alnemri, T. *et al.* The pyroptosome: a supramolecular assembly of ASC dimers mediating inflammatory cell death via caspase-1 activation. *Cell Death Differ* **14**, 1590-1604, doi:10.1038/sj.cdd.4402194 (2007).
51 Mariathasan, S. *et al.* Differential activation of the inflammasome by caspase-1 adaptors ASC and Ipaf. *Nature* **430**, 213-218, doi:10.1038/nature02664 (2004).
52 Nicholson, D. W. Caspase structure, proteolytic substrates, and function during apoptotic cell death. *Cell Death Differ* **6**, 1028-1042, doi:10.1038/sj.cdd.4400598 (1999).
53 Lee, D. J. *et al.* Regulation and Function of the Caspase-1 in an Inflammatory Microenvironment. *J Invest Dermatol* **135**, 2012-2020, doi:10.1038/jid.2015.119 (2015).
54 Denes, A., Lopez-Castejon, G. & Brough, D. Caspase-1: is IL-1 just the tip of the ICEberg? *Cell Death Dis* **3**, e338, doi:10.1038/cddis.2012.86 (2012).
55 Fink, S. L. & Cookson, B. T. Caspase-1-dependent pore formation during pyroptosis leads to osmotic lysis of infected host macrophages. *Cellular microbiology* **8**, 1812-1825, doi:10.1111/j.1462-5822.2006.00751.x (2006).
56 Bergsbaken, T., Fink, S. L. & Cookson, B. T. Pyroptosis: host cell death and inflammation. *Nature reviews. Microbiology* **7**, 99-109, doi:10.1038/nrmicro2070 (2009).

57 Yi, Y.-S. Caspase-11 non-canonical inflammasome: a critical sensor of intracellular lipopolysaccharide in macrophage-mediated inflammatory responses. *Immunology* **152**, 207-217, doi:10.1111/imm.12787 (2017).
58 Man, S. M. & Kanneganti, T. D. Converging roles of caspases in inflammasome activation, cell death and innate immunity. *Nature reviews. Immunology* **16**, 7-21, doi:10.1038/nri.2015.7 (2016).
59 Man, S. M., Karki, R. & Kanneganti, T. D. Molecular mechanisms and functions of pyroptosis, inflammatory caspases and inflammasomes in infectious diseases. *Immunological reviews* **277**, 61-75, doi:10.1111/imr.12534 (2017).
60 Zhang, J. M. & An, J. Cytokines, inflammation, and pain. *Int Anesthesiol Clin* **45**, 27-37, doi:10.1097/AIA.0b013e318034194e (2007).
61 Miagkov, A. V. *et al.* NF-kappaB activation provides the potential link between inflammation and hyperplasia in the arthritic joint. *Proceedings of the National Academy of Sciences of the United States of America* **95**, 13859-13864, doi:10.1073/pnas.95.23.13859 (1998).
62 Ramos-Junior, E. S. & Morandini, A. C. Gasdermin: A new player to the inflammasome game. *Biomedical Journal* **40**, 313-316, doi:https://doi.org/10.1016/j.bj.2017.10.002 (2017).
63 Lopez-Castejon, G. & Brough, D. Understanding the mechanism of IL-1β secretion. *Cytokine Growth Factor Rev* **22**, 189-195, doi:10.1016/j.cytogfr.2011.10.001 (2011).
64 Afonina, Inna S., Müller, C., Martin, Seamus J. & Beyaert, R. Proteolytic Processing of Interleukin-1 Family Cytokines: Variations on a Common Theme. *Immunity* **42**, 991-1004, doi:https://doi.org/10.1016/j.immuni.2015.06.003 (2015).
65 Miao, E. A., Rajan, J. V. & Aderem, A. Caspase-1-induced pyroptotic cell death. *Immunological reviews* **243**, 206-214, doi:10.1111/j.1600-065X.2011.01044.x (2011).
66 Chen, X. *et al.* Pyroptosis is driven by non-selective gasdermin-D pore and its morphology is different from MLKL channel-mediated necroptosis. *Cell Research* **26**, 1007, doi:10.1038/cr.2016.100

https://www.nature.com/articles/cr2016100 - supplementary-information (2016).
67 Sborgi, L. *et al.* GSDMD membrane pore formation constitutes the mechanism of pyroptotic cell death. *Embo j* **35**, 1766-1778, doi:10.15252/embj.201694696 (2016).
68 Wright, J. A. & Bryant, C. E. The killer protein Gasdermin D. *Cell Death And Differentiation* **23**, 1897, doi:10.1038/cdd.2016.100 (2016).
69 Aglietti, R. A. *et al.* GsdmD p30 elicited by caspase-11 during pyroptosis forms pores in membranes. *Proceedings of the National Academy of Sciences* **113**, 7858-7863, doi:10.1073/pnas.1607769113 (2016).
70 Evavold, C. L. & Kagan, J. C. Defying Death: The (W)hole Truth about the Fate of GSDMD Pores. *Immunity* **50**, 15-17, doi:https://doi.org/10.1016/j.immuni.2018.12.032 (2019).
71 Taabazuing, C. Y., Okondo, M. C. & Bachovchin, D. A. Pyroptosis and Apoptosis Pathways Engage in Bidirectional Crosstalk in Monocytes and Macrophages. *Cell Chemical Biology* **24**, 507-514.e504, doi:https://doi.org/10.1016/j.chembiol.2017.03.009 (2017).
72 Orning, P. *et al.* Pathogen blockade of TAK1 triggers caspase-8-dependent cleavage of gasdermin D and cell death. *Science (New York, N.Y.)* **362**, 1064-1069, doi:10.1126/science.aau2818 (2018).
73 Vince, J. E. & Silke, J. The intersection of cell death and inflammasome activation. *Cellular and molecular life sciences : CMLS* **73**, 2349-2367, doi:10.1007/s00018-016-2205-2 (2016).

74 Glick, D., Barth, S. & Macleod, K. F. Autophagy: cellular and molecular mechanisms. *J Pathol* **221**, 3-12, doi:10.1002/path.2697 (2010).
75 Kim, Y. K., Shin, J. S. & Nahm, M. H. NOD-Like Receptors in Infection, Immunity, and Diseases. *Yonsei Med J* **57**, 5-14, doi:10.3349/ymj.2016.57.1.5 (2016).
76 Dupont, N. *et al.* Autophagy-based unconventional secretory pathway for extracellular delivery of IL-1β. *Embo j* **30**, 4701-4711, doi:10.1038/emboj.2011.398 (2011).
77 Rathinam, Vijay A. K. & Fitzgerald, Katherine A. Inflammasome Complexes: Emerging Mechanisms and Effector Functions. *Cell* **165**, 792-800, doi:https://doi.org/10.1016/j.cell.2016.03.046 (2016).
78 Deretic, V. & Levine, B. Autophagy, immunity, and microbial adaptations. *Cell host & microbe* **5**, 527-549, doi:10.1016/j.chom.2009.05.016 (2009).
79 Davis, S., Wang, J. & Ferro-Novick, S. Crosstalk between the Secretory and Autophagy Pathways Regulates Autophagosome Formation. *Developmental Cell* **41**, 23-32, doi:https://doi.org/10.1016/j.devcel.2017.03.015 (2017).
80 Kimura, T. *et al.* Dedicated SNAREs and specialized TRIM cargo receptors mediate secretory autophagy. *The EMBO Journal* **36**, 42-60, doi:10.15252/embj.201695081 (2017).
81 Rühl, S. *et al.* ESCRT-dependent membrane repair negatively regulates pyroptosis downstream of GSDMD activation. *Science (New York, N.Y.)* **362**, 956-960, doi:10.1126/science.aar7607 (2018).
82 Jimenez, A. J. *et al.* ESCRT Machinery Is Required for Plasma Membrane Repair. *Science (New York, N.Y.)* **343**, 1247136, doi:10.1126/science.1247136 (2014).
83 Jimenez, A. J. & Perez, F. Plasma membrane repair: the adaptable cell life-insurance. *Current Opinion in Cell Biology* **47**, 99-107, doi:https://doi.org/10.1016/j.ceb.2017.03.011 (2017).
84 Petiot, A. *et al.* Alix differs from ESCRT proteins in the control of autophagy. *Biochemical and Biophysical Research Communications* **375**, 63-68, doi:https://doi.org/10.1016/j.bbrc.2008.07.136 (2008).
85 Sadoul, R. Do Alix and ALG-2 really control endosomes for better or for worse? *Biology of the Cell* **98**, 69-77, doi:10.1042/bc20050007 (2006).
86 Martin-Serrano, J., Yarovoy, A., Perez-Caballero, D. & Bieniasz, P. D. Divergent retroviral late-budding domains recruit vacuolar protein sorting factors by using alternative adaptor proteins. *Proceedings of the National Academy of Sciences of the United States of America* **100**, 12414-12419, doi:10.1073/pnas.2133846100 (2003).
87 Kingsbury, S. R., Conaghan, P. G. & McDermott, M. F. The role of the NLRP3 inflammasome in gout. *J Inflamm Res* **4**, 39-49, doi:10.2147/jir.s11330 (2011).
88 Martinon, F., Pétrilli, V., Mayor, A., Tardivel, A. & Tschopp, J. Gout-associated uric acid crystals activate the NALP3 inflammasome. *Nature* **440**, 237-241, doi:10.1038/nature04516 (2006).
89 Busso, N. & So, A. Mechanisms of inflammation in gout. *Arthritis Res Ther* **12**, 206, doi:10.1186/ar2952 (2010).
90 Wannamaker, W. *et al.* (S)-1-((S)-2-{[1-(4-amino-3-chloro-phenyl)-methanoyl]-amino}-3,3-dimethyl-butanoy l)-pyrrolidine-2-carboxylic acid ((2R,3S)-2-ethoxy-5-oxo-tetrahydro-furan-3-yl)-amide (VX-765), an orally available selective interleukin (IL)-converting enzyme/caspase-1 inhibitor, exhibits potent anti-inflammatory activities by inhibiting the release of IL-1beta and IL-18. *J Pharmacol Exp Ther* **321**, 509-516, doi:10.1124/jpet.106.111344 (2007).
91 Guo, B., Fu, S., Zhang, J., Liu, B. & Li, Z. Targeting inflammasome/IL-1 pathways for cancer immunotherapy. *Scientific Reports* **6**, 36107, doi:10.1038/srep36107

https://www.nature.com/articles/srep36107 - supplementary-information (2016).

92 Moossavi, M., Parsamanesh, N., Bahrami, A., Atkin, S. L. & Sahebkar, A. Role of the NLRP3 inflammasome in cancer. *Molecular Cancer* **17**, 158, doi:10.1186/s12943-018-0900-3 (2018).
93 Dupaul-Chicoine, J. *et al. The Nlrp3 Inflammasome Suppresses Colorectal Cancer Metastatic Growth in the Liver by Promoting Natural Killer Cell Tumoricidal Activity*. Vol. 43 (2015).
94 Allen, I. C. *et al.* The NLRP3 inflammasome functions as a negative regulator of tumorigenesis during colitis-associated cancer. *J Exp Med* **207**, 1045-1056, doi:10.1084/jem.20100050 (2010).
95 Dorhoi, A. *et al.* Activation of the NLRP3 inflammasome by Mycobacterium tuberculosis is uncoupled from susceptibility to active tuberculosis. *European Journal of Immunology* **42**, 374-384, doi:10.1002/eji.201141548 (2012).
96 (WHO), W. *Global Tuberculosis Raport*, 2016).
97 Ehrt, S. & Schnappinger, D. Mycobacterial survival strategies in the phagosome: defence against host stresses. *Cellular microbiology* **11**, 1170-1178, doi:10.1111/j.1462-5822.2009.01335.x (2009).
98 Pauwels, A.-M., Trost, M., Beyaert, R. & Hoffmann, E. Patterns, Receptors, and Signals: Regulation of Phagosome Maturation. *Trends in Immunology* **38**, 407-422, doi:https://doi.org/10.1016/j.it.2017.03.006 (2017).
99 Eklund, D. *et al. Human Gene Variants Linked to Enhanced NLRP3 Activity Limit Intramacrophage Growth of Mycobacterium tuberculosis*. Vol. 209 (2013).
100 Briken, V., Ahlbrand, S. E. & Shah, S. Mycobacterium tuberculosis and the host cell inflammasome: a complex relationship. *Front Cell Infect Microbiol* **3**, 62, doi:10.3389/fcimb.2013.00062 (2013).
101 Mayer-Barber, K. D. *et al.* Caspase-1 independent IL-1beta production is critical for host resistance to mycobacterium tuberculosis and does not require TLR signaling in vivo. *J Immunol* **184**, 3326-3330, doi:10.4049/jimmunol.0904189 (2010).
102 Master, S. S. *et al.* Mycobacterium tuberculosis prevents inflammasome activation. *Cell host & microbe* **3**, 224-232, doi:10.1016/j.chom.2008.03.003 (2008).
103 Shah, S. *et al.* Cutting edge: Mycobacterium tuberculosis but not nonvirulent mycobacteria inhibits IFN-β and AIM2 inflammasome-dependent IL-1β production via its ESX-1 secretion system. *J Immunol* **191**, 3514-3518, doi:10.4049/jimmunol.1301331 (2013).
104 Evavold, C. L. *et al.* The Pore-Forming Protein Gasdermin D Regulates Interleukin-1 Secretion from Living Macrophages. *Immunity* **48**, 35-44.e36, doi:https://doi.org/10.1016/j.immuni.2017.11.013 (2018).
105 Garneau, J. E. *et al.* The CRISPR/Cas bacterial immune system cleaves bacteriophage and plasmid DNA. *Nature* **468**, 67, doi:10.1038/nature09523

https://www.nature.com/articles/nature09523 - supplementary-information (2010).
106 Ran, F. A. *et al.* Genome engineering using the CRISPR-Cas9 system. *Nat Protoc* **8**, 2281-2308, doi:10.1038/nprot.2013.143 (2013).
107 Ratan, Z. A. *et al.* CRISPR-Cas9: a promising genetic engineering approach in cancer research. *Ther Adv Med Oncol* **10**, 1758834018755089, doi:10.1177/1758834018755089 (2018).
108 Sun, L., Lutz, B. M. & Tao, Y. X. The CRISPR/Cas9 system for gene editing and its potential application in pain research. *Transl Perioper Pain Med* **1**, 22-33 (2016).
109 *GeneArt Genomic Cleavage Detection Kit*, <https://www.thermofisher.com/document-connect/document-connect.html?url=https%3A%2F%2Fassets.thermofisher.com%2FTFS-Assets%2FLSG%2Fmanuals%2FA24372_GeneArt_GenomicCleavage_Detect_Kit_man.pdf&titl

e=R2VuZUFydCZyZWc7IEdlbm9taWMgQ2xlYXZhZ2UgRGV0ZWN0aW9uIEtpdCAtIFVzZXIgR3VpZGU=> (
110 Mahmood, T. & Yang, P. C. Western Blot: Technique, Theory, and Trouble Shooting. *North American Journal of Medical Sciences* **4**, 429-434, doi:10.4103/1947-2714.100998 (2012).
111 Addgene. *Plasmids 101: Gateway Cloning*, <https://blog.addgene.org/plasmids-101-gateway-cloning> (2017).
112 Maheaswari, R., Kshirsagar, J. T. & Lavanya, N. Polymerase chain reaction: A molecular diagnostic tool in periodontology. *J Indian Soc Periodontol* **20**, 128-135, doi:10.4103/0972-124x.176391 (2016).
113 Chan, F. K., Moriwaki, K. & De Rosa, M. J. Detection of necrosis by release of lactate dehydrogenase activity. *Methods in molecular biology (Clifton, N.J.)* **979**, 65-70, doi:10.1007/978-1-62703-290-2_7 (2013).
114 *LDH cytotoxicity detection kit user manual*, <http://radio.cuci.udg.mx/bch/EN/Manuals/LDH-INT_Clontech.pdf> (2007).
115 Scientific, T. *Overview of ELISA*, <https://www.thermofisher.com/no/en/home/life-science/protein-biology/protein-biology-learning-center/protein-biology-resource-library/pierce-protein-methods/overview-elisa.html - 2> (
116 Rapino, F. *et al.* C/EBPα Induces Highly Efficient Macrophage Transdifferentiation of B Lymphoma and Leukemia Cell Lines and Impairs Their Tumorigenicity. *Cell reports* **3**, 1153-1163, doi:https://doi.org/10.1016/j.celrep.2013.03.003 (2013).
117 Gaidt, M., Rapino, F., Graf, T. & Hornung, V. Vol. 1714 57-66 (2018).
118 Platform, B. I. G. P. *GPP Web Portal*, <https://portals.broadinstitute.org/gpp/public/analysis-tools/sgrna-design> (2019).
119 Doench, J. G. *et al.* Optimized sgRNA design to maximize activity and minimize off-target effects of CRISPR-Cas9. *Nature Biotechnology* **34**, 184, doi:10.1038/nbt.3437

https://www.nature.com/articles/nbt.3437 - supplementary-information (2016).
120 Addgene. *Lntiviral Guide*, <https://www.addgene.org/viral-vectors/lentivirus/lenti-guide/> (
121 Invivogen. Lentiviral Vector Production and Cell Transduction. *Invivogen Insight*.
122 Brinkman, E. K., Chen, T., Amendola, M. & van Steensel, B. Easy quantitative assessment of genome editing by sequence trace decomposition. *Nucleic Acids Res* **42**, e168, doi:10.1093/nar/gku936 (2014).
123 Brinkman et al. *Nucl.Acids Res*, <https://tide.deskgen.com/> (2014).
124 Harris, J. *et al.* Autophagy controls IL-1beta secretion by targeting pro-IL-1beta for degradation. *J Biol Chem* **286**, 9587-9597, doi:10.1074/jbc.M110.202911 (2011).
125 Sborgi, L. *et al.* GSDMD membrane pore formation constitutes the mechanism of pyroptotic cell death. *The EMBO Journal*, e201694696, doi:10.15252/embj.201694696 (2016).
126 Rathkey, J. *et al. Live cell visualization of gasdermin D-driven pyroptotic cell death*. Vol. 292 (2017).
127 He, W.-t. *et al.* Gasdermin D is an executor of pyroptosis and required for interleukin-1β secretion. *Cell Research* **25**, 1285, doi:10.1038/cr.2015.139

https://www.nature.com/articles/cr2015139 - supplementary-information (2015).
128 Ding, J. *et al.* Pore-forming activity and structural autoinhibition of the gasdermin family. *Nature* **535**, 111-116, doi:10.1038/nature18590 (2016).
129 Liu, X. *et al.* Inflammasome-activated gasdermin D causes pyroptosis by forming membrane pores. *Nature* **535**, 153, doi:10.1038/nature18629

https://www.nature.com/articles/nature18629 - supplementary-information (2016).
130 Hara, T. *et al.* FIP200, a ULK-interacting protein, is required for autophagosome formation in mammalian cells. *J Cell Biol* **181**, 497-510, doi:10.1083/jcb.200712064 (2008).
131 Gaj, T., Gersbach, C. A. & Barbas, C. F., 3rd. ZFN, TALEN, and CRISPR/Cas-based methods for genome engineering. *Trends Biotechnol* **31**, 397-405, doi:10.1016/j.tibtech.2013.04.004 (2013).
132 Riordan, S. M., Heruth, D. P., Zhang, L. Q. & Ye, S. Q. Application of CRISPR/Cas9 for biomedical discoveries. *Cell & Bioscience* **5**, 33, doi:10.1186/s13578-015-0027-9 (2015).
133 Young, S. A., Aitken, R. J. & Ikawa, M. Advantages of using the CRISPR/Cas9 system of genome editing to investigate male reproductive mechanisms using mouse models. *Asian journal of andrology* **17**, 623-627, doi:10.4103/1008-682x.153851 (2015).
134 Cong, L. *et al.* Multiplex genome engineering using CRISPR/Cas systems. *Science (New York, N.Y.)* **339**, 819-823, doi:10.1126/science.1231143 (2013).
135 Zhang, X.-H., Tee, L. Y., Wang, X.-G., Huang, Q.-S. & Yang, S.-H. Off-target Effects in CRISPR/Cas9-mediated Genome Engineering. *Molecular Therapy - Nucleic Acids* **4**, e264, doi:https://doi.org/10.1038/mtna.2015.37 (2015).
136 Brinkman, E. K., Chen, T., Amendola, M. & van Steensel, B. Easy quantitative assessment of genome editing by sequence trace decomposition. *Nucleic Acids Research* **42**, e168-e168, doi:10.1093/nar/gku936 (2014).
137 Qi, L. S. *et al.* Repurposing CRISPR as an RNA-guided platform for sequence-specific control of gene expression. *Cell* **152**, 1173-1183, doi:10.1016/j.cell.2013.02.022 (2013).
138 Chanput, W., Mes, J. J. & Wichers, H. J. THP-1 cell line: An in vitro cell model for immune modulation approach. *International Immunopharmacology* **23**, 37-45, doi:https://doi.org/10.1016/j.intimp.2014.08.002 (2014).
139 Hostettler, L. *et al.* The Bright Fluorescent Protein mNeonGreen Facilitates Protein Expression Analysis In Vivo. *G3: Genes|Genomes|Genetics* **7**, 607-615, doi:10.1534/g3.116.038133 (2017).
140 Scientific, T. (ThermoFisher Scienctific).

9 Appendices

9.1 Appendix I

Overview of guide sequences (CRISPR/Cas9 oligos and primers) and Gateway cloning/HIFI/IVA primers (in blue) used in this study. All the primers were ordered from Sigma-Aldrich and designed by K.S.Beckwith.

Primer	**Sequence**
FIP200_sgRNA_1_s	CACCGTTTCTAACAGCTCTATTACG
FIP200_sgRNA_1_as	AAACCGTAATAGAGCTGTTAGAAAC
FIP200_sgRNA_2_s	CACCGCTGGTTAGGCACTCCAACAG
FIP200_sgRNA_2_as	AAACCTGTTGGAGTGCCTAACCAGC
FIP200_sg2_seq_fw	GCCTCTCTCTGCTAAACTAGAC
FIP200_sg2_seq_rv	CAGATCACCATCTTTAGTGTCAATCG
FIP200_sg1_seq_fw	CCCAAATGATGGAGTGATTTTTCCC
FIP200_sg1_seq_rv	CATGAAGTATGCTACAGAAAATCCAAGC
SEC22B_sgRNA_1_s	CACCGTTCGTCCTCCTGCATCGAGG
SEC22B_sgRNA_1_as	AAACCCTCGATGCAGGAGGACGAAC
SEC22B_sgRNA_2_s	CACCGAAAAGCCAACTTCTTAGGGA
SEC22B_sgRNA_2_as	AAACTCCCTAAGAAGTTGGCTTTTC
SEC22B_sg1_seq_fw	AGCTGGATCTCCGGTAACTG
SEC22B_sg1_seq_rv	CACTGGGTGATCACAATCAACC
SEC22B_sg2_seq_fw	GACTCTCGTTTAGCCAGCCTC

SEC22B_sg2_seq_rv	GGGGGAAAGATCAAAAGACTAGAG

PDCD6_sgRNA_1_s	CACCGTGCCGGACCAGAGCTTCCTG
PDCD6_sgRNA_1_as	AAACCAGGAAGCTCTGGTCCGGCAC
PDCD6_sgRNA_2_s	CACCGAGGGTCGATAAAGACAGGAG
PDCD6_sgRNA_2_as	AAACCTCCTGTCTTTATCGACCCTC
PDCD6_sg1_seq_fw	GATAATGCCAGGCCCTGC
PDCD6_sg1_seq_rv	CTCTGCATCTTGGGAAGGG
PDCD6_sg2_seq_fw	CTTAGGGGAAGACCACACTGG
PDCD6_sg2_seq_rv	GCTTCCTATTCCCCTCCTAAACC
ALIX_sgRNA2_seq_fw	GCTGATCATGGCGACATTCATCTC
ALIX_sgRNA2_seq_rv	AGATCAGTACAGGGCAGACTGC
ALIX_sgRNA2_s	CACCGCGTCCGCTGGACAAGCACGA
ALIX_sgRNA2_as	AAACTCGTGCTTGTCCAGCGGACGC
ALIX_sgRNA1_seq_fw	GTAGGTCAGATGTTTTAGATTGGTTTTGC
ALIX_sgRNA1_seq_rv	GATCTATTTCATGACTTCAAACACAGCC
ALIX_sgRNA1_s	CACCGCTTAAGTCGAGAGCCGACCG
ALIX_sgRNA1_as	AAACCGGTCGGCTCTCGACTTAAGC

GSDMD-m1_rv	CAGGTGACTTCGGCTCCGCA
GSDMD-m2_fw	CACCTACCCCAAGCAACCCTG

GSDMD-m2_rv	GCGTCTTCCCTCCCCTGACA
GSDMD_cc1-fw	GCTCATGGTTCTGGAAACCCC
GSDMD_cc1-rv	GCCGAGATAGCAAAACCTCACC
hGSDMD-cc1-sgRNA-s	CACCGGACAGGCAAAGATCGCAGG
hGSDMD-cc1_sgRNA-as	AAACCCTGCGATCTTTGCCTGTCC
hGSDMD-cc2-sgRNA-as	AAACCGCCTGCGATCTTTGCCTGTC
hGSDMD-cc2-sgRNA-s	CACCGACAGGCAAAGATCGCAGGCG
hGSDMD-m1-sgRNA-as	AAACCTTGTGGGTGCGCGTGACTTC
hGSDMD-m1-sgRNA-s	CACCGAAGTCACGCGCACCCACAAG
hGSDMD-m2-sgRNA-as	AAACGACTCGAGGTGCGGCCCCCTC
hGSDMD-m2-sgRNA-s	CACCGAGGGGGCCGCACCTCGAGTC
hGSDMD-p1-sgRNA-as	AAACGGTGTTAGGGTCCACACTCAC
hGSDMD-p1-sgRNA-s	CACCGTGAGTGTGGACCCTAACACC

GSDMD_attB1_fw	AAAGCAGGCTTCATGGGGTCGGCCTTTGAG
GSDMD_attB2_rv	GAAAGCTGGGTTGTGGGGCTCCTGGCTCA
GSDMD_3'UTR_rv	GCAAACACTCTGCCCTGCTG
GSDMD_K248_fw	CGTTCCACGAGCGAAGGC
GSDMD_K248_rv	CTTGTGGCCTGTCGCGG
GSDMD_K248_FLAG_fw	ACAAAGACGATGACGACAAGCGTTCCACGAGCGAAGGC

GSDMD_K248_FLAG_rv	GTCGTCATCGTCTTTGTAGTCCTTGTGGCCTGTCGCGG
GSDMD_mNG_fw	CGCGACAGGCCACAAGATGGTGAGCAAGGGCGAG
GSDMD_mNG_rv	CTTCGCTCGTGGAACGCTTGTACAGCTCGTCCATGCC

9.2 Appendix II

Schematic drawings (Snapgene) of pEntry_GsDMD_L1L2 vector and map of destination vector plex307 used in Gateway molecular cloning

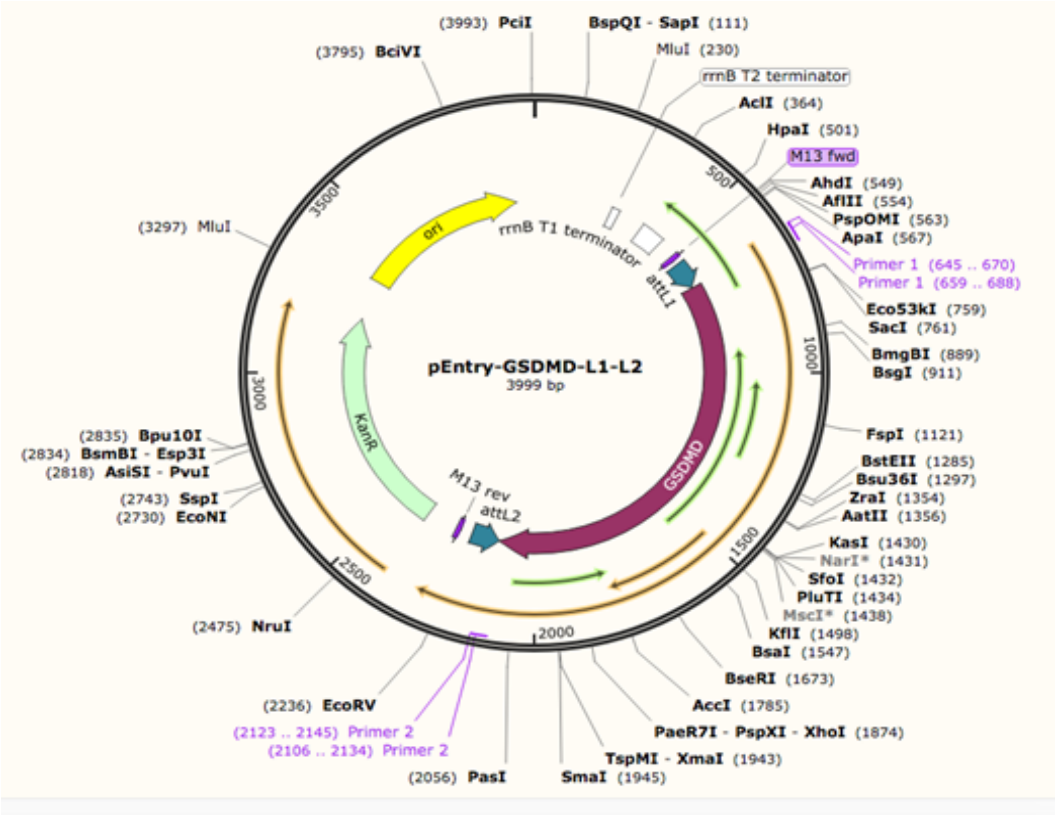

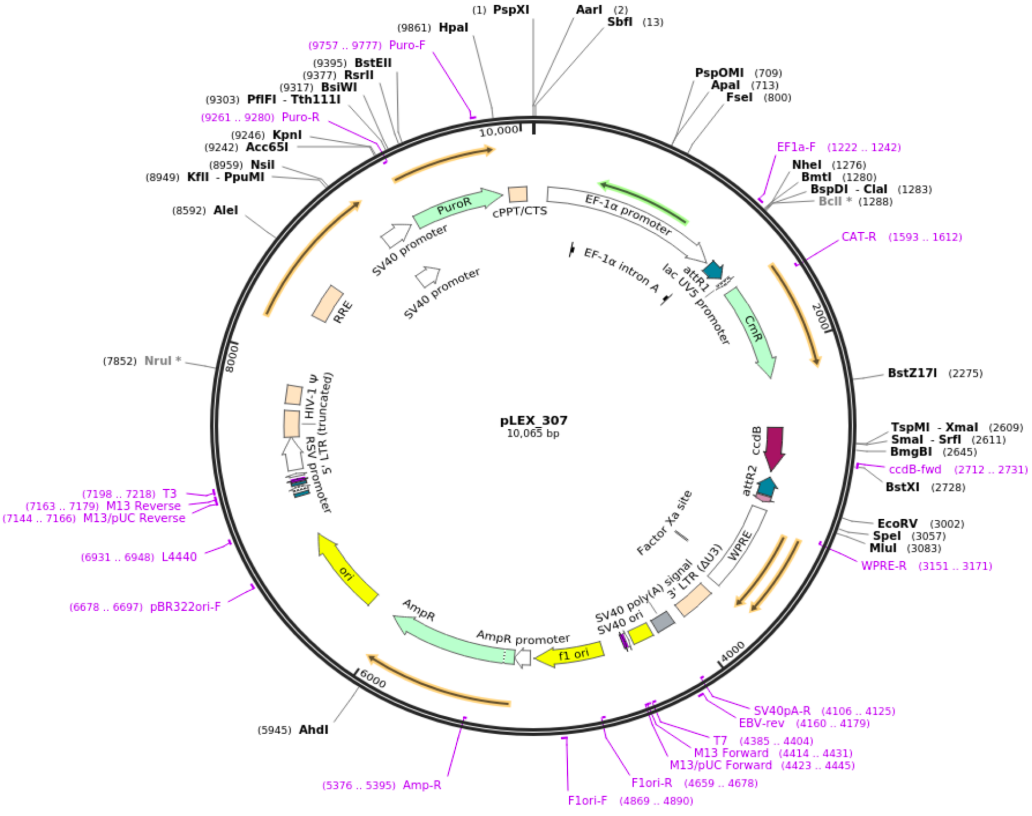

9.3 Appendix III

PCR products (top) and cleaved products after enzyme digestion (bottom) of GSDMD KOs reporters

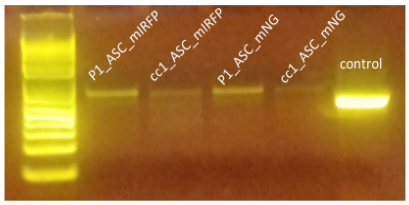

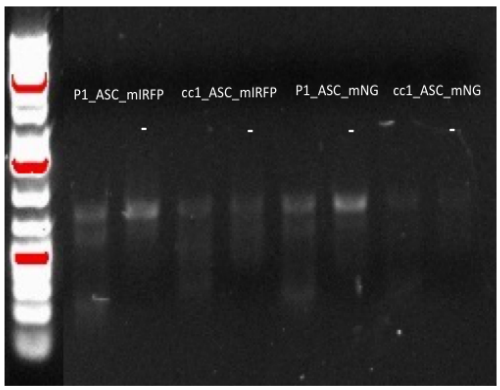

9.4 Appendix IV

PCR products (top) and cleaved products after enzyme digestion (bottom) of FIP200, SEC22B sg2, PDCD6 sg1 and ALIXsg1 KOs

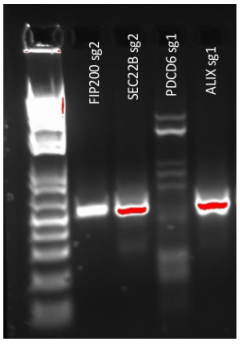

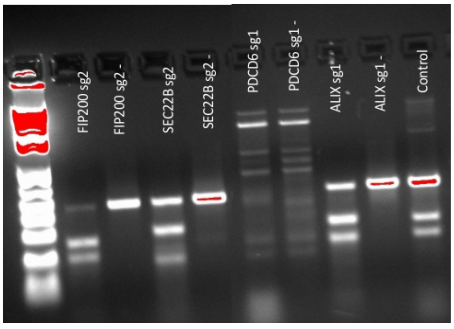

9.5 Appendix V

Calculated cleaved efficiency of KO cell lines using the formula previously described in Method 3.7.5.

KO cell lines	Cleavage efficiency (%)
WT	0
cc1	34
cc2	33
m1	Not quantified
m2	30
p1	Not quantified
FIP200 sg1	56
FIP200 sg2	68
SEC22b sg1	73
SEC22b sg2	37
PDCD6 (ALG2) sg2	19
NLRP3	Not quantified
ALIX sg1	42
ALIX sg2	59

9.6 Appendix VI

EVOS imaging of NLRP3 KO and ASC_mNG (control). A) Fluorescent images of NLRP3 KO and ASC_mNG cell lines of untreated and LPS+nigericin. a) Raw(mean value) live/dead cell count data with SEM B) Fluorescent images of NLRP3 KO and ASC_mNG cell lines of untreated and M.tub b) Raw live/dead (mean value) cell count data with SEM

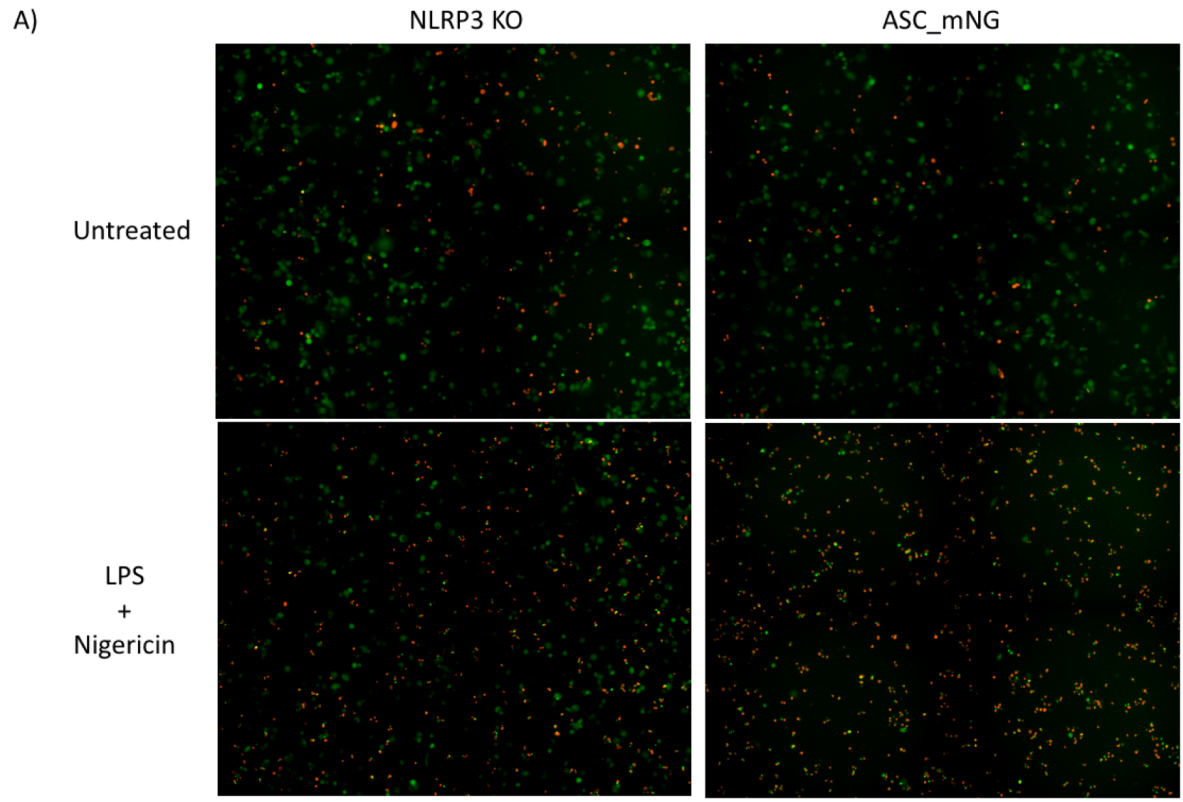

a)

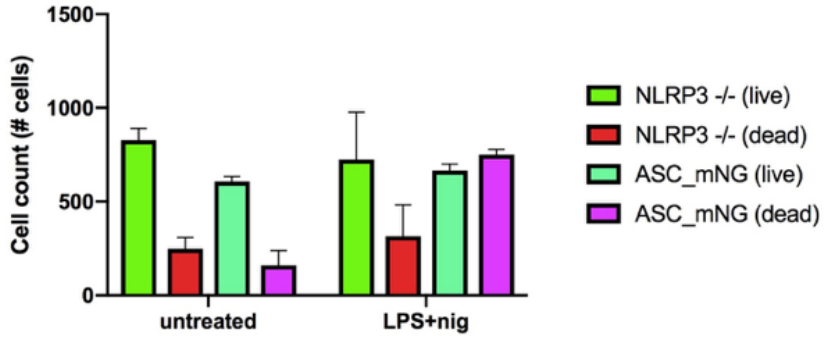

B)

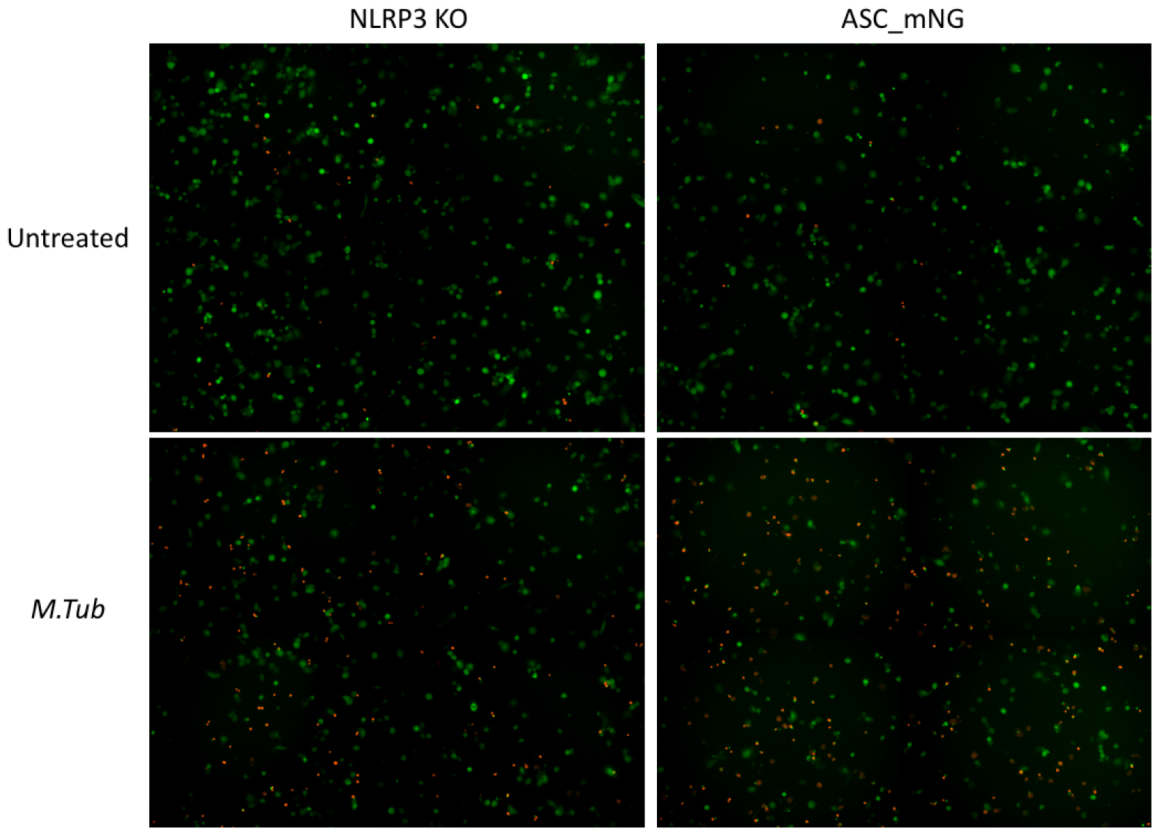
NLRP3 KO
ASC_mNG
Untreated
M.Tub

b)

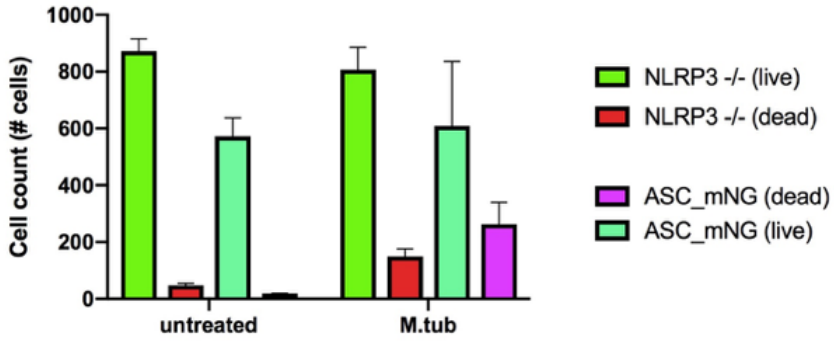
1000
800
600
400
200
0
Cell count (# cells)
untreated
M.tub
NLRP3 -/- (live)
NLRP3 -/- (dead)
ASC_mNG (dead)
ASC_mNG (live)

9.7 Appendix VII

CRISPR KOs TIDE Indel spectrum result

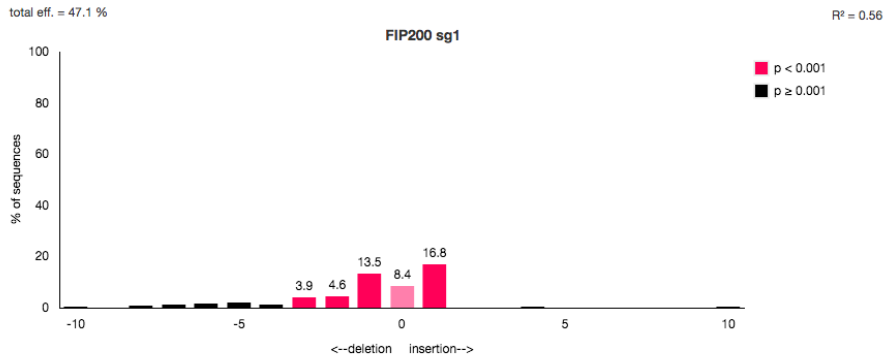

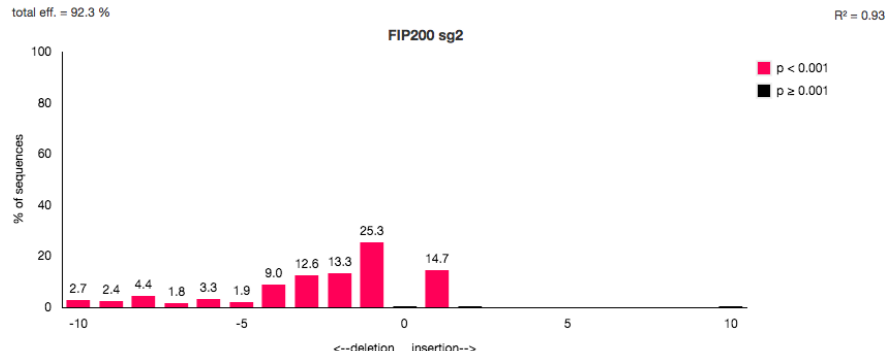

Indel Spectrum

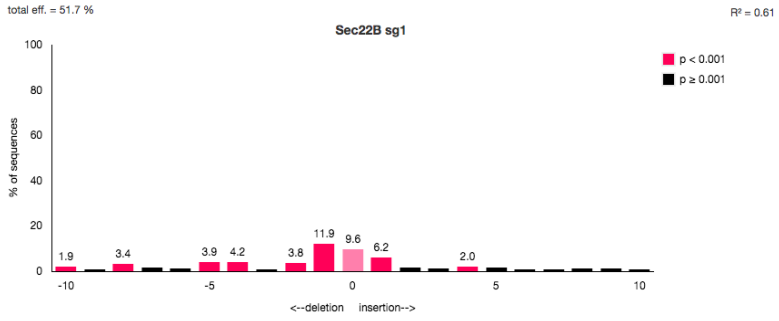

Indel Spectrum

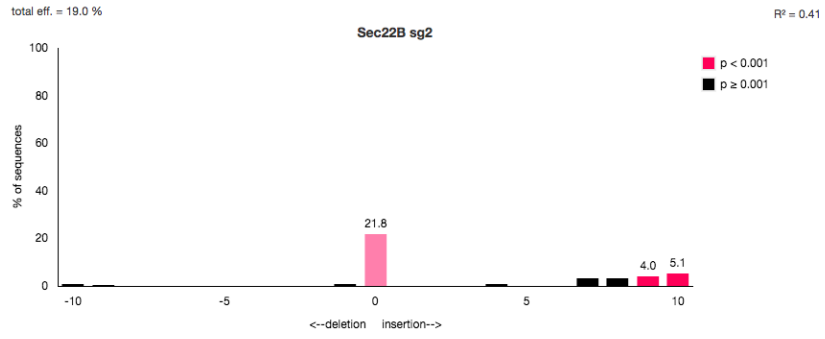

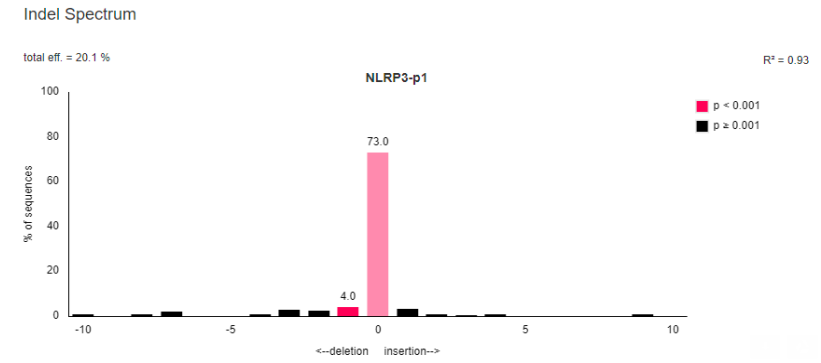

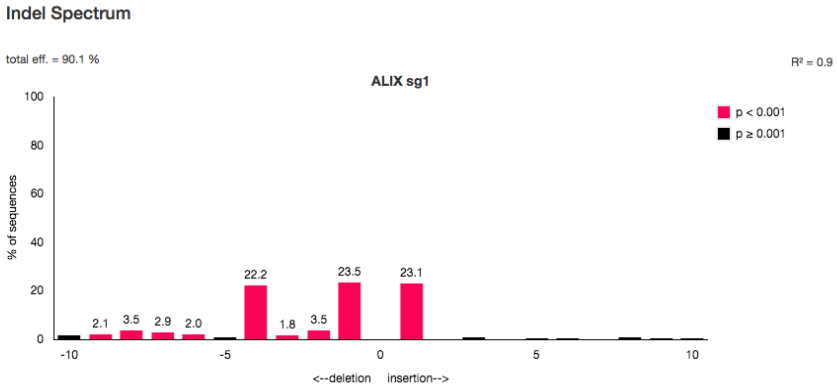

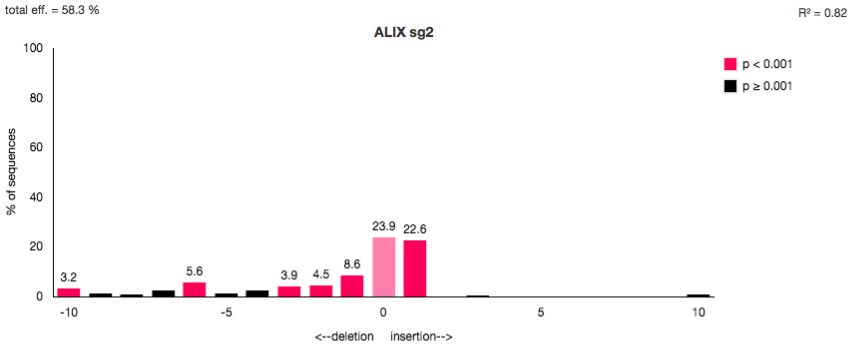

9.8 Appendix VIII

Geneplus 1kb plus DNA ladder[140]

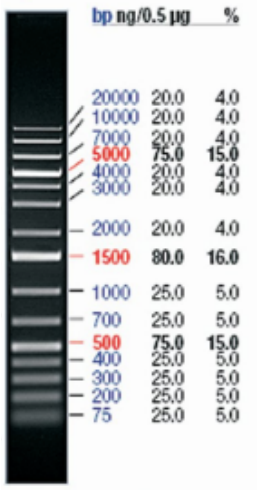

NTNU
Norwegian University of
Science and Technology